UNIVERSIDADE ESTADUAL DE CAMPINAS

Instituto de Matemática, Estatística e Computação Científica

GUILHERME TAVARES DA SILVA

Non-Smooth Dynamical Systems with Singular Switching Manifolds: the Double Discontinuity case

Sistemas Dinâmicos Não Suaves com Variedades de Descontinuidade Singulares: o caso da Descontinuidade Dupla

Campinas

2021

Guilherme Tavares da Silva

Non-Smooth Dynamical Systems with Singular Switching Manifolds: the Double Discontinuity case

Sistemas Dinâmicos Não Suaves com Variedades de Descontinuidade Singulares: o caso da Descontinuidade Dupla

Tese apresentada ao Instituto de Matemática, Estatística e Computação Científica da Universidade Estadual de Campinas como parte dos requisitos exigidos para a obtenção do título de Doutor em Matemática.

Thesis presented to the Institute of Mathematics, Statistics and Scientific Computing of the University of Campinas in partial fulfillment of the requirements for the degree of Doctor in Mathematics.

Supervisor: Ricardo Miranda Martins

Este trabalho corresponde à versão final da Tese defendida pelo aluno Guilherme Tavares da Silva e orientada pelo Prof. Dr. Ricardo Miranda Martins.

Campinas

2021

Ficha catalográfica
Universidade Estadual de Campinas
Biblioteca do Instituto de Matemática, Estatística e Computação Científica
Ana Regina Machado - CRB 8/5467

Si38n

Silva, Guilherme Tavares da, 1991-
Non-smooth dynamical systems with singular switching manifolds : the double discontinuity case / Guilherme Tavares da Silva. – Campinas, SP : [s.n.], 2021.

Orientador: Ricardo Miranda Martins.
Tese (doutorado) – Universidade Estadual de Campinas, Instituto de Matemática, Estatística e Computação Científica.

1. Sistemas dinâmicos. 2. Sistemas de Filippov. 3. Perturbação singular (Matemática). 4. Estabilidade estrutural. I. Martins, Ricardo Miranda, 1983-. II. Universidade Estadual de Campinas. Instituto de Matemática, Estatística e Computação Científica. III. Título.

Informações para Biblioteca Digital

Título em outro idioma: Sistemas dinâmicos não suaves com variedades de descontinuidade singulares : o caso da descontinuidade dupla
Palavras-chave em inglês:
Dynamical systems
Filippov systems
Singular perturbations (Mathematics)
Structural stability
Área de concentração: Matemática
Titulação: Doutor em Matemática
Banca examinadora:
Ricardo Miranda Martins [Orientador]
Gabriel Ponce
Marco Antonio Teixeira
Rodrigo Donizete Euzébio
Ana Cristina de Oliveira Mereu
Data de defesa: 15-03-2021
Programa de Pós-Graduação: Matemática

Identificação e informações acadêmicas do(a) aluno(a)
- ORCID do autor: https://orcid.org/0000-0002-3079-7458
- Currículo Lattes do autor: http://lattes.cnpq.br/4771859106417880

Tese de Doutorado defendida em 15 de março de 2021 e aprovada pela banca examinadora composta pelos Profs. Drs.

Prof(a). Dr(a). RICARDO MIRANDA MARTINS

Prof(a). Dr(a). GABRIEL PONCE

Prof(a). Dr(a). MARCO ANTONIO TEIXEIRA

Prof(a). Dr(a). RODRIGO DONIZETE EUZÉBIO

Prof(a). Dr(a). ANA CRISTINA DE OLIVEIRA MEREU

A Ata da Defesa, assinada pelos membros da Comissão Examinadora, consta no SIGA/Sistema de Fluxo de Dissertação/Tese e na Secretaria de Pós-Graduação do Instituto de Matemática, Estatística e Computação Científica.

To my parents, Izaura Flauzino and José Cícero.

Acknowledgements

I would like to thank...

...my family, for the affection and support.

...my girlfriend, Ana Clara, for the love and complicity.

...my supervisor, Prof. Ricardo Miranda, for the trust, patience, and friendship.

...all my professors, for the knowledge and experience shared.

...all IMECC employees, for the competence and helpfulness.

...the thesis committee, for the helpful suggestions and advice.

This study was financed in part by the Coordenação de Aperfeiçoamento de Pessoal de Nível Superior - Brasil (CAPES) — Finance Code 001.

The best way to predict the future is to invent it.
—Alan Kay

Resumo

Uma das hipóteses mais comuns na Teoria dos Sistemas Dinâmicos Não Suaves consiste na regularidade da variedade de descontinuidade, caso no qual existe a bem definida e estabelecida dinâmica de Filippov. Entretanto, apesar da presença em muitos modelos relevantes, sistemas com variedade de descontinuidade singular carecem de uma dinâmica igualmente bem estabelecida. Neste trabalho, apresentamos uma metodologia que, através de blow-ups e perturbação singular, permite a extensão da dinâmica de Filippov para o caso singular. Mais especificamente, focamos em sistemas em $\mathbb{R}^2$ e $\mathbb{R}^3$ cuja variedade de descontinuidade consiste em uma variedade algébrica com auto-interseção transversal, em formato de cruz. Em $\mathbb{R}^2$, estudamos a realização e estabilidade estrutural de uma configuração conhecida como Sela Deslizante. Em $\mathbb{R}^3$, estudamos a dinâmica e estabilidade estrutural da parte singular de uma configuração conhecida como Descontinuidade Dupla. Em ambos os casos, focamos em sistemas dados por campos vetoriais afins.

Palavras-chave: Sistemas dinâmicos. Sistemas de Filippov. Perturbação singular (Matemática). Estabilidade estrutural.

Abstract

One of the most common hypotheses on the Theory of Non-Smooth Dynamical Systems is a regular surface as switching manifold, at which case there is at least the well-defined and established Filippov dynamics. However, although present in many relevant models, systems with singular switching manifolds still lack such well-established dynamics. At this work, we present a framework that, through blow-ups and singular perturbation, allows the extension of Filippov dynamics to the singular case. More specifically, we focus on systems in $\mathbb{R}^2$ and $\mathbb{R}^3$ whose switching manifold consists of an algebraic manifold with transversal, cross-like, self-intersection. In $\mathbb{R}^2$, we study the realization and structural stability of a configuration known as Sliding Saddle. In $\mathbb{R}^3$, we study the dynamics and structural stability of the singular part of a configuration known as Double Discontinuity. In both cases, we focus on systems given by affine vector fields.

Keywords: Dynamical systems. Filippov systems. Singular perturbations (Mathematics). Structural stability.

List of Figures

List of Tables

Contents

Introduction

A dynamical system is a mathematical rule governing the time evolution of the points in a given geometrical space. Having its origins in Newtonian Mechanics, we might think of the Theory of Dynamical Systems as a mathematical generalization of it. Permeating practically all areas of science through the creation of models with temporal evolution, the Theory of Dynamical System is one of the most active and important areas of modern Mathematics.

Formally, a dynamical system consists of an action of a 1-parameter group of maps into a set. The two more common ways this action presents itself consist of the iteration of a diffeomorphism or the solutions of an ordinary differential equation. In both cases, we might attribute the success and importance of the theory to the philosophy employed in the study of these actions: prioritizing qualitative instead of quantitative analysis. In particular, the holy grail of the theory is to prove the *structural stability* of a given system which, roughly speaking, means that the dynamics of the system do not change upon small perturbations of its parameters.

The Theory of Dynamical Systems given by ordinary differential equations

$$\dot{\mathbf{x}} = \mathbf{F}(\mathbf{x}), \tag{1}$$

where $\mathbf{F} : \mathbb{R}^n \to \mathbb{R}^n$ is at least a continuous vector field evolved naturally with the birth of Calculus itself, with [2] and [32] being exceptional modern references on the subject. In fact, the machinery provided by this theory has been used in the study of models all around science: from classical Newtonian Mechanics to modern Machine Learning [55].

However, either naturally or due to simplifications and practicality, many of these phenomena are better approached with non-smooth models, i.e., where the vector field $\mathbf{F}$ above has discontinuities. More specifically, given $U \subset \mathbb{R}^n$ open, $h : U \to \mathbb{R}$ continually differentiable having 0 as a **regular value** and two vector fields $\mathbf{F}_\pm : U \to \mathbb{R}^n$ of class $C^k(U)$ with $k \geqslant 1$, we understand as a Non-Smooth Dynamical System that given by a differential equation as (1) where

$$\mathbf{F}(\mathbf{x}) = \begin{cases} \mathbf{F}_+(\mathbf{x}), & \text{if } \mathbf{x} \in \Sigma_+, \\ \mathbf{F}_-(\mathbf{x}), & \text{if } \mathbf{x} \in \Sigma_-, \end{cases} \tag{2}$$

with $\Sigma_+ = \{\mathbf{x} \in U;\ h(\mathbf{x}) \geqslant 0\}$ and $\Sigma_- = \{\mathbf{x} \in U;\ h(\mathbf{x}) \leqslant 0\}$ intersecting at a regular surface Σ called **switching manifold**. We denote the set of vector fields $\mathbf{F}$ defined as above by

$$\mathcal{R}^k(U) \equiv C^k(U, \mathbb{R}^n) \times C^k(U, \mathbb{R}^n)$$

which we consider equipped with the Whitney topology. Generally, we write $\mathbf{F} = (\mathbf{F}_+, \mathbf{F}_-)$ to denote the elements of this set. These systems arise frequently, for instance, in the study of mechanical systems with impact or friction [6, 27, 33, 56], electronic circuits with switches [4, 5, 12, 52], biological and climate models with abrupt changes [3, 10, 34, 41, 42], economics and politics [1, 51, 53], etc. Hence, not only due to its applications, but also its mathematical beauty, the theory of Non-Smooth Dynamical System is a very active field, attracting and mobilizing scientists from all around the world.

In this endeavor, the establishment of definitions is one of the main challenges. The definition of solution for a non-smooth system, for instance, is not always clear. Nevertheless, in this context, one of the greatest contributions came from Filippov in [22], which introduced a convention to define such solutions in such a way that, apparently, is both geometrically beautiful and consistent with the physical world[1]. More specifically, for points $\mathbf{x} \in U \backslash \Sigma$, the usual local dynamics of the fields $\mathbf{F}_\pm$ is considered. On the other hand, roughly speaking, for points $\mathbf{x} \in \Sigma$ and considering the Lie derivative $\mathbf{F}_\pm h(\mathbf{x}) := \nabla h(\mathbf{x}) \cdot \mathbf{F}_\pm(\mathbf{x})$, the switching manifold Σ splits into three regions:

- **Crossing Region**: $\Sigma^{cr} = \{\mathbf{x} \in \Sigma;\ \mathbf{F}_+ h(\mathbf{x}) \mathbf{F}_- h(\mathbf{x}) > 0\}$. In this case, any trajectory which meets Σ_{cr} cross Σ through concatenation.
- **Sliding Region**: $\Sigma^{sl} = \{\mathbf{x} \in \Sigma;\ \mathbf{F}_+ h(\mathbf{x}) > 0,\ \mathbf{F}_- h(\mathbf{x}) < 0\}$. In this case, any trajectory which meets Σ_{sl} remains tangent to Σ for positive time.
- **Escaping Region**: $\Sigma^{es} = \{\mathbf{x} \in \Sigma;\ \mathbf{F}_+ h(\mathbf{x}) < 0,\ \mathbf{F}_- h(\mathbf{x}) > 0\}$. In this case, any trajectory which meets Σ_{es} remains tangent to Σ for negative time.

Due to the continuity, all regions above are open sets separated by the so-called **tangency points** $\mathbf{x} \in \Sigma$ where $\mathbf{F}_+ h(\mathbf{x}) \mathbf{F}_- h(\mathbf{x}) = 0$ which, dynamically, acts as singularities. Moreover, for points $\mathbf{x} \in \Sigma^s := \Sigma^{sl} \cup \Sigma^{es}$, the trajectory slides tangent to Σ according to a well-defined **sliding vector field** $\mathbf{F}^s : \Sigma^s \to T\Sigma^s$ given by

$$\mathbf{F}^s(\mathbf{x}) = \frac{\mathbf{F}_- h(\mathbf{x}) \mathbf{F}_+(\mathbf{x}) - \mathbf{F}_+ h(\mathbf{x}) \mathbf{F}_-(\mathbf{x})}{\mathbf{F}_- h(\mathbf{x}) - \mathbf{F}_+ h(\mathbf{x})}, \tag{3}$$

which consists of the single vector in the intersection $\mathrm{Conv}(\{\mathbf{F}_+(\mathbf{x}), \mathbf{F}_-(\mathbf{x})\}) \cap \Sigma$, where $\mathrm{Conv}(\cdot)$ represents **convex hull**.

[1] It is important to remark, however, that other conventions exist with equal beauty. Filippov's convention just happens to be the most accepted one nowadays. For instance, we cite here Carathéodory [47] and Utkin [50] conventions. See also [23] for some historical aspects.

Using the above construction, many advances have been achieved on this class of systems concerning, for instance, its bifurcations [25], regularization [40, 46, 49], structural stability [7, 24, 48] and uncountable works regarding minimal sets. However, as previously observed, the theory established by Filippov's convention has a fundamental hypothesis: a regular surface as switching manifold between the smooth parts of the system, i.e., a surface $\Sigma = h^{-1}(\{0\})$ where 0 is a regular value of h. Many relevant phenomena, however, require a model where Σ is, actually, the preimage of a singular value. Generally speaking, models where two or more abrupt changes might occur. See, for instance, the "On or Off Genes" section in [30, p. 28], where a model is presented for two genes interacting in an organic cell of a living system in order to produce proteins. At that same reference, [30, p. 30], the section "Jittery Investments" presents another interesting model for a game with two players buying or selling stocks of a company.

In this context, an important class of Non-Smooth Dynamical Systems in $\mathbb{R}^3$ with singular switching manifold, known as Gutierrez-Sotomayor and described in [26], is obtained when the regularity condition is broken in a dynamically stable manner. More precisely, in order to avoid non-trivial recurrence on non-orientable manifolds, a restriction to Σ is imposed so that its smooth parts are either orientable or diffeomorphic to an open set of $\mathbb{P}^2$ (projective plane), $\mathbb{K}^2$ (Klein's bottle) or $G^2 = \mathbb{T}^2 \# \mathbb{P}^2$ (torus with cross-cap). After a proper coordinates normalization, this restriction leads to five algebraic manifolds, with a regular configuration

$$\mathcal{R} = \left\{(x, y, z) \in \mathbb{R}^3;\ z = 0\right\}. \tag{4}$$

known as **regular discontinuity** and four singular configurations given by

$$\begin{aligned} \mathcal{D} &= \left\{(x, y, z) \in \mathbb{R}^3;\ xy = 0\right\}, \\ \mathcal{T} &= \left\{(x, y, z) \in \mathbb{R}^3;\ xyz = 0\right\}, \\ \mathcal{C} &= \left\{(x, y, z) \in \mathbb{R}^3;\ z^2 - x^2 - y^2 = 0\right\}, \\ \mathcal{W} &= \left\{(x, y, z) \in \mathbb{R}^3;\ zx^2 - y^2 = 0\right\}, \end{aligned} \tag{5}$$

and known as **double**, **triple**, **cone** and **Whitney discontinuities**, respectively. See Figure 1.

For systems whose switching manifold is homeomorphic to (4), the Filippov dynamics described above is fully applicable. In fact, these systems exactly corresponds to those described at the beginning of this text. However, for systems whose switching manifold is homeomorphic to one of the singular configurations (5), Filippov dynamics is not directly applicable to the whole manifold Σ. More precisely, the switching manifold

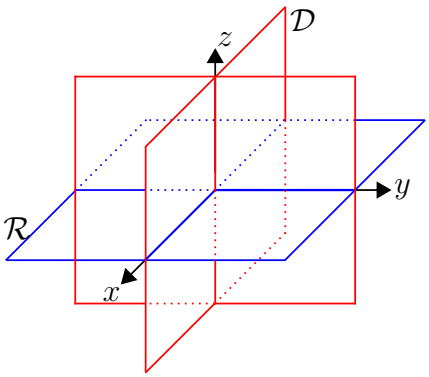

(a) $\mathcal{R}$ in blue, $\mathcal{D}$ in red and $\mathcal{T} = \mathcal{R} \cup \mathcal{D}$.

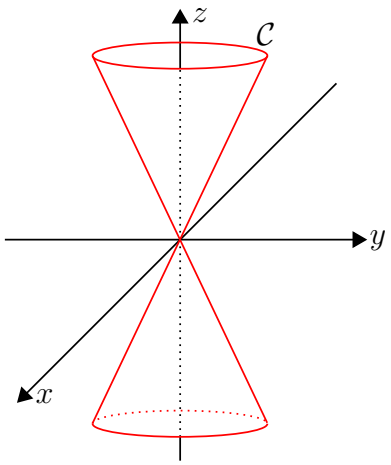

(b) $\mathcal{C}$ in red.

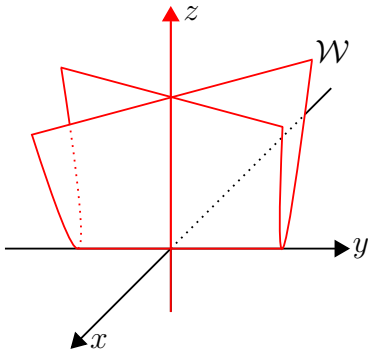

(c) $\mathcal{W}$ in red.

Figure 1 – Gutierrez-Sotomayor algebraic manifolds.

can be decomposed in the following disjoint union:

$$\Sigma = \Sigma_{\mathcal{R}} \cup \Sigma_{\mathcal{S}} \tag{6}$$

where $\Sigma_{\mathcal{R}}$ consists, locally, of regular discontinuities; and $\Sigma_{\mathcal{S}}$ consists of points where Σ self-intersects, difficulting direct application of the usual Filippov dynamics. In fact, an attempt to directly generalize the Filippov convention to points in $\Sigma_{\mathcal{S}}$, leads to the existence of up to infinite possible sliding fields, as proved at Lemma 2.4 of [28, p. 1087]. See Figure 2a.

In other words, the class of Non-Smooth Dynamical Systems $\mathbf{F} = (\mathbf{F}_i)$ whose switching manifold is homeomorphic to one of those at (5), in the sense of Gutierrez-Sotomayor, represents the simplest singular systems. However, besides its many applications, knowledge of its dynamics is scarce. In particular, over the last decade, three main frameworks arose to study these systems. Not necessarily in chronological order, these frameworks are briefly presented below.

The first one, presented in [28] by *Jeffrey*, propose an extension of the Filippov dynamics to $\Sigma_{\mathcal{S}}$ through the so-called "canopy", a convex-like ruled surface, built with the convex hull $\text{Conv}(\{\mathbf{F}_i\})$, which can be proved to intersect Σ at a finite number of points, see Figure 2b. Each one of these intersections represents a sliding vector and, therefore, this methodology leads again to non-uniqueness of the sliding field. To deal with this lack of uniqueness, the author there conjectures the so-called "dummy dynamics" acting over the canopy. This idea led to many results such as, for instance, [29, 31, 54]. However, as stated at [28, p. 1102], a justification for the dummy dynamics remains an open problem.

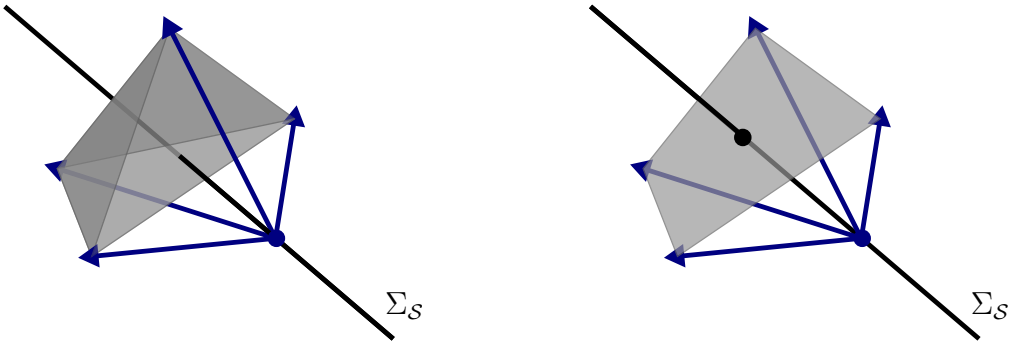

(a) Hull. (b) Canopy.

Figure 2 – Convex hull and canopy.

The next one, presented in [13] by *Dieci et al.*, although older than the previous methodology, proposes a similar construction where, again, non-uniqueness of sliding vectors happens. Here, however, the authors show that, imposing certain attractivity hypothesis on the switching manifold Σ, many conclusions can be proved on the behavior of the dynamics. In fact, this idea led to the sequence of works [14–20] where several aspects of the dynamics are explored under different types of attractivity: from minimal sets to structural stability. However, imposing conditions on Σ is a fundamental and restrictive hypothesis here.

Finally, [8] by *Buzzi et al.*, propose an extension of the Filippov dynamics to $\Sigma_{\mathcal{S}}$ through the application of a proper blow-up and use of Geometrical Singular Perturbation Theory (see [21, 49]), or GSP-Theory for short, to study the resulting slow-fast systems. Although distant from a direct generalization of Filippov's convention, this methodology is also a natural approach with advantages over the previous ones. In fact, while the non-uniqueness of the sliding field is also predicted, here it is managed naturally, as will be seen over the text. Moreover, yet in comparison with the previous ones, due to the blow-up, this methodology provides a broader view of the dynamics. Even more, no assumptions neither on Σ or the underlying vector fields $\mathbf{F}_i$ are required here. However, both [8] and the posterior works [35, 37, 40] lack a clear presentation and justification for the dynamics induced over $\Sigma_{\mathcal{S}}$. Up to our knowledge, there are no works focused on the study of this

dynamics for any class of fields $\mathbf{F}_i$ such as, for instance, linear ones. In fact, the main focus of the above cited works above lies on the verification that, after the blow-up, the resulting system contains only regular discontinuities.

Given the arguments above, for this text, we embrace and improve the blow-up based methodology to study the dynamics associated with singular switching manifolds, since it

1. does not depend on imposing conditions on Σ;
2. deals naturally with the non-uniqueness of sliding vectors; and
3. provide a broader view of the dynamics over $\Sigma_{\mathcal{S}}$.

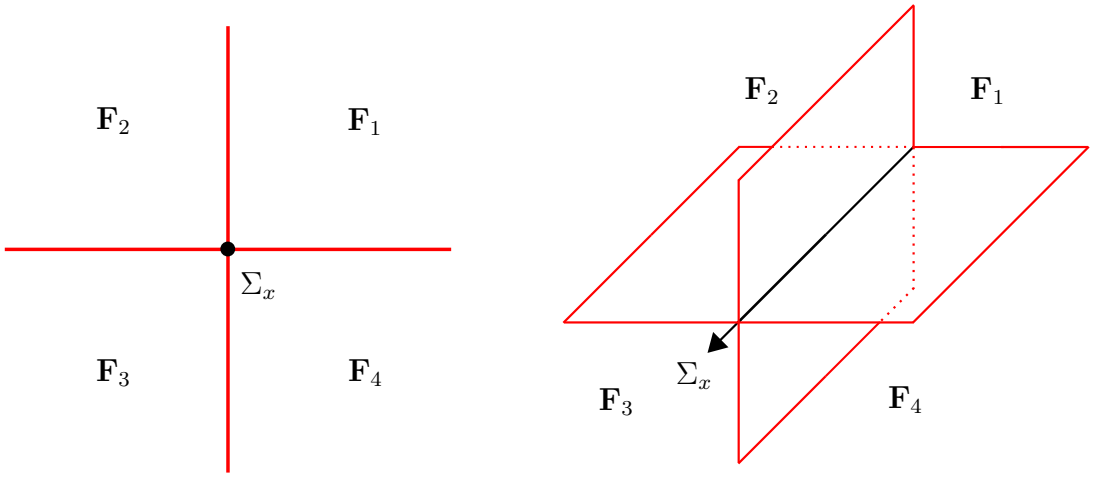

(a) $\mathcal{D}_2^k$ (b) $\mathcal{D}_3^k$

Figure 3 – Double discontinuity.

More specifically, we deal essentially with the Gutierrez-Sotomayor algebraic manifold $\mathcal{D}$, the double discontinuity, both an equivalent in $\mathbb{R}^2$ and the traditional in $\mathbb{R}^3$, whose classes of vector fields are henceforth denoted $\mathcal{D}_2^k$ and $\mathcal{D}_3^k$, respectively, see Figure 3. Geometrically, these configurations represent transversal self-intersections of the switching manifold. We focus on systems given by affine vector fields

$$\mathbf{F}_i(\mathbf{x}) = \mathbf{A}_i\mathbf{x} + \mathbf{b}_i,$$

where $\mathbf{A}_i$ and $\mathbf{b}_i$ are real matrices for every $i \in \{1, 2, 3, 4\}$ respectively of sizes $j \times j$ and $j \times 1$, with $j \in \{2, 3\}$ representing the dimension and progressively increasing its complexity: starting at the constant case ($\mathbf{A}_i = \mathbf{0}$), linear ($\mathbf{b}_i = \mathbf{0}$) and then, finally, the complete affine case. We denote these classes of constant, linear and affine vector fields, respectively,

as $\mathcal{C}_j$, $\mathcal{L}_j$ and $\mathcal{A}_j$. This program assures a progressive and effective increase on the intuition and understanding of the dynamics.

First, in $\mathbb{R}^2$, we deal with the class $\mathcal{D}_2^k$ of piecewise vector fields having a cross-like singular switching manifold which is just a slice of the Double Discontinuity, see Figure 3a. In this context, inspired by the works of *Dieci et al* in [13–20], we study the realization and structural stability of a particular configuration which we baptized as Sliding Saddle, where saddle-like attractivity conditions as imposed on Σ. Regarding its realization, we not only provide explicit conditions on the parameters for each one of the classes of vector fields $\mathcal{C}_2$, $\mathcal{L}_2$ and $\mathcal{A}_2$, but also conjecture a relation between the sliding saddles realized by $\mathcal{L}_l$ and $\mathcal{A}_2$ at Conjecture 3.1:

Conjecture 3.1. *Given* $\mathbf{F} = (\mathbf{F}_1, \cdots, \mathbf{F}_4) \in \mathcal{L}_2$*, there exists translations* $\mathbf{T}_1, \cdots, \mathbf{T}_4$ *such that* $\tilde{\mathbf{F}} = (\mathbf{T}_1 \circ \mathbf{F}_1, \cdots, \mathbf{T}_4 \circ \mathbf{F}_4) \in \mathcal{A}_2$ *realize a sliding saddle if, and only if,*

(a) $\mathbf{F}$ *realizes a sliding saddle; and*

(b) $\mathbf{T}_i$ *does not create visible singularities in* $\mathbf{F}_i$*.*

Regarding structural stability, as we will see, Sotomayor-Teixeira regularization plays a major role. In fact, we provide results establishing a relation between the structural stability of the regularization and that of the sliding field of the piecewise vector field or, in other words, a converse to the main result of [46]. More precisely, we state Theorem 3.1 below for the case $\mathcal{R}$ of regular Filippov systems and also provide Conjecture 3.2, which has a similar statement, but regarding the case $\mathcal{D}_2^k$ of planar double discontinuities.

Theorem 3.1. *Let* $\varphi : \mathbb{R} \to \mathbb{R}$ *be a monotonous transition function,* $\mathcal{N} \subset \mathcal{R}^k$ *a subset satisfying the (PH) hypothesis and* $\mathbf{F} \in \mathcal{N}$ *such that* $\mathbf{F}^\varepsilon$ *is structurally stable in* $\mathcal{N}^\varepsilon$*. Then, there exists an open neighborhood* $\mathcal{W} \subset \mathcal{N}$ *of* $\mathbf{F}$ *such that*

$$\mathbf{G} \in \mathcal{W} \qquad \Rightarrow \qquad \mathbf{G}^s \sim \mathbf{F}^s,$$

i.e., $\mathbf{F}^s$ *is structurally stable upon small perturbations of* $\mathbf{F}$ *in* $\mathcal{N}$*.*

Next, in $\mathbb{R}^3$, we deal with the class $\mathcal{D}_3^k$ of piecewise vector fields having the traditional[2] Double Discontinuity as switching manifold, see Figure 3b. Here, we tackle the main problem of defining a dynamics over $\Sigma_{\mathcal{S}}$, given by a straight line Σ_x. In particular, we use the cylindrical blow-up suggested in [37] to induce a dynamics over Σ_x, with GSP-Theory playing a major role. As a result, we obtain the **Fundamental Lemma 4.1** stated below:

[2] As presented in Figure 1a.

Lemma 4.1 (Fundamental Dynamics)**.** *Given $\mathbf{F} \in \mathcal{D}^k_3$ with components $\mathbf{F}_i = (w_i, p_i, q_i)$, let $\tilde{\mathbf{F}} \in \tilde{\mathcal{D}}^k_3$ be the vector field induced by the blow-up*

$$\phi_1(x, \theta, r) = (x, r\cos\theta, r\sin\theta).$$

Then, this blow-up associates the dynamics over Σ_x with the following dynamics over the cylinder $C = \mathbb{R} \times S^1 = S_1 \cup \ldots \cup S_4$: over each stripe S_i acts a slow-fast dynamics whose reduced dynamics is given by

$$\begin{cases} \dot{x} = w_i \\ 0 = q_i \cos\theta - p_i \sin\theta \end{cases}, \tag{4.9}$$

with slow radial dynamics $\dot{r} = p_i \cos\theta + q_i \sin\theta$; and layer dynamics given by

$$\begin{cases} x' = 0 \\ \theta' = q_i \cos\theta - p_i \sin\theta \end{cases}, \tag{4.10}$$

with fast radial dynamics $r' = 0$. Finally, at every equation above the functions w_i, p_i and q_i must be calculated at the point $\phi_1(x, \theta, 0) = (x, 0, 0)$.

We note here that no blowing-down is ever carried out over this text, i.e., once we have the blow-up induced (fundamental) dynamics above over the cylinder C, the inverse operation is never performed to recover a dynamics over Σ_x with the original coordinates. Actually, this operation would make little to no sense most of the times given the higher codimension of Σ_x, i.e., most of the information on the dynamics would be lost. For instance, under the so-called **fundamental hypothesis** (WFH) or (SFH), the fundamental lemma assures not only the sequence of qualitative theorems bellow for the general, non-linear case, but also most of the original results in this text and, hence, its name.

Theorem 4.2. *The radial dynamics can only be transversal ($\dot{r} \neq 0$) to the cylinder C over the slow manifold $\mathcal{M}_i$. More over, under (WFH), it is in fact transversal.*

Theorem 4.3. *The slow manifold $\mathcal{M}_i$ is locally a graph $(x, \theta(x))$ under (WFH). However, if $\|(f_i)_\theta\|$ admits a global positive minimum, then $\mathcal{M}_i$ is globally a graph $(x, \theta(x))$. Either way, $\theta(x)$ is of class C^k.*

Theorem 4.4. *The slow manifold $\mathcal{M}_i$ is normally hyperbolic at every point that satisfies (WFH).*

Theorem 4.5. *The hyperbolic singularities of the reduced system (4.9) acts as hyperbolic saddle or node singularities of S_i under (WFH).*

Then, using these fundamental dynamics, we focus on the constant ($\mathcal{C}_3$) and affine ($\mathcal{A}_3$) cases, to fully describe the respective induced dynamics over the cylinder as stated in Theorem 4.6 for the constant case and Theorem 4.7 below for the affine case.

Theorem 4.7 (Affine Dynamics)**.** *Given $\mathbf{F} \in \mathcal{A}_3$ with affine components $\mathbf{F}_i$ given by (4.16) and such that $\gamma_i \neq 0$, let $\tilde{\mathbf{F}} \in \tilde{\mathcal{A}}_3$ be the vector field induced by the blow-up $\phi_1(x, \theta, r) = (x, r\cos\theta, r\sin\theta)$. Then, this blow-up associates the dynamics over Σ_x with the following dynamics over the cylinder $C = \mathbb{R} \times S^1 = S_1 \cup \ldots \cup S_4$: over each stripe S_i acts a slow-fast dynamics whose slow manifold is given by $\mathcal{M}_i = A_i \cup A_i^\pi$, where A_i^π is a π-translation of A_i in θ and*

1. *case $a_{i2} \neq 0$, then*

$$A_i = \{(x,\theta) \in [-\infty, \alpha_i] \times [0, 2\pi]\,;\ \theta = \theta_i(x) + \pi\} \cup$$
$$\cup\, \{(x,\theta) \in [\alpha_i, +\infty] \times [0, 2\pi]\,;\ \theta = \theta_i(x)\}$$

   with $\theta_i(x) = \arctan\left(\dfrac{a_{i3}x + d_{i3}}{a_{i2}x + d_{i2}}\right)$, which consists in an arctangent-like curve inside the cylinder C with $\theta = \beta_i + \pi$ and $\theta = \beta_i$ as negative and positive horizontal asymptotes, respectively;

2. *case $a_{i2} = 0$, then*

$$A_i = \{(x,\theta) \in \mathbb{R} \times [0, 2\pi]\,;\ \theta = \theta_i(x)\}$$

   with $\theta_i(x) = \arctan\left(\dfrac{a_{i3}x + d_{i3}}{d_{i2}}\right)$, which consists in an arctangent-like curve inside the cylinder C with $\theta = \sigma_{i-}$ and $\theta = \sigma_{i+}$ as negative and positive horizontal asymptotes, respectively.

Both arctangents are increasing if $\gamma_i > 0$ and decreasing if $\gamma_i < 0$. Over them act the reduced dynamics $\dot{x} = a_{i1}x + d_{i1}$ and, around them, acts the layer dynamics described in Table 3, but exchanging a_{i2} with d_{i2} if $a_{i2} = 0$. Finally, the new parameters above are given by $\alpha_i = -\dfrac{d_{i2}}{a_{i2}}$, $\beta_i = \arctan\left(\dfrac{a_{i3}}{a_{i2}}\right)$, $\gamma_i = a_{i3}d_{i2} - d_{i3}a_{i2}$, $\delta_i = -\dfrac{d_{i1}}{a_{i1}}$ and $\sigma_{i\pm} = \pm\,\mathrm{sgn}\,(\gamma_i)\dfrac{\pi}{2}$.

Finally, combining this fine-grained control of the dynamics with the structural stability characterization provided by [7], we also derive Peixoto-like theorems characterizing semi-local structural stability of the dynamics over the cylinder for both the constant (Theorem 4.8) and affine (Theorem 4.9 as stated below) cases.

Theorem 4.9 (Affine Dynamics Stability)**.** *Let* $\mathbf{F} \in \mathcal{A}_3$ *be given by (4.22) with* $\gamma_i \neq 0$*. Given* $\Sigma_{\theta_0} \in \tilde{\mathcal{I}}_C$*, let* $\mathbf{X} = (\mathbf{X}_-, \mathbf{X}_+)$ *be the Filippov system induced around* Σ_{θ_0} *and inside a convex compact set* $K \subset C_+ \cup C_-$*, where* C_+ *and* C_- *are two consecutive stripes meeting at* Σ_{θ_0}*. Then,* $\mathbf{F}$ *is* (Σ_{θ_0}, K)*-semi-local structurally stable in* $\mathcal{A}_3$ *if, and only if,* $\mathbf{X}_+$ *and* $\mathbf{X}_-$ *satisfies*

1. $a_{i1} \neq 0$ *and* $\mathbf{P} \notin \Sigma_{\theta_0}$*, where* $\mathbf{P}$ *is the only singularity of* $\mathbf{X}_\pm$*;*
2. *conditions (C.6) — (C.9) of Proposition 4.2.*

For clarification on the technicalities involved, especially in the statement above, we encourage the interested reader to please consult the respective chapter in the text, which is structured as follows:

Chapter 1. To establish notations and terminologies, we formally introduce the Theory of Non-Smooth Dynamical Systems. In particular, we formally introduce the Filippov systems.

Chapter 2. First, we introduce the regularization process developed by Sotomayor and Teixeira. Next, we show how this process connects with Filippov dynamics through GSP-Theory.

Chapter 3. Here, we formally introduce the concept of Sliding Saddle and obtain sets of conditions to realize it with affine vector fields. Finally, we study its regularization and structural stability.

Chapter 4. In this chapter, we formally introduce the concept of Double Discontinuity. Next, we use a proper blow-up and GSP-Theory to induce dynamics over the singular parts. Finally, we study its semi-local structural stability.

Chapter 5. We provide interesting further directions of investigation for the topics here discussed.

1 Non-Smooth Systems

In this chapter, we have as a goal to establish notations and terminologies, as well as to introduce the main protagonist of this text: the Filippov Systems. In the first section, we introduce the piecewise vector fields, whose dynamics we are willing to study. In the second section, we present the differential inclusions, which is the fundamental tool used to define the dynamics given by such vector fields, and finally, we define the Filippov systems in the last section.

1.1 Piecewise Vector Fields

Definition 1.1. *Let $U \subset \mathbb{R}^n$ be an open set, $\mathbf{F}_{\pm} : U \to \mathbb{R}^n$ vector fields of class C^k with $k \geqslant 1$ and $h : U \to \mathbb{R}$ a function of class C^1 which has 0 as a regular value. We say that $\mathbf{F} : U \to \mathbb{R}^n$ given by*

$$\mathbf{F}(\mathbf{x}) = \begin{cases} \mathbf{F}_+(\mathbf{x}), & \text{if } h(\mathbf{x}) \geqslant 0, \\ \mathbf{F}_-(\mathbf{x}), & \text{if } h(\mathbf{x}) \leqslant 0, \end{cases} \tag{1.1}$$

*is a **piecewise (or discontinuous) vector field**.*

As 0 is a regular value of h, then $\Sigma = h^{-1}(0)$ is a codimension 1 regular submanifold. Hence, $U \backslash \Sigma$ consists of two regions $\Sigma_+ = h^{-1}(0, +\infty)$ and $\Sigma_- = h^{-1}(-\infty, 0)$, where acts $\mathbf{F}_+$ and $\mathbf{F}_-$, respectively. We say that Σ is the **switching manifold** of the vector field $\mathbf{F}$. See Figure 4.

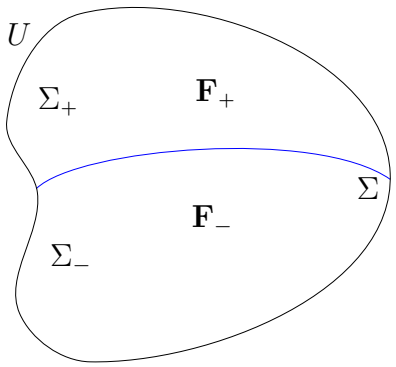

Figure 4 – Piecewise vector field.

The set of all vector fields $\mathbf{F}$ defined as above will be denoted

$$\mathcal{R}^k(U) \equiv C^k(U, \mathbb{R}^n) \times C^k(U, \mathbb{R}^n)$$

and equipped with the usual Whitney product topology. Generally, we write $\mathbf{F} = (\mathbf{F}_+, \mathbf{F}_-)$ to denote the elements of this set.

We would like to define a possible dynamics for piecewise (or discontinuous) differential equations given by

$$\dot{\mathbf{x}} = \mathbf{F}(\mathbf{x}), \tag{1.2}$$

where $\mathbf{F} \in \mathcal{R}^k(U)$ and $\dot{\mathbf{x}} = \frac{d\mathbf{x}}{dt}$; we would then say that (1.2) gives birth to a **piecewise (or discontinuous, or non-smooth) dynamical system**. Observe that there is an obstacle associated to the definition of such dynamics. In fact, given a point $\mathbf{p} \in \Sigma$, if $\mathbf{F}_+(\mathbf{p})$ and $\mathbf{F}_-(\mathbf{p})$ are vectors pointing to the same side of Σ, then it is reasonable to say that the local trajectory of $\mathbf{p}$ consists in the concatenation of the trajectories of $\mathbf{F}_+$ and $\mathbf{F}_-$ through $\mathbf{p}$. However, if $\mathbf{F}_+(\mathbf{p})$ and $\mathbf{F}_-(\mathbf{p})$ are vectors pointing to opposite sides of Σ, then there is no obvious definition for the local trajectory of $\mathbf{p}$. In the next sections, we will present the solution to this problem as proposed in [22]. We start by introducing the concept of differential inclusion.

1.2 Differential Inclusions

Differential inclusions are a generalization of the concept of ordinary differential equations. In order to define and study them, we need to understand first the concept of multivalued vector fields and their continuity. See [45] for details.

Definition 1.2. *Given $U \subset \mathbb{R}^n$ an open set, we say that $\mathcal{F} : U \to P(\mathbb{R}^n)$, where $P(\mathbb{R}^n)$ is the powerset of $\mathbb{R}^n$, is a* ***multivalued vector field****.*

In other words, multivalued fields are "fields" whose image of each point in its domain is not necessarily a single point in the codomain. The continuity of these vector fields is presented in the definition below.

Definition 1.3. *Let $\mathcal{F} : U \to P(\mathbb{R}^n)$ be a multivalued vector field and $\mathbf{p} \in U$. Then, we say that $\mathcal{F}$ is*

(a) ***upper semi-continuous*** *at $\mathbf{p}$ if, for every open neighborhood $B \subset \mathbb{R}^n$ of $\mathcal{F}(\mathbf{p})$, there exists an open neighborhood $A \subset U$ of $\mathbf{p}$ such that $\mathcal{F}(A) \subset B$;*

(b) ***lower semi-continuous*** *at $\mathbf{p}$ if, for every open set $B \subset \mathbb{R}^n$ such that $B \cap \mathcal{F}(\mathbf{p}) \neq \varnothing$, there exists an open neighborhood $A \subset U$ of $\mathbf{p}$ such that $\mathcal{F}(\mathbf{x}) \cap B \neq \varnothing$ for every $\mathbf{x} \in A$;*

(c) ***continuous*** *at $\mathbf{p}$ if it is upper and lower semi-continuous at $\mathbf{p}$.*

Now we can define the concept of a differential inclusion which, as previously said, is nothing more than a generalization of the concept of ordinary differential equations. More specifically:

Definition 1.4. *Let $\mathcal{F} : U \to P(\mathbb{R}^n)$ be a multivalued vector field. We say that the expression*

$$\dot{\mathbf{x}} \in \mathcal{F}(\mathbf{x}) \tag{1.3}$$

*is an **ordinary differential inclusion**.*

In order to motivate the definition of solution for a differential inclusion, remember that, if $\mathbf{F} : U \to \mathbb{R}^n$ is a usual vector field, then a solution of the ordinary Initial Value Problem

$$\begin{cases} \dot{\mathbf{x}} = \mathbf{F}(\mathbf{x}) \\ \mathbf{x}(0) = \mathbf{p} \end{cases}$$

is a differentiable curve $\varphi : [-T, T] \to U$ such that

$$\dot{\varphi}(t) = \mathbf{F}(\varphi(t)) \qquad \text{e} \qquad \varphi(0) = \mathbf{p}$$

or, equivalently,

$$\varphi(t) = \mathbf{p} + \int_0^t \mathbf{F}(\varphi(s))ds \qquad \Leftrightarrow \qquad \varphi(t) = \mathbf{p} + \int_0^t \dot{\varphi}(s)ds.$$

Definition 1.5. *We say that the curve $\varphi : [-T, T] \to U$ is **absolutely continuous** if there exists $\mathbf{p} \in U$ and an integrable function $g : [-T, T] \to \mathbb{R}^n$ such that*

$$\varphi(t) = \mathbf{p} + \int_0^t g(s)ds$$

or, equivalently,

$$\varphi(t) = \mathbf{p} + \int_0^t \dot{\varphi}(s)ds$$

since, in this case, φ is differentiable almost everywhere and, therefore, $\dot{\varphi}(s) = g(s)$ almost everywhere.

The set of all absolutely continuous curves $\varphi : [-T, T] \to U$ defined as above will be denoted by

$$\mathrm{AC}([-T,T],U) \equiv \mathbb{R}^n \times L_1([-T,T],U)$$

and equipped with the norm

$$\|\varphi\| = \|\varphi(0)\| + \int_0^T \|\dot{\varphi}(s)\| ds$$

which transforms it in a Banach space.

Definition 1.6. *Let $\mathcal{F} : U \to P(\mathbb{R}^n)$ be a multivalued vector field. We say that $\varphi \in AC([-T,T],U)$ is a* ***solution of the differential inclusion***

$$\dot{\mathbf{x}} \in \mathcal{F}(\mathbf{x})$$

if

$$\dot{\varphi}(t) \in \mathcal{F}(\varphi(t))$$

for almost every $t \in [-T,T]$.

The set of all solutions of the differential inclusion $\dot{\mathbf{x}} \in \mathcal{F}(\mathbf{x})$ such that $\varphi(0) = \mathbf{p} \in U$ will be denoted by

$$S_{\mathcal{F}}(\mathbf{p}) = \{\varphi \in \mathrm{AC}([-T,T],U);\ \dot{\varphi}(t) \in \mathcal{F}(\varphi(t)) \quad e \quad \varphi(0) = \mathbf{p}\}\,.$$

Observe that, generally, due to the multivalued nature of the definition of differential inclusion, we cannot expect uniqueness of solutions through a given point $\mathbf{p} \in U$. In particular, the maps $\mathbf{x} \mapsto S_{\mathcal{F}}(\mathbf{x})$ and $(\mathbf{x},t) \mapsto S_{\mathcal{F}}(\mathbf{x})(t) = \{\varphi(t);\ \varphi \in S_{\mathcal{F}}(\mathbf{x})\}$ are multivalued. However, as to the existence of solutions we have the following:

Theorem 1.1 (retrieved from [45], page 98)**.** *Let $U \subset \mathbb{R}^n$ be an open set and $\mathcal{F} : U \to \mathbb{R}^n$ be a multivalued vector field. Suppose that $\mathcal{F}$ is upper semi-continuous and, for every $\mathbf{x} \in U$, $\mathcal{F}(\mathbf{x})$ is convex. Then,*

(a) $S_{\mathcal{F}}(\mathbf{p}) \neq \varnothing$,

(b) $S_{\mathcal{F}}(\mathbf{p}) \subset AC([-T,T],U)$ and $S_{\mathcal{F}}(\mathbf{p})(t) \subset \mathbb{R}^n$ are connected sets,

for every $\mathbf{p} \in U$.

As for the dependency of solutions relative to initial conditions we have the following:

Theorem 1.2 (retrieved from [45], page 109)**.** *Let $U \subset \mathbb{R}^n$ be an open set and $\mathcal{F} : U \to \mathbb{R}^n$ be a multivalued vector field. Suppose that $\mathcal{F}$ is upper semi-continuos and, for every $\mathbf{x} \in U$, $\mathcal{F}(\mathbf{x})$ is convex and compact. Then, $\mathbf{x} \mapsto S_{\mathcal{F}}(\mathbf{x})$ and $(\mathbf{x}, t) \mapsto S_{\mathcal{F}}(\mathbf{x})(t)$ are upper semi-continuous.*

1.3 Filippov Systems

Let $U \subset \mathbb{R}^n$ be an open bounded set and $\mathbf{F} = (\mathbf{F}_+, \mathbf{F}_-) \in \mathcal{R}^k(U)$ be a piecewise vector field. In order to define a dynamics for the non-smooth differential equation

$$\dot{\mathbf{x}} = \mathbf{F}(\mathbf{x}), \tag{1.4}$$

with switching manifold $\Sigma = h^{-1}(0)$, consider the multivalued vector field given by

$$\mathcal{Z}_{\mathbf{F}}(\mathbf{x}) = \begin{cases} \{\mathbf{F}_+(\mathbf{x})\}, & \text{if } h(\mathbf{x}) > 0, \\ \{\mathbf{F}_-(\mathbf{x})\}, & \text{if } h(\mathbf{x}) < 0, \\ \text{Conv}(\{\mathbf{F}_+(\mathbf{x}), \mathbf{F}_-(\mathbf{x})\}), & \text{if } h(\mathbf{x}) = 0, \end{cases} \tag{1.5}$$

where

$$\text{Conv}(\{\mathbf{F}_+(\mathbf{x}), \mathbf{F}_-(\mathbf{x})\}) = \left\{ \frac{1+\lambda}{2}\mathbf{F}_+(\mathbf{x}) + \frac{1-\lambda}{2}\mathbf{F}_-(\mathbf{x});\ -1 \leqslant \lambda \leqslant 1 \right\}$$

is the **convex hull** of the set $\{\mathbf{F}_+(\mathbf{x}), \mathbf{F}_-(\mathbf{x})\}$. See Figure 5, where the convex hull is represented in gray.

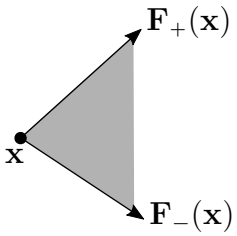

Figure 5 – Convex hull of the set $\{\mathbf{F}_+(\mathbf{x}), \mathbf{F}_-(\mathbf{x})\}$.

For every $\mathbf{x} \in U$, we have that $\mathcal{Z}_{\mathbf{F}}(\mathbf{x})$ is a convex and compact set. Even more, due to Proposition 2.2 of [45] we also have that $\mathcal{Z}_{\mathbf{F}}$ is upper semi-continuous. Hence, the

conclusions of Theorem 1.1 and Theorem 1.2 are true for this multivalued field. In other words, the differential inclusion

$$\dot{\mathbf{x}} \in \mathcal{Z}_{\mathbf{F}}(\mathbf{x}) \tag{1.6}$$

admits solutions which are upper semi-continuous with respect to initial conditions. Therefore, in [22], Aleksei Fedorovich Filippov introduced the following convention[1] to define the solutions of the non-smooth differential equation (1.4):

Definition 1.7. *(Filippov's Convention) We say that φ is a solution of the non-smooth differential equation (1.4) if φ is a solution of the differential inclusion (1.6). We say that (1.4) with this dynamics is a* ***Filippov system****.*

Now that we have a dynamics associated to the differential equation (1.4), we would like to describe its local trajectories. For that, observe initially that, from (1.5) follow that the local trajectory of points $\mathbf{p} \notin \Sigma$ is given by the usual smooth dynamics of the vector fields $\mathbf{F}_+$ or $\mathbf{F}_-$. On the other hand, in order to describe the local trajectory of points $\mathbf{p} \in \Sigma$, the following operation will be useful:

Definition 1.8. *Let $U \subset \mathbb{R}^n$ be an open set, $\mathbf{F} : U \to \mathbb{R}^n$ a vector field of class C^k and $h : U \to \mathbb{R}$ a function of class C^1. We say that $\mathbf{F}h : U \to \mathbb{R}$ given by*

$$\mathbf{F}h(\mathbf{p}) = \nabla h(\mathbf{p}) \cdot \mathbf{F}(\mathbf{p})$$

is the ***Lie derivative*** *of h relative to the field $\mathbf{F}$ at the point $\mathbf{p}$, where $\cdot$ is the usual inner product of $\mathbb{R}^n$. Generally, we write*

$$\mathbf{F}^n h(\mathbf{p}) = \nabla(\mathbf{F}h)^{n-1}(\mathbf{p}) \cdot \mathbf{F}(\mathbf{p}),$$

to denote the n-th Lie derivative.

Geometrically, the Lie derivative tells us which side of Σ the field $\mathbf{F}$ points to. In fact, as 0 is a regular value of h, then $\Sigma = h^{-1}(0)$ is an orientable surface. Therefore, we have the following cases:

(a) If $\mathbf{F}h(\mathbf{p}) > 0$, then $\mathbf{F}(\mathbf{p})$ and $\nabla h(\mathbf{p})$ points to the same side of $T_{\mathbf{p}}\Sigma$.

(b) If $\mathbf{F}h(\mathbf{p}) < 0$, then $\mathbf{F}(\mathbf{p})$ and $\nabla h(\mathbf{p})$ points to opposite sides of $T_{\mathbf{p}}\Sigma$.

(c) If $\mathbf{F}h(\mathbf{p}) = 0$, then $\mathbf{F}(\mathbf{p}) \in T_{\mathbf{p}}\Sigma$.

[1] As remarked at the Introduction, other conventions exist with equal beauty and importance, for instance, Carathéodory [47] and Utkin [50] conventions. Naturally, under these other conventions, many of the dynamical aspects described on this section would be different.

1.3.1 Crossing Region

Definition 1.9. *We say that the open subset Σ^c of the switching manifold Σ given by*

$$\Sigma^c = \{\mathbf{p} \in \Sigma;\ \mathbf{F}_+h(\mathbf{p})\mathbf{F}_-h(\mathbf{p}) > 0\}\,,$$

*is the **crossing region** and every $\mathbf{p} \in \Sigma^c$ is a **crossing point**.*

In this case, due to the geometrical interpretation of the Lie derivative given above, we have that the fields $\mathbf{F}_+$ and $\mathbf{F}_-$ both points to the same side of Σ. In particular, it can be proved that there will be no intersection between $\mathrm{Conv}(\{\mathbf{F}_+(\mathbf{p}), \mathbf{F}_-(\mathbf{p})\})$ and $T_{\mathbf{p}}\Sigma$, as represented at Figure 6. More precisely:

Proposition 1.1. *If $\mathbf{p} \in \Sigma^c$, then $\mathcal{Z}_{\mathbf{F}}(\mathbf{p}) \cap T_{\mathbf{p}}\Sigma = \varnothing$.*

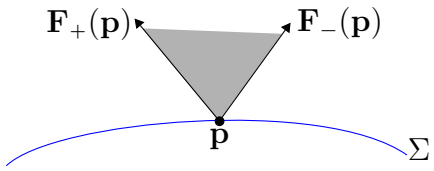

Figure 6 – Vector fields at a crossing point.

Therefore, given $\mathbf{p} \in \Sigma^c$, if $\varphi_\pm(t, \mathbf{p})$ are the respective solutions for the Initial Value Problems

$$\begin{cases} \dot{\mathbf{x}} = \mathbf{F}_\pm(\mathbf{x}) \\ \mathbf{x}(0) = \mathbf{p} \end{cases}$$

then this curves behaves locally as represented at Figure 7.

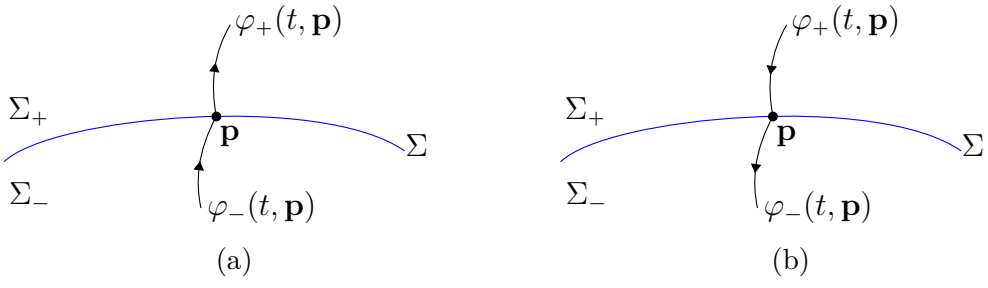

Figure 7 – All local trajectories through a crossing point.

For both cases, let $\varphi(t, \mathbf{p})$ be a local concatenation of the curves $\varphi_\pm(t, \mathbf{p})$. More precisely, for the case Figure 7a, define

$$\varphi(t, \mathbf{p}) = \begin{cases} \varphi_-(t, \mathbf{p}), & t \in [-T, 0], \\ \varphi_+(t, \mathbf{p}), & t \in [0, T], \end{cases}$$

and, for the case Figure 7b, define

$$\varphi(t, \mathbf{p}) = \begin{cases} \varphi_+(t, \mathbf{p}), & t \in [-T, 0], \\ \varphi_-(t, \mathbf{p}), & t \in [0, T], \end{cases}$$

where $T > 0$ is sufficiently small.

Proposition 1.2. *Given $\mathbf{p} \in \Sigma^c$, the curve $\varphi(t, \mathbf{p})$ defined as above is the only local trajectory of (1.4) through $\mathbf{p}$.*

1.3.2 Sliding Region

Definition 1.10. *We say that the open subset Σ^s of the switching manifold Σ given by*

$$\Sigma^s = \{\mathbf{p} \in \Sigma;\ \mathbf{F}_+h(\mathbf{p})\mathbf{F}_-h(\mathbf{p}) < 0\}$$

*is the **sliding region** and every $\mathbf{p} \in \Sigma^s$ is a **sliding point**.*

In this case, due to the geometrical interpretation of the Lie derivative given above, we have that the fields $\mathbf{F}_+$ and $\mathbf{F}_-$ points to opposite sides of Σ. In particular, it can be proved that there is intersection between $\text{Conv}(\{\mathbf{F}_+(\mathbf{p}), \mathbf{F}_-(\mathbf{p})\})$ and $T_\mathbf{p}\Sigma$, as represented at Figure 8. More precisely:

Proposition 1.3. *If $\mathbf{p} \in \Sigma^s$, then $\mathcal{Z}_\mathbf{F}(\mathbf{p}) \cap T_\mathbf{p}\Sigma = \{\mathbf{F}^s(\mathbf{p})\}$, where*

$$\mathbf{F}^s(\mathbf{p}) = \frac{\mathbf{F}_-h(\mathbf{p})\mathbf{F}_+(\mathbf{p}) - \mathbf{F}_+h(\mathbf{p})\mathbf{F}_-(\mathbf{p})}{\mathbf{F}_-h(\mathbf{p}) - \mathbf{F}_+h(\mathbf{p})}. \tag{1.7}$$

Even more,

$$\begin{aligned} \mathbf{F}^s : \Sigma^s &\to T\Sigma^s \\ \mathbf{p} &\mapsto \mathbf{F}^s(\mathbf{p}) \end{aligned}$$

is a well-defined vector field over Σ^s.

We say that $\mathbf{F}^s$ is the **sliding field** of (1.4). Its trajectories give birth to local trajectories of (1.4). More precisely:

Proposition 1.4. *Given $\mathbf{p} \in \Sigma^s$, if $\varphi^s(t, \mathbf{p})$ is a solution for the Initial Value Problem*

$$\begin{cases} \dot{\mathbf{x}} = \mathbf{F^s}(\mathbf{x}) \\ \mathbf{x}(0) = \mathbf{p} \end{cases},$$

then $\varphi^s(t, \mathbf{p})$ *is a local trajectory of (1.4) through* $\mathbf{p}$.

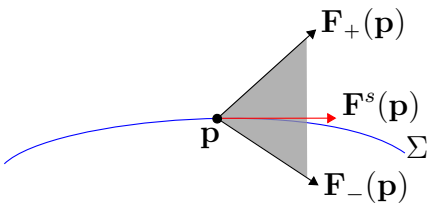

Figure 8 – Vector fields at a sliding point.

Beyond that, given $\mathbf{p} \in \Sigma^c$, if $\varphi_\pm(t, \mathbf{p})$ are the respective solutions for the Initial Value Problems

$$\begin{cases} \dot{\mathbf{x}} = \mathbf{F}_\pm(\mathbf{x}) \\ \mathbf{x}(0) = \mathbf{p} \end{cases}$$

then these curves behave locally as represented at Figure 9, where a possible curve $\varphi^s(t, \mathbf{p})$ was also represented for illustrative purposes only.

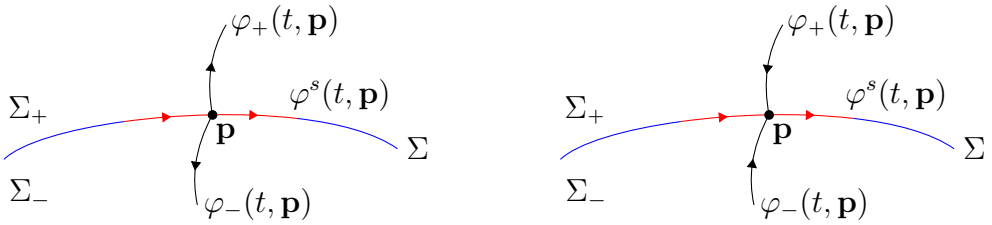

Figure 9 – Some local trajectories through a sliding point.

For both cases[2], again, concatenation gives birth to local trajectories of (1.4). More precisely, in the case of Figure 9a, define

$$\psi^\pm(t, \mathbf{p}) = \begin{cases} \varphi^s(t, \mathbf{p}), & t \in [-T, 0], \\ \varphi_\pm(t, \mathbf{p}), & t \in [0, T], \end{cases}$$

and, in the case of Figure 9b, define

$$\psi^\pm(t, \mathbf{p}) = \begin{cases} \varphi_\pm(t, \mathbf{p}), & t \in [-T, 0], \\ \varphi^s(t, \mathbf{p}), & t \in [0, T], \end{cases}$$

where $T > 0$ is sufficiently small.

[2] The cases presented at Figure 9 are called **escaping** and **sliding**, respectively. In this text, we will often commit the language abuse of calling both cases as sliding.

Proposition 1.5. *Given* $\mathbf{p} \in \Sigma^s$*, the curves* $\psi^{\pm}(t, \mathbf{p})$ *defined as above are local trajectories of (1.4) through* $\mathbf{p}$*.*

Recall that from Theorem 1.1 it follows that the set of solutions $S_{\mathcal{Z}_\mathbf{F}}(\mathbf{p})$ is connected. However, up until now, we constructed only three points of this set. In order to connect these points, making the set connected, in the case of Figure 9a, define

$$\Gamma^{\pm}_{\varepsilon}(t, \mathbf{p}) = \begin{cases} \varphi^s(t, \mathbf{p}), & t \in [-T, \varepsilon], \\ \varphi_{\pm}(t - \varepsilon, \varphi^s(\varepsilon, \mathbf{p})), & t \in [\varepsilon, T], \end{cases}$$

and, in the case of Figure 9b, define

$$\Gamma^{\pm}_{\varepsilon}(t, \mathbf{p}) = \begin{cases} \varphi_{\pm}(t + \varepsilon, \varphi^s(-\varepsilon, \mathbf{p})), & t \in [-T, -\varepsilon], \\ \varphi^s(t, \mathbf{p}), & t \in [-\varepsilon, T], \end{cases}$$

where $T > 0$ is sufficiently small and $0 \leqslant \varepsilon \leqslant T$. Observe that $\Gamma^{\pm}_0 = \psi^{\pm}$ and $\Gamma^{\pm}_T = \varphi^s$. In Figure 10 we represent in gray the region covered by the solutions $\Gamma^{\pm}_{\varepsilon}$ with $0 < \varepsilon < T$.

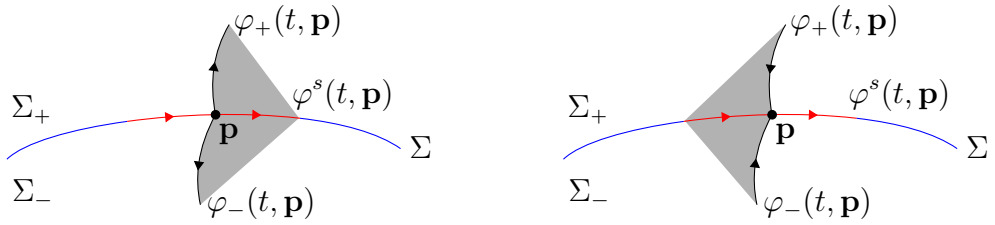

Figure 10 – All local trajectories through a sliding point.

Proposition 1.6. *Given* $\mathbf{p} \in \Sigma^s$*, the curves* $\Gamma^{\pm}_{\varepsilon}(t, \mathbf{p})$ *defined as above are the only local trajectories of (1.4) through* $\mathbf{p}$*.*

1.3.3 Singularities

A careful reading of the text so far reveals the existence of three types of points associated with Filippov systems which deserve to be called singularities. In fact, outside the switching manifold Σ we have the usual singularities of the vector fields $\mathbf{F}_{\pm}$. Over the manifold Σ we have the singularities of the sliding field $\mathbf{F}^s$ and, finally, we also have the tangencies, i.e., points where $\mathbf{F}_{\pm}h(\mathbf{p}) = 0$. In what follows, we formally define these singularities.

We start with the singularities of the vector fields $\mathbf{F}_{\pm}$ which lie outside the manifold Σ. Observe that these singularities may or may not be inside the respective acting region of the field, i.e., $\Sigma^{\pm}$. More precisely:

Definition 1.11. *We say that* $\mathbf{p} \in \Sigma^{\pm}$ *with* $\mathbf{F}_{\pm}(\mathbf{p}) = 0$ *is a* ***visible usual singularity*** *of (1.4). We say that* $\mathbf{p} \in \Sigma^{\mp}$ *with* $\mathbf{F}_{\pm}(\mathbf{p}) = 0$ *is an* ***invisible usual singularity*** *of (1.4).*

The usual singularities behave locally as expected, i.e., as the well-known and established results for smooth dynamics dictate. In particular, we remark that these singularities are stationary trajectories reached in infinite time.

Furthermore, over the sliding region Σ^s of the switching manifold, we have the singularities of the sliding field $\mathbf{F}^s$. More precisely:

Definition 1.12. *We say that* $\mathbf{p} \in \Sigma^s$ *with* $\mathbf{F}^s(\mathbf{p}) = 0$ *is a* ***pseudo-equilibrium*** *of (1.4).*

Just like in the previous case, over the sliding region, the pseudo-equilibriums behave as expected, i.e., as the well known and established results for smooth dynamics dictate. However, over $U \backslash \Sigma$, due to Proposition 1.6, we remark that these singularities can have a stationary component reached in finite time.

Finally, still over the switching manifold, we have the tangencies of the fields $\mathbf{F}_{\pm}$ with Σ. More precisely:

Definition 1.13. *Let* $n \geqslant 2$ *be a natural number. We say that* $\mathbf{p} \in \Sigma$ *such that*

$$\mathbf{F}_{\pm}h(\mathbf{p}) = (\mathbf{F}_{\pm})^2 h(\mathbf{p}) = \cdots = (\mathbf{F}_{\pm})^{n-1} h(\mathbf{p}) = 0 \qquad \textit{and} \qquad (\mathbf{F}_{\pm})^n h(\mathbf{p}) \neq 0$$

is a ***tangency of order*** *n of (1.4). In particular, if* $n = 2$*, then we say that* $\mathbf{p}$ *is a* ***fold*** *point; if* $n = 3$*, then we say that* $\mathbf{p}$ *is a* ***cusp*** *point.*

We say that

$$S_{\mathbf{F}_{\pm}} = \{\mathbf{p} \in \Sigma : \ \mathbf{F}_{\pm}h(\mathbf{p}) = 0\}$$

are the **tangency sets** of the vector fields $\mathbf{F}_{\pm}$. The tangencies, especially the folds, are some of the most interesting singularities of Filippov systems. For instance, folds can give birth to a phenomenon known as T-singularity[3], which exhibits nondeterministic chaos [11].

Geometrically, the fold points are those where quadratic tangencies of the fields $\mathbf{F}_{\pm}$ with the manifold Σ occur. These tangencies are classified as **visible** or **invisible**, see Figure 11, and can be distinguished as presented in the proposition below.

[3] So named in honor to its discoverer, Marco Antonio Teixeira, in [48].

Proposition 1.7. *Let* $\mathbf{p} \in \Sigma$. *Supposing that* $\mathbf{F}_+h(\mathbf{p}) = 0$, *then* $\mathbf{p}$ *is a fold point*

(a) visible if $(\mathbf{F}_+)^2h(\mathbf{p}) > 0$;

(b) invisible if $(\mathbf{F}_+)^2h(\mathbf{p}) < 0$.

Supposing that $\mathbf{F}_-h(\mathbf{p}) = 0$, *then* $\mathbf{p}$ *is a fold point*

(c) visible if $(\mathbf{F}_-)^2h(\mathbf{p}) < 0$;

(d) invisible if $(\mathbf{F}_-)^2h(\mathbf{p}) > 0$.

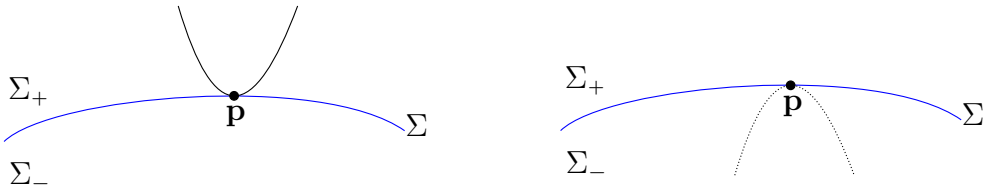

(a) Visible fold. (b) Invisible fold.

Figure 11 – Fold points of the vector field $\mathbf{F}_+$.

1.3.4 Structural Stability

The study of structural stability of certain Filippov systems is one of the goals of this text. Therefore, we recall here the classical definition (given in [48]) for this concept. First, we define the concept of local topological equivalence between Filippov systems:

Definition 1.14. *Let* $\mathbf{F}, \tilde{\mathbf{F}} \in \mathcal{R}^k(U)$ *and* $\mathbf{p} \in U$. *We say that* $\mathbf{F}$ *and* $\tilde{\mathbf{F}}$ *are* ***topologically equivalent*** *at* $\mathbf{p}$ *if there exists neighborhoods* V *and* $\tilde{V}$ *of* $\mathbf{p}$ *in* $\mathbb{R}^n$ *and a homeomorphism* $\phi : V \to \tilde{V}$ *which keeps* Σ *invariant and takes trajectories of* $\mathbf{F}$ *into trajectories of* $\tilde{\mathbf{F}}$ *preserving time orientation.*

Now, we can define the concept of local structural stability between Filippov systems naturally:

Definition 1.15. *We say that* $\mathbf{F} \in \mathcal{R}^k(U)$ *is* ***structurally stable*** *at* $\mathbf{p} \in U$ *if there exists an open neighborhood* W *of* $\mathbf{F}$ *in* $\mathcal{R}^k(U)$ *such that, if* $\tilde{\mathbf{F}} \in W$, *then* $\tilde{\mathbf{F}}$ *and* $\mathbf{F}$ *are topologically equivalent at* $\mathbf{p}$.

The concept of global structural stability can be naturally obtained from the following definition of global topological equivalence:

Definition 1.16. *Let* $\mathbf{F}, \tilde{\mathbf{F}} \in \mathcal{R}^k(U)$*. We say that* $\mathbf{F}$ *and* $\tilde{\mathbf{F}}$ *are* ***topologically equivalent*** *and denote* $\mathbf{F} \sim \tilde{\mathbf{F}}$ *if there exists a homeomorphism* $\phi : U \to U$ *that keeps* Σ *invariant and takes orbits of* $\mathbf{F}$ *into orbits of* $\tilde{\mathbf{F}}$ *preserving time orientation.*

2 Regularization

In this chapter, we have as a goal to introduce the concept of regularization developed by Jorge Sotomayor and Marco Antonio Teixeira in [46]. In the first section, given a piecewise vector field, we construct its regularization, which consists of a 1-parameter family of smooth vector fields which converges to the given piecewise field. Next, in the second section, we introduce part of the Geometric Singular Perturbation Theory developed by Neil Fenichel in [21] and its connection with Filippov dynamics through regularization.

2.1 Sotomayor-Teixeira

Let $\mathbf{F} = (\mathbf{F}_+, \mathbf{F}_-) \in \mathcal{R}^k(U)$ be a piecewise smooth vector field as defined above with a switching manifold $\Sigma = h^{-1}(0)$. A Sotomayor-Teixeira regularization of $\mathbf{F}$, as described at [46], is a 1-parameter family of smooth vector fields $\mathbf{F}^\varepsilon$ that converges pointwisely to $\mathbf{F}$ as $\varepsilon \to 0$. More precisely, for $\mathbf{x} \in U \backslash \Sigma$, observe that the field $\mathbf{F}$ can be written in the form

$$\mathbf{F}(\mathbf{x}) = \left[\frac{1 + \operatorname{sgn}(h(\mathbf{x}))}{2}\right] \mathbf{F}_+(\mathbf{x}) + \left[\frac{1 - \operatorname{sgn}(h(\mathbf{x}))}{2}\right] \mathbf{F}_-(\mathbf{x}), \tag{2.1}$$

where $\operatorname{sgn} : \mathbb{R} \to \mathbb{R}$ is the **signal function** given by

$$\operatorname{sgn}(x) = \begin{cases} -1, & \text{if } x < 0, \\ 0, & \text{if } x = 0, \\ 1, & \text{if } x > 0, \end{cases}$$

which is a discontinuous function whose graph if represented at Figure 12a.

In order to approximate the piecewise smooth vector $\mathbf{F}$ with a 1-parameter family of smooth vector fields, we approximate the signal function at (2.1) with a certain type of smooth function. More precisely:

Definition 2.1. *We say that a smooth function $\varphi : \mathbb{R} \to \mathbb{R}$ is a* ***monotonous***[1] ***transition function*** *if*

$$\varphi(x) = \begin{cases} -1, & \text{if } x \leqslant -1, \\ 1, & \text{if } x \geqslant 1, \end{cases}$$

[1] A study on the regularization process with non-monotonous transition functions can be found at the chapter 6 of [38].

and $\varphi'(x) > 0$ *for* $-1 < x < 1$.

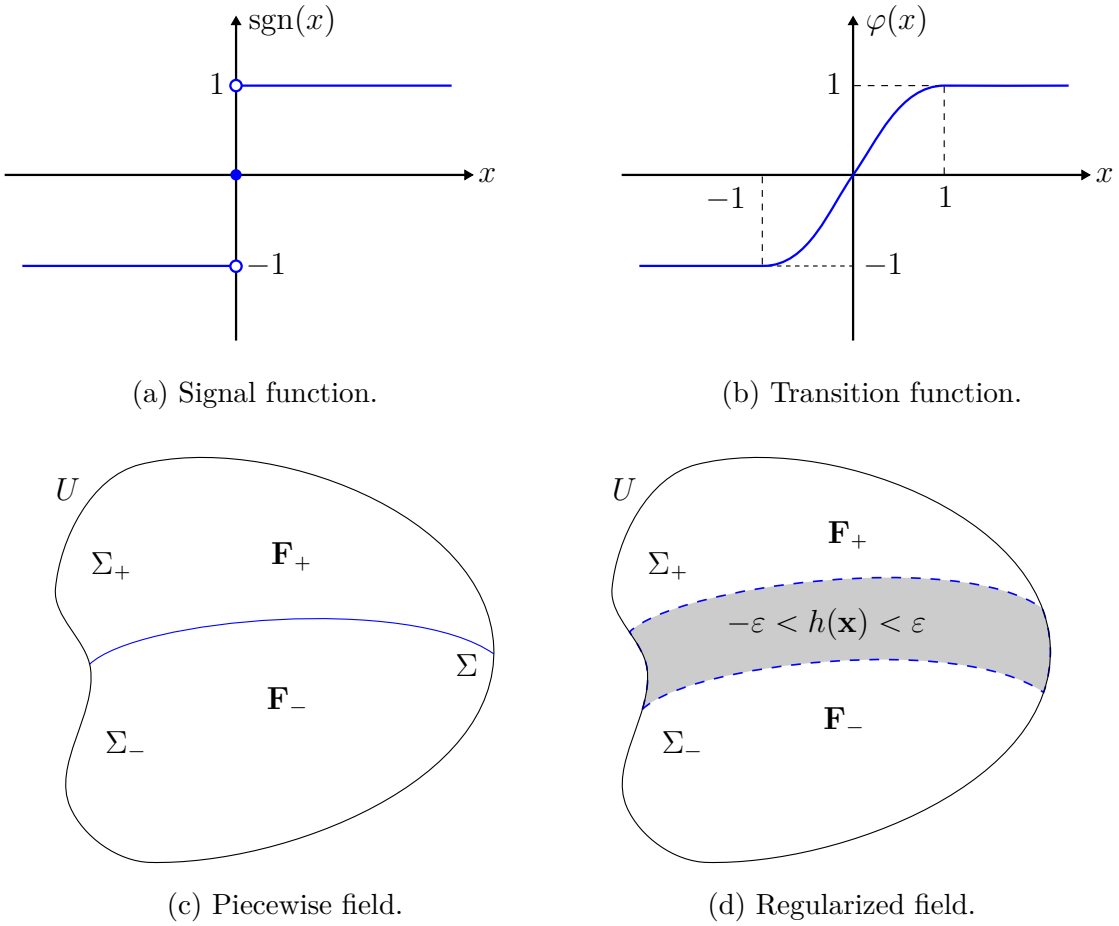

(a) Signal function.

(b) Transition function.

(c) Piecewise field.

(d) Regularized field.

Figure 12 – Grid representation of the Sotomayor-Teixeira's regularization with the signal function (a) associated to the piecewise smooth vector field (c) and the transition function (b) associated to the regularized vector field (d).

The graph of a typical transition function is represented at Figure 12b. Observe that, if we define $\varphi^\varepsilon(x) = \varphi\left(\frac{x}{\varepsilon}\right)$, where $\varepsilon > 0$, then clearly $\varphi^\varepsilon \to \text{sgn}$ pointwisely when $\varepsilon \to 0$, as long as their domains are restricted to the set $\mathbb{R}\backslash\{0\}$. In particular, if we define

$$\mathbf{F}^\varepsilon(\mathbf{x}) = \left[\frac{1+\varphi^\varepsilon(h(\mathbf{x}))}{2}\right]\mathbf{F}_+(\mathbf{x}) + \left[\frac{1-\varphi^\varepsilon(h(\mathbf{x}))}{2}\right]\mathbf{F}_-(\mathbf{x}), \tag{2.2}$$

then we get a 1-parameter family of vector fields $\mathbf{F}^\varepsilon \in C^k(U)$ such that $\mathbf{F}^\varepsilon \to \mathbf{F}$ pointwisely when $\varepsilon \to 0$, as long as their domains are restricted to the set $\mathbb{R}\backslash\{0\}$.

Definition 2.2. *Let* $\varphi : \mathbb{R} \to \mathbb{R}$ *be a monotonous transition function. We say that (2.2) is a* φ^ε*-**regularization** of (2.1).*

Observe that the regularization $\mathbf{F}^\varepsilon$ coincides with $\mathbf{F}$ outside the rectangle given by $-\varepsilon < h(\mathbf{x}) < \varepsilon$. In fact,

$$\mathbf{F}^{\varepsilon}(\mathbf{x}) = \begin{cases} \mathbf{F}_{+}(\mathbf{x}), & \text{if } h(\mathbf{x}) \geqslant \varepsilon, \\ \mathbf{F}_{-}(\mathbf{x}), & \text{if } h(\mathbf{x}) \leqslant -\varepsilon, \end{cases}$$

as represented at Figure 12d. In particular, it is clear that $\mathbf{F}^{\varepsilon}$ recovers the smooth component of the Filippov dynamics given by $\mathbf{F}$, i.e., that associated to the region $U\backslash\Sigma$, as long as we take $\varepsilon > 0$ small enough. As described in the next section, $\mathbf{F}^{\varepsilon}$ also recovers the non-smooth component of the Filippov dynamics, i.e., that associated to the region Σ.

2.2 Geometrical Singular Perturbation Theory

Let $W \subset \mathbb{R}^{m+n}$ be an open set whose elements are represented by $(\mathbf{x}, \mathbf{y})$. Let also $\mathbf{f} : W \times [0,1] \to \mathbb{R}^m$ and $\mathbf{g} : W \times [0,1] \to \mathbb{R}^n$ be vector fields of class C^k with $k \geqslant 1$. Given $0 < \xi < 1$, consider the system of differential equations

$$\begin{cases} \mathbf{x}' = \mathbf{f}(\mathbf{x}, \mathbf{y}, \xi) \\ \mathbf{y}' = \xi \mathbf{g}(\mathbf{x}, \mathbf{y}, \xi) \end{cases}, \tag{2.3}$$

where $\square' = {}^{d\square}/_{d\tau}$, $\mathbf{x} = \mathbf{x}(\tau)$ and $\mathbf{y} = \mathbf{y}(\tau)$. Applying at the previous system the time rescaling given by $t = \xi\tau$, we obtain the new system

$$\begin{cases} \xi\dot{\mathbf{x}} = \mathbf{f}(\mathbf{x}, \mathbf{y}, \xi) \\ \dot{\mathbf{y}} = \mathbf{g}(\mathbf{x}, \mathbf{y}, \xi) \end{cases}, \tag{2.4}$$

where $\dot{\square} = {}^{d\square}/_{dt}$, $\mathbf{x} = \mathbf{x}(t)$ and $\mathbf{y} = \mathbf{y}(t)$.

As $0 < \xi < 1$, then (2.3) and (2.4) have exactly the same phase portrait, except for the trajectories speed, which is greater for first system and smaller for the second. Therefore, the following definition makes sense:

Definition 2.3. *We say that (2.3) and (2.4) form a (m,n)-**slow-fast system** with **fast system** given by (2.3) and **slow system** given by (2.4).*

Taking $\xi \to 0$ in (2.3), we get the so-called **layer system**

$$\begin{cases} \mathbf{x}' = \mathbf{f}(\mathbf{x}, \mathbf{y}, 0) \\ \mathbf{y}' = \mathbf{0} \end{cases}, \tag{2.5}$$

which has dimension m. Taking $\xi \to 0$ in (2.4), we get the so-called **reduced system**

$$\begin{cases} \mathbf{0} = \mathbf{f}(\mathbf{x}, \mathbf{y}, 0) \\ \dot{\mathbf{y}} = \mathbf{g}(\mathbf{x}, \mathbf{y}, 0) \end{cases}, \tag{2.6}$$

which has dimension n. Beyond that, we say that the set

$$\mathcal{M} = \{(\mathbf{x}, \mathbf{y}) \in W;\ \mathbf{f}(\mathbf{x}, \mathbf{y}, 0) = \mathbf{0}\}$$

is the **slow manifold**. Observe that, on one hand, $\mathcal{M}$ represents the set of singularities of the layer system; on the other hand, $\mathcal{M}$ represents the manifold over which the dynamics of the reduced system takes place.

The main idea of Geometrical Singular Perturbation Theory, or GSP-Theory for short, established by Fenichel in [21], consists of combining the dynamics of the limit systems (layer and reduced) to recover the dynamics of the initial system (slow-fast) with $\xi > 0$ small. In fact, considering ξ as an additional variable of the slow system (2.4) we get the new one

$$\begin{cases} \mathbf{x}' = \mathbf{f}(\mathbf{x}, \mathbf{y}, \xi) \\ \mathbf{y}' = \xi \mathbf{g}(\mathbf{x}, \mathbf{y}, \xi) \\ \xi' = 0 \end{cases}, \tag{2.7}$$

whose Jacobian matrix at $(\mathbf{x}_0, \mathbf{y}_0, 0) \in \mathcal{M} \times \{0\}$ is

$$\mathbf{J}_{\text{fast}} = \begin{bmatrix} \mathbf{f_x} & \mathbf{f_y} & 0 \\ \mathbf{0} & \mathbf{0} & 0 \\ \mathbf{0} & \mathbf{0} & 0 \end{bmatrix}, \tag{2.8}$$

where $\mathbf{f_x}$ and $\mathbf{f_y}$ represent the partial derivatives calculated at the point $(\mathbf{x}_0, \mathbf{y}_0, 0)$. The matrix above has the trivial eigenvalue $\lambda = 0$ with algebraic multiplicity $n + 1$. The remaining eigenvalues, called **non-trivial**, are divided in three categories: negative, zero or positive real parts; we denote the number of such eigenvalues by k^s, k^c and k^u, respectively.

Definition 2.4. *We say that* $(\mathbf{x}_0, \mathbf{y}_0, 0) \in \mathcal{M} \times \{0\}$ *is* ***normally hyperbolic*** *if every non-trivial eigenvalue of (2.8) have non-zero real part, i.e.,* $k^c = 0$.

Fenichel, in [21], proved that normal hyperbolicity allows the persistence of invariant compact parts of the slow manifold under singular perturbation, i.e., the dynamical structure of such parts with $\xi = 0$ persists for $\xi > 0$ small. Even more, with predictable stability. More precisely:

Theorem 2.1 (Retrieved from [49], page 1953)**.** *Let* $\mathcal{N}$ *be a normally hyperbolic compact invariant* j*-dimensional submanifold of* $\mathcal{M}$*. Suppose that the stable and unstable manifolds of* $\mathcal{N}$*, with respect to the reduced system, have dimensions* $j + j^s$ *and* $j + j^u$*, respectively. Then, there exists a 1-parameter family of invariant submanifolds* $\{\mathcal{N}_\xi;\ \xi \sim 0\}$ *such that* $\mathcal{N}_0 = \mathcal{N}$ *and* $\mathcal{N}_\xi$ *has stable and unstable manifolds with dimensions* $j + j^s + k^s$ *and* $j + j^u + k^u$*, respectively.*

The reverse idea of GSP-Theory can also be used to recover the non-smooth component of the Filippov dynamics, given by the piecewise vector field ($\varepsilon = 0$), from its regularization ($\varepsilon > 0$). In fact, let $\mathbf{F} = (\mathbf{F}_+, \mathbf{F}_-) \in \mathcal{R}^k(U, h)$ be a piecewise smooth vector field with switching manifold $\Sigma = h^{-1}(\{0\})$. Let also $\varphi : \mathbb{R} \to \mathbb{R}$ be a monotonous transition function and $\mathbf{F}^\varepsilon$ the φ^ε-regularization of $\mathbf{F}$.

We need to transform $\mathbf{F}^\varepsilon$ in a slow-fast system. In order to do so, observe that, as 0 is a regular value of h, then from the Local Normal Form for Submersions follows that, without loss of generality, we can admit that $h(x_1, \ldots, x_n) = x_1$ in a neighborhood of a given point $\mathbf{x} \in \Sigma$. Therefore, if we write $\mathbf{F}_+ = (f_1^+, \ldots, f_n^+)$ and $\mathbf{F}_- = (f_1^-, \ldots, f_n^-)$, then follows that $\mathbf{F}^\varepsilon$ can be written as

$$\dot{x}_i = \left[\frac{1 + \varphi^\varepsilon(x_1)}{2}\right] f_i^+(x_1, \ldots, x_n) + \left[\frac{1 + \varphi^\varepsilon(x_1)}{2}\right] f_i^-(x_1, \ldots, x_n),$$

where $i \in \{1, \ldots, n\}$. Now, applying to the system above the polar blow-up given by $x_1 = \xi \cos\theta$ and $\varepsilon = \xi \sin\theta$, where $\xi \geqslant 0$ and $\theta \in [0, \pi]$, we obtain a $(1, n-1)$-slow-fast system given by

$$\begin{cases} \xi\dot{\theta} = \alpha_1(\theta, x_2, \ldots, x_n, \xi) \\ \dot{x}_i = \alpha_i(\theta, x_2, \ldots, x_n, \xi) \end{cases}, \tag{2.9}$$

where $i \in \{2, \ldots, n\}$.

Observe that, for $\xi = 0$, we have $x_1 = 0$ and $\varepsilon = 0$, i.e., we are at the non-regularized system $\mathbf{F}$ over the manifold Σ. In the other hand, for $\xi > 0$ and $\theta \in (0, \pi)$, we have $-\xi < x_1 < \xi$ and $0 < \varepsilon < \xi$, i.e., we are at the regularized system $\mathbf{F}^\varepsilon$ over the rectangle where it does not coincide to $\mathbf{F}$, see Figure 12d. The authors of [49] then proved the result below:

Theorem 2.2 (Retrieved from [49], page 1950)**.** *Consider the piecewise smooth vector field* $\mathbf{F}$ *and the slow-fast system (2.9). The sliding region* Σ^s *is homeomorphic to the slow manifold given by*

$$\alpha_1(\theta, x_2, \ldots, x_n, 0) = 0$$

and the dynamics of the sliding vector field $\mathbf{F}^s$ *over* Σ^s *is topologically equivalent to that of the reduced system given by*

$$\begin{cases} 0 = \alpha_1(\theta, x_2, \ldots, x_n, 0) \\ \dot{x}_i = \alpha_i(\theta, x_2, \ldots, x_n, 0) \end{cases},$$

where $i \in \{2, \ldots, n\}$.

Concisely, the Filippov dynamics of $\mathbf{F}$ is completely recovered by its regularization $\mathbf{F}^\varepsilon$. In order to do so, the following steps, described in details above, are necessary:

1. Normalization of the switching manifold.
2. Regularization of the piecewise smooth vector field.
3. Polar blow-up of the regularization.
4. Analysis of the resulting limit systems (layer and reduced).

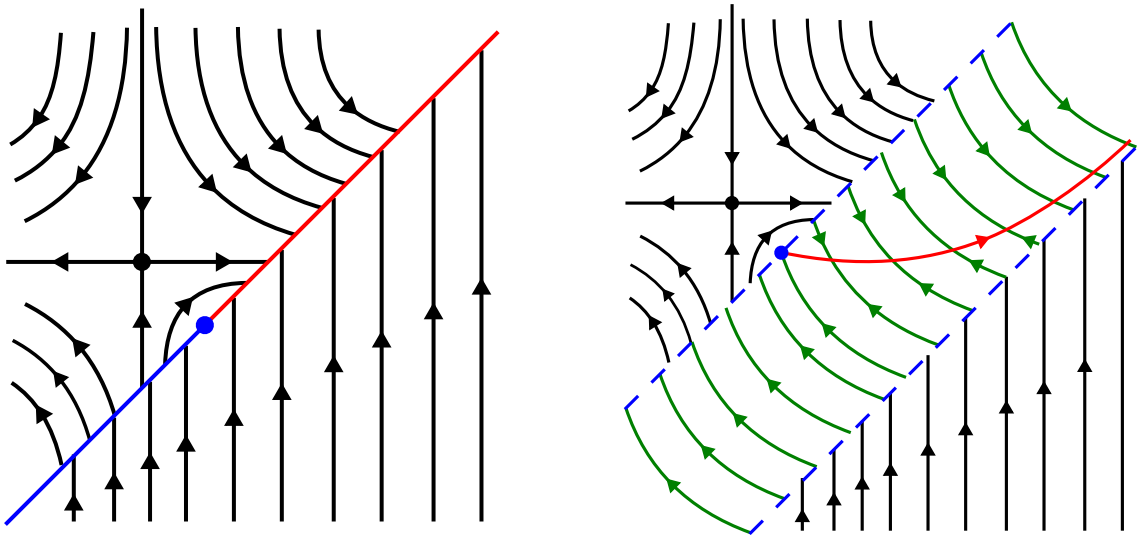

(a) Piecewise field. (b) Regularized field.

Figure 13 – Complete regularization process.

Example 2.1. *Let* $\mathbf{F}_-(x,y) = (x+1, -y+1)$ *and* $\mathbf{F}_+(x,y) = (0,1)$ *be vector fields in* $\mathbb{R}^2$ *and* $\mathbf{F} = (\mathbf{F}_+, \mathbf{F}_-)$ *be the piecewise smooth vector field given by*

$$\mathbf{F}(x,y) = \begin{cases} \mathbf{F}_-(x,y), & \text{if } y \geqslant x \\ \mathbf{F}_+(x,y), & \text{if } y \leqslant x \end{cases},$$

with switching manifold given by $\Sigma = h^{-1}(0)$, *where* $h : \mathbb{R}^2 \to \mathbb{R}$ *is given ny* $h(x,y) = x - y$, *i.e.,* $\Sigma = \{(x,y) \in \mathbb{R}^2;\ y = x\}$. *Therefore, we have the Filippov system represented at Figure 13a, where clearly the red sliding region is given by* $\Sigma^s = \{(x,x);\ x > 0\}$. *Lets see how the regularization process described above recovers the sliding dynamics:*

1. *(Normalization)*
   Applying a $\frac{\pi}{4}$ *radians rotation we get the normalized vector field*

$$\tilde{\mathbf{F}}(x,y) = \begin{cases} \frac{\sqrt{2}}{2}(x+y, x-y+2), & \text{if } x \leqslant 0 \\ \frac{\sqrt{2}}{2}(-1,1), & \text{if } x \geqslant 0 \end{cases},$$

i.e., now the switching manifold is given by the map $(x,y) \mapsto x$.

2. *(Regularization)*
Let $\varphi : \mathbb{R} \to \mathbb{R}$ *be an arbitrary monotonous transition function. Applying the* φ^ε*-regularization to* $\tilde{\mathbf{F}}$ *we get the 1-parameter family of smooth vector fields*

$$\tilde{\mathbf{F}}^\varepsilon(x,y) = \tfrac{\sqrt{2}}{4}(-1+x+y-(1+x+y)\varphi^\varepsilon(x), \\ 3+x-y+(-1-x+y)\varphi^\varepsilon(x))$$

where $\varepsilon > 0$.

3. *(Blow-up)*
Applying the polar blow-up given by $x = \xi\cos\theta$ *and* $\varepsilon = \xi\sin\theta$*, where* $\xi \geqslant 0$ *and* $\theta \in [0,\pi]$*, to the regularization* $\tilde{\mathbf{F}}^\varepsilon$ *we get the slow system*

$$\begin{cases} \xi\dot{\theta} = \frac{\sqrt{2}}{4}\sin\theta\,(1-\xi\cos\theta-y+(1+\xi\cos\theta+y)\varphi(\cot\theta)) \\ \dot{y} = \frac{\sqrt{2}}{4}\,(3+\xi\cos\theta-y+(-1-\xi\cos\theta+y)\varphi(\cot\theta)) \end{cases}.$$

4. *(Analysis of the singular perturbation problem)*
Taking $\xi = 0$ *in the slow system above, we get that the slow manifold is the curve* $y(\theta)$ *given by*

$$\varphi(\cot\theta) = \frac{y-1}{y+1}$$

connecting the points $(\theta,y) = (0,+\infty)$ *and* $(\theta,y) = (\pi,0)$*. Beyond that, the reduced system is given by*

$$\dot{y} = \frac{\sqrt{2}}{4}\left(3-y+(-1+y)\frac{y-1}{y+1}\right) = \frac{\sqrt{2}}{y+1} > 0,$$

since, as seen above, $y > 0$ *over the slow manifold. On the other hand, the layer system is given by*

$$\theta' = \frac{\sqrt{2}}{4}\sin\theta\,(1-y+(1+y)\varphi(\cot\theta))$$

and, therefore, $\theta' > 0$ *below the slow manifold and* $\theta' < 0$ *above it. Therefore, the recovery of the initial Filippov dynamics through regularization and GSP-Theory can*

be represented as in Figure 13b, where the reduced system is represented in red and the layer system is represented in green.[2]

[2] A new rotation by and angle of $-\frac{\pi}{4}$ was applied in order to bring back the system to the original coordinates.

3 Sliding Saddle

In this chapter, we have as a goal to study the realization and structural stability of a particular configuration of the sliding region that we baptise as *sliding saddle*. In the first section, we classify the Filippov systems in $\mathbb{R}^2$ given by affine vector fields which realizes a sliding saddle. In the second section, we study the regularization and local structural stability of the sliding saddles obtained in the previous section.

3.1 Realization

Let $\mathbf{F}_i : \mathbb{R}^2 \to \mathbb{R}$ be vector fields of class C^k with $i \in \{1, 2, 3, 4\}$ and $k \geqslant 1$. Consider the piecewise vector field $\mathbf{F} = (\mathbf{F}_1, \ldots, \mathbf{F}_4)$ given by

$$\mathbf{F}(x, y) = \begin{cases} \mathbf{F}_1(x, y), & \text{if } x \geqslant 0 \text{ and } y \geqslant 0, \\ \mathbf{F}_2(x, y), & \text{if } x \leqslant 0 \text{ and } y \geqslant 0, \\ \mathbf{F}_3(x, y), & \text{if } x \leqslant 0 \text{ and } y \leqslant 0, \\ \mathbf{F}_4(x, y), & \text{if } x \geqslant 0 \text{ and } y \leqslant 0, \end{cases} \tag{3.1}$$

i.e., whose switching manifold Σ is the cross given by the union of the lines $x = 0$ and $y = 0$, as represented at Figure 14. The set of all vector fields $\mathbf{F}$ defined as above will be denoted by

$$\mathcal{D}_2^k \equiv C^k(\mathbb{R}^2) \times C^k(\mathbb{R}^2) \times C^k(\mathbb{R}^2) \times C^k(\mathbb{R}^2)$$

and equipped with the Whitney product topology.

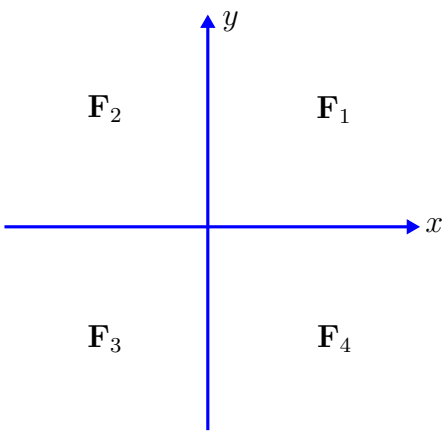

Figure 14 – Cross switching manifold.

Consider the Filippov system given by $\mathbf{F}$. Observe that, whenever necessary, we have a sliding field $\mathbf{F}^s$ well-defined at $\Sigma\backslash\{(0,0)\}$. At the origin $(0,0)$, however, there is no well-defined Filippov dynamics. In fact, $\Sigma = h^{-1}(0)$, where $h : \mathbb{R}^2 \to \mathbb{R}$ given by $h(x,y) = xy$ has 0 as a singular value, since $Dh(0,0)$ is not surjective.

In this section, given a Filippov system as above and considering $\Sigma\backslash\{(0,0)\}$, we would like to study the realization of the sliding region configuration represented at Figure 15. We say that this configuration is a **sliding saddle**.

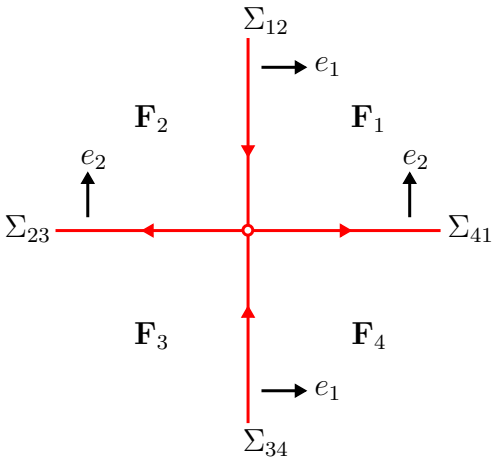

Figure 15 – Sliding saddle.

In order to formally define a sliding saddle, consider the partition $\Sigma\backslash\{(0,0)\} = \Sigma_{12} \cup \Sigma_{23} \cup \Sigma_{34} \cup \Sigma_{41}$, where

$$\begin{aligned}
\Sigma_{12} &= \{(0,y);\ y > 0\} = \pi_1^{-1}\big|_{(0,\infty)}(0),\\
\Sigma_{23} &= \{(x,0);\ x < 0\} = \pi_2^{-1}\big|_{(0,-\infty)}(0),\\
\Sigma_{34} &= \{(0,y);\ y < 0\} = \pi_1^{-1}\big|_{(0,-\infty)}(0),\\
\Sigma_{41} &= \{(x,0);\ x > 0\} = \pi_2^{-1}\big|_{(0,\infty)}(0),
\end{aligned}$$

are open subsets and $\pi_1, \pi_2 : \mathbb{R}^2 \to \mathbb{R}$ are the canonical projections. Beyond that, remembering the geometrical interpretation of the Lie derivative given at Section 1.3, without loss of generality, we will simplify the calculations considering reference vectors $e_1 = (1,0)$ at Σ_{41} and Σ_{23}; and $e_2 = (0,1)$ at Σ_{12} and Σ_{34}, as represented at Figure 15. Even more, let

$$\mathbf{F}^s_{ij} = \frac{(\mathbf{F}_j \cdot e_\square)\mathbf{F}_i - (\mathbf{F}_i \cdot e_\square)\mathbf{F}_j}{(\mathbf{F}_j \cdot e_\square) - (\mathbf{F}_i \cdot e_\square)}$$

be the sliding field at Σ_{ij}, where $\square = 1$ for Σ_{12} and Σ_{34}; and $\square = 2$ for Σ_{41} and Σ_{23}.

To assure the sliding configuration at Σ_{12} represented at Figure 15, the field $\mathbf{F}_1$ should point from Σ_{12} to Σ_{41}; whereas the field $\mathbf{F}_2$ should point from Σ_{12} to Σ_{23}. Beyond

that, the sliding field $\mathbf{F}_{12}^s$ should be decreasing. More specifically, the following conditions should be assured:

$$\Sigma_{12} : \begin{cases} y > 0 \\ \mathbf{F}_1(0,y) \cdot e_1 > 0 \\ \mathbf{F}_2(0,y) \cdot e_1 < 0 \\ \pi_2 \circ \mathbf{F}_{12}^s(0,y) < 0 \end{cases} . \tag{3.2}$$

Similarly, in order to assure the configurations at Σ_{23}, Σ_{34} and Σ_{41} represented at 15, the following respective sets of conditions should be verified:

$$\Sigma_{23} : \begin{cases} x < 0 \\ \mathbf{F}_2(x,0) \cdot e_2 < 0 \\ \mathbf{F}_3(x,0) \cdot e_2 > 0 \\ \pi_1 \circ \mathbf{F}_{23}^s(x,0) < 0 \end{cases} , \tag{3.3}$$

$$\Sigma_{34} : \begin{cases} y < 0 \\ \mathbf{F}_3(0,y) \cdot e_1 < 0 \\ \mathbf{F}_4(0,y) \cdot e_1 > 0 \\ \pi_2 \circ \mathbf{F}_{12}^s(0,y) > 0 \end{cases} , \tag{3.4}$$

$$\Sigma_{41} : \begin{cases} x > 0 \\ \mathbf{F}_4(x,0) \cdot e_2 > 0 \\ \mathbf{F}_1(x,0) \cdot e_2 < 0 \\ \pi_1 \circ \mathbf{F}_{23}^s(x,0) > 0 \end{cases} . \tag{3.5}$$

Definition 3.1. *We say that the switching manifold of the Filippov system (3.1) is a* ***sliding saddle*** *if the sets of conditions (3.2), (3.3), (3.4) and (3.5) are satisfied.*

Now that we have formally defined the sliding saddle, we will study its realization with affine vector fields $\mathbf{F}_i$. More precisely, at the following subsections, we will consider vector fields[1]

$$\mathbf{F}_i(x,y) = \mathbf{A}_i \begin{bmatrix} x \\ y \end{bmatrix} + \mathbf{b}_i = \begin{bmatrix} a_{i1} & a_{i2} \\ a_{i3} & a_{i4} \end{bmatrix} \begin{bmatrix} x \\ y \end{bmatrix} + \begin{bmatrix} b_{i1} \\ b_{i2} \end{bmatrix} , \tag{3.6}$$

where $\mathbf{A}_i$ and $\mathbf{b}_i$ are real matrices for every $i \in \{1,2,3,4\}$, progressively increasing its complexity: starting at the constant case ($\mathbf{A}_i = \mathbf{0}$), linear ($\mathbf{b}_i = \mathbf{0}$) and then, finally, the affine case (3.6).

[1] Sometimes, without loss of generality, we will commit the abuse of terminology of confusing matrix with vector notation.

3.1.1 Constant Fields

Let $\mathcal{C}_2$ be the set of constant fields given by (3.6) with $\mathbf{A}_i = \mathbf{0}$. In order to realize a sliding saddle with $\mathbf{F} \in \mathcal{C}_2$, we apply the sets of conditions (3.2), (3.3), (3.4) and (3.5) to obtain the following new sets of conditions:

$$\Sigma_{12}: \begin{cases} y > 0 \\ b_{11} > 0 \\ b_{21} < 0 \\ \frac{b_{21}b_{12}-b_{11}b_{22}}{b_{21}-b_{11}} < 0 \end{cases} \Rightarrow \quad \Sigma_{12}: \begin{cases} b_{11} > 0 \\ b_{21} < 0 \end{cases}, \tag{3.7}$$

$$\Sigma_{23}: \begin{cases} x < 0 \\ b_{22} < 0 \\ b_{32} > 0 \\ \frac{b_{32}b_{21}-b_{22}b_{31}}{b_{32}-b_{22}} < 0 \end{cases} \Rightarrow \quad \Sigma_{23}: \begin{cases} b_{22} < 0 \\ b_{32} > 0 \end{cases}, \tag{3.8}$$

$$\Sigma_{34}: \begin{cases} y < 0 \\ b_{31} < 0 \\ b_{41} > 0 \\ \frac{b_{41}b_{32}-b_{31}b_{42}}{b_{41}-b_{31}} > 0 \end{cases} \Rightarrow \quad \Sigma_{34}: \begin{cases} b_{31} < 0 \\ b_{41} > 0 \end{cases}, \tag{3.9}$$

$$\Sigma_{41}: \begin{cases} x > 0 \\ b_{42} > 0 \\ b_{12} < 0 \\ \frac{b_{12}b_{41}-b_{42}b_{11}}{b_{12}-b_{42}} > 0 \end{cases} \Rightarrow \quad \Sigma_{41}: \begin{cases} b_{42} > 0 \\ b_{12} < 0 \end{cases}. \tag{3.10}$$

Observe that, considering the three first lines of each left-hand side set above, the fourth line is automatically satisfied and, therefore, is unnecessary. Even more, the first lines become unnecessary. Therefore, we obtain the right-hand side final sets of conditions.

Example 3.1. *Applying the sets of conditions (3.7), (3.8), (3.9) and (3.10), one can verify that the constant vector fields*

$$\begin{aligned} \mathbf{F}_2(x,y) &= \begin{bmatrix} -1 \\ -1 \end{bmatrix}, \qquad \mathbf{F}_1(x,y) = \begin{bmatrix} 1 \\ -1 \end{bmatrix}, \\ \mathbf{F}_3(x,y) &= \begin{bmatrix} -1 \\ 1 \end{bmatrix}, \qquad \mathbf{F}_4(x,y) = \begin{bmatrix} 1 \\ 1 \end{bmatrix}, \end{aligned} \tag{3.11}$$

represented at Figure 16, realize a sliding saddle.

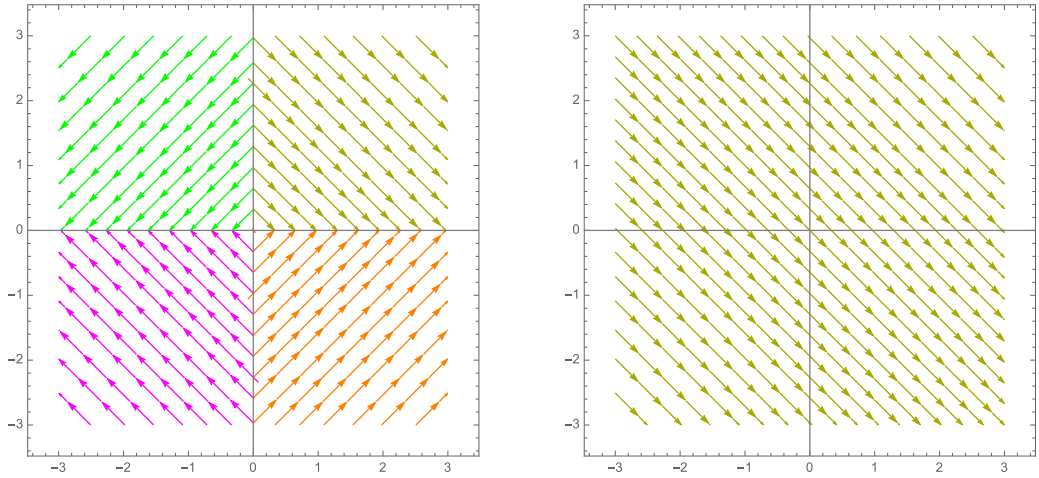

(a) $\mathbf{F} = (\mathbf{F}_1, \ldots, \mathbf{F}_4)$ (b) $\mathbf{F}_1$

Figure 16 – Constant vector fields realizing a sliding saddle.

3.1.2 Linear Fields

Let $\mathcal{L}_2$ be the set of linear fields given by (3.6) with $\mathbf{b}_i = \mathbf{0}$. In order to realize a sliding saddle with $\mathbf{F} \in \mathcal{L}_2$, we apply the sets of conditions (3.2), (3.3), (3.4) and (3.5) to obtain the following new sets of conditions:

$$\Sigma_{12} : \begin{cases} y > 0 \\ a_{12} > 0 \\ a_{22} < 0 \\ \frac{a_{22}a_{14} - a_{12}a_{24}}{a_{22} - a_{12}} y < 0 \end{cases} \Rightarrow \quad \Sigma_{12} : \begin{cases} a_{12} > 0 \\ a_{22} < 0 \\ a_{22}a_{14} - a_{12}a_{24} > 0 \end{cases}, \tag{3.12}$$

$$\Sigma_{23} : \begin{cases} x < 0 \\ a_{23} > 0 \\ a_{33} < 0 \\ \frac{a_{33}a_{21} - a_{23}a_{31}}{a_{33} - a_{23}} x < 0 \end{cases} \Rightarrow \quad \Sigma_{23} : \begin{cases} a_{23} > 0 \\ a_{33} < 0 \\ a_{33}a_{21} - a_{23}a_{31} < 0 \end{cases}, \tag{3.13}$$

$$\Sigma_{34} : \begin{cases} y < 0 \\ a_{32} > 0 \\ a_{42} < 0 \\ \frac{a_{42}a_{34} - a_{32}a_{44}}{a_{42} - a_{32}} y > 0 \end{cases} \Rightarrow \quad \Sigma_{34} : \begin{cases} a_{32} > 0 \\ a_{42} < 0 \\ a_{42}a_{34} - a_{32}a_{44} > 0 \end{cases}, \tag{3.14}$$

$$\Sigma_{41} : \begin{cases} x > 0 \\ a_{43} > 0 \\ a_{13} < 0 \\ \frac{a_{13}a_{41} - a_{43}a_{11}}{a_{13} - a_{43}} x > 0 \end{cases} \Rightarrow \quad \Sigma_{41} : \begin{cases} a_{43} > 0 \\ a_{13} < 0 \\ a_{13}a_{41} - a_{43}a_{11} < 0 \end{cases}. \tag{3.15}$$

Observe that, considering the three first lines of each left-hand side set above, the fourth line can be simplified. Even more, the first lines become unnecessary. Therefore, we obtain the right-hand side final sets of conditions.

Example 3.2. *Applying the sets of conditions (3.12), (3.13), (3.14) and (3.15) one can verify that the linear vector fields*

$$\begin{aligned} \mathbf{F}_2(x,y) &= \begin{bmatrix} 1 & -1 \\ 1 & -2 \end{bmatrix} \begin{bmatrix} x \\ y \end{bmatrix}, & \mathbf{F}_1(x,y) &= \begin{bmatrix} 1 & 1 \\ -1 & -2 \end{bmatrix} \begin{bmatrix} x \\ y \end{bmatrix}, \\ \mathbf{F}_3(x,y) &= \begin{bmatrix} 1 & 1 \\ -1 & -2 \end{bmatrix} \begin{bmatrix} x \\ y \end{bmatrix}, & \mathbf{F}_4(x,y) &= \begin{bmatrix} 1 & -1 \\ 1 & -2 \end{bmatrix} \begin{bmatrix} x \\ y \end{bmatrix}, \end{aligned} \tag{3.16}$$

represented at Figure 17, realize a sliding saddle.

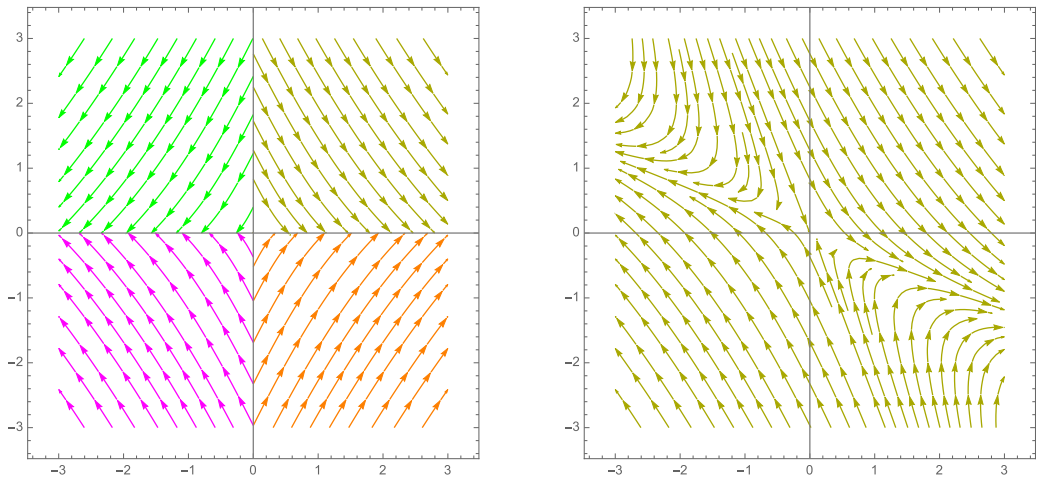

(a) $\mathbf{F} = (\mathbf{F}_1, \ldots, \mathbf{F}_4)$ (b) $\mathbf{F}_1$

Figure 17 – Linear vector fields realizing a sliding saddle.

3.1.3 Affine Fields

Let $\mathcal{A}_2$ be the set of affine fields given by (3.6). In order to realize a sliding saddle with $\mathbf{F} \in \mathcal{A}_2$, we apply the sets of conditions (3.2), (3.3), (3.4) and (3.5) to obtain the following new sets of conditions:

$$\Sigma_{12} : \begin{cases} y > 0 \\ a_{12}y + b_{11} > 0 \\ a_{22}y + b_{21} < 0 \\ (a_{22}y + b_{21})(a_{14}y + b_{12}) - (a_{12}y + b_{11})(a_{24}y + b_{22}) > 0 \end{cases}, \tag{3.17}$$

$$\Sigma_{23}:\begin{cases} x<0 \\ a_{23}x+b_{22}<0 \\ a_{33}x+b_{32}>0 \\ (a_{33}x+b_{32})(a_{21}x+b_{21})-(a_{23}x+b_{22})(a_{31}x+b_{31})<0 \end{cases}, \tag{3.18}$$

$$\Sigma_{34}:\begin{cases} y<0 \\ a_{32}y+b_{31}<0 \\ a_{42}y+b_{41}>0 \\ (a_{42}y+b_{41})(a_{34}y+b_{32})-(a_{32}y+b_{31})(a_{44}y+b_{42})>0 \end{cases}, \tag{3.19}$$

$$\Sigma_{41}:\begin{cases} x>0 \\ a_{43}x+b_{42}>0 \\ a_{13}x+b_{12}<0 \\ (a_{13}x+b_{12})(a_{41}x+b_{41})-(a_{43}x+b_{42})(a_{11}x+b_{11})<0 \end{cases}. \tag{3.20}$$

Observe that, considering the three first lines of each left-hand side set above, the fourth line has already been simplified. Even more, the final sets of conditions here resemble those for the linear case above. In fact, given linear vector fields that realize a sliding saddle, applying proper translations, it is easy to obtain affine fields that also realize a sliding saddle.

Example 3.3. *Consider the linear fields* $\mathbf{F}_i$ *obtained at Example 3.2. Moving the singularity of* $\mathbf{F}_1$ *to* $(-1,-1)$*, of* $\mathbf{F}_2$ *to* $(1,-1)$*, of* $\mathbf{F}_3$ *to* $(1,1)$ *and of* $\mathbf{F}_4$ *to* $(-1,1)$*, one obtain the affine fields* $\tilde{\mathbf{F}}_i$ *given by*

$$\begin{aligned} \tilde{\mathbf{F}}_2(x,y)&=\begin{bmatrix}1&-1\\1&-2\end{bmatrix}\begin{bmatrix}x\\y\end{bmatrix}+\begin{bmatrix}-2\\-3\end{bmatrix}, & \tilde{\mathbf{F}}_1(x,y)&=\begin{bmatrix}1&1\\-1&-2\end{bmatrix}\begin{bmatrix}x\\y\end{bmatrix}+\begin{bmatrix}2\\-3\end{bmatrix}, \\ \tilde{\mathbf{F}}_3(x,y)&=\begin{bmatrix}1&1\\-1&-2\end{bmatrix}\begin{bmatrix}x\\y\end{bmatrix}+\begin{bmatrix}-2\\3\end{bmatrix}, & \tilde{\mathbf{F}}_4(x,y)&=\begin{bmatrix}1&-1\\1&-2\end{bmatrix}\begin{bmatrix}x\\y\end{bmatrix}+\begin{bmatrix}2\\3\end{bmatrix}, \end{aligned} \tag{3.21}$$

represented at Figure 17, which realize a sliding saddle, as can be verified using the sets of conditions (3.17), (3.18), (3.19) and (3.20).

Therefore, given the evidence provided by both the previous example and other similar ones, we formulate the following conjecture, which provides an alternative method to construct sliding saddles with affine vector fields:

Conjecture 3.1. *Given* $\mathbf{F} = (\mathbf{F}_1, \cdots, \mathbf{F}_4) \in \mathcal{L}_2$*, there exists translations* $\mathbf{T}_1, \cdots, \mathbf{T}_4$ *such that* $\tilde{\mathbf{F}} = (\mathbf{T}_1 \circ \mathbf{F}_1, \cdots, \mathbf{T}_4 \circ \mathbf{F}_4) \in \mathcal{A}_2$ *realize a sliding saddle if, and only if,*

(a) $\mathbf{F}$ *realizes a sliding saddle; and*

(b) $\mathbf{T}_i$ *does not create visible singularities in* $\mathbf{F}_i$*.*

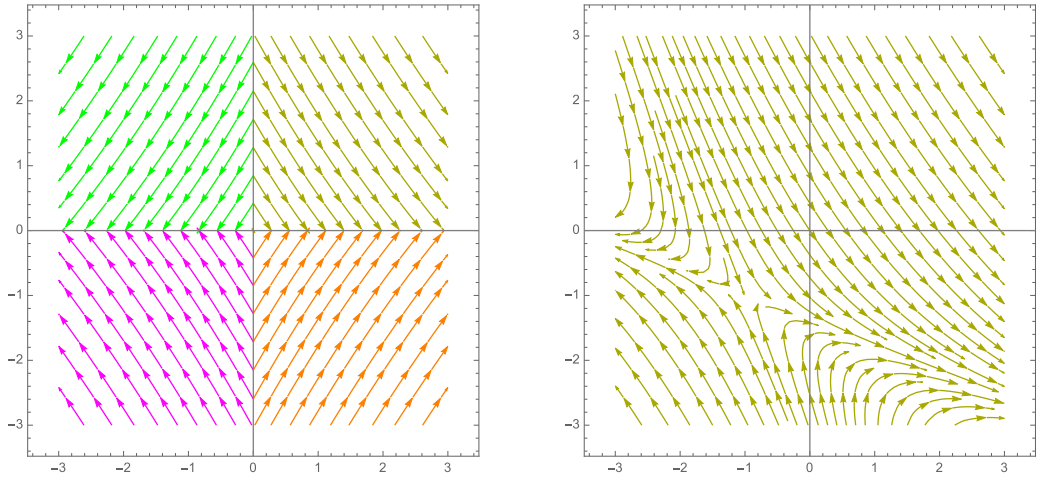

(a) $\mathbf{F} = (\mathbf{F}_1, \ldots, \mathbf{F}_4)$ (b) $\mathbf{F}_1$

Figure 18 – Affine vector fields realizing a sliding saddle.

3.2 Stability

Let $\mathbf{F} = (\mathbf{F}_1, \cdots, \mathbf{F}_4) \in \mathcal{D}_2^k$ be a piecewise vector field with a cross as switching manifold. In this section, first, we will build a regularization of $\mathbf{F}$ and, next, we present a possible way to study the structural stability of its sliding field through the study of its regularization. In particular, we will study the local structural stability of sliding saddles.

3.2.1 Regularization

Given $\varphi : \mathbb{R} \to \mathbb{R}$ a monotonous transition function, the regularization of $\mathbf{F}$ will be constructed applying a double Sotomayor-Teixeira φ-regularization, as represented at Figure 19. More specifically, first we apply a horizontal (see Figure 19b) φ^ε-regularization, i.e., considering Σ_{41} and Σ_{23}, obtaining smooth fields

$$\mathbf{F}_{41}^\varepsilon(\mathbf{x}) = \left[\frac{1+\varphi^\varepsilon(\pi_2(\mathbf{x}))}{2}\right]\mathbf{F_1}(\mathbf{x}) + \left[\frac{1-\varphi^\varepsilon(\pi_2(\mathbf{x}))}{2}\right]\mathbf{F_4}(\mathbf{x}) =$$
$$= \left[\frac{1+\varphi^\varepsilon(y)}{2}\right]\mathbf{F_1}(\mathbf{x}) + \left[\frac{1-\varphi^\varepsilon(y)}{2}\right]\mathbf{F_4}(\mathbf{x})$$

when considering Σ_{41}, and

$$\begin{aligned}\mathbf{F}^{\varepsilon}_{23}(\mathbf{x}) &= \left[\frac{1+\varphi^{\varepsilon}(\pi_2(\mathbf{x}))}{2}\right]\mathbf{F_2}(\mathbf{x}) + \left[\frac{1-\varphi^{\varepsilon}(\pi_2(\mathbf{x}))}{2}\right]\mathbf{F_3}(\mathbf{x}) = \\ &= \left[\frac{1+\varphi^{\varepsilon}(y)}{2}\right]\mathbf{F_2}(\mathbf{x}) + \left[\frac{1-\varphi^{\varepsilon}(y)}{2}\right]\mathbf{F_3}(\mathbf{x})\end{aligned}$$

when considering Σ_{23}. Now, we apply a vertical (see Figure 19c) φ^{δ}-regularization, i.e., considering Σ_{12} and Σ_{34}, obtaining the smooth field

$$\begin{aligned}\mathbf{F}^{\varepsilon,\delta}(\mathbf{x}) &= \left[\frac{1+\varphi^{\delta}(\pi_1(\mathbf{x}))}{2}\right]\mathbf{F}^{\varepsilon}_{41}(\mathbf{x}) + \left[\frac{1-\varphi^{\delta}(\pi_1(\mathbf{x}))}{2}\right]\mathbf{F}^{\varepsilon}_{23}(\mathbf{x}) = \\ &= \left[\frac{1+\varphi^{\delta}(x)}{2}\right]\mathbf{F}^{\varepsilon}_{41}(\mathbf{x}) + \left[\frac{1-\varphi^{\delta}(x)}{2}\right]\mathbf{F}^{\varepsilon}_{23}(\mathbf{x})\end{aligned}$$

which can be written as

$$\begin{aligned}\mathbf{F}^{\varepsilon,\delta}(\mathbf{x}) = &\left[\frac{1-\varphi^{\delta}(x)}{2}\right]\left[\frac{1+\varphi^{\varepsilon}(y)}{2}\right]\mathbf{F_2}(\mathbf{x}) + \left[\frac{1+\varphi^{\delta}(x)}{2}\right]\left[\frac{1+\varphi^{\varepsilon}(y)}{2}\right]\mathbf{F_1}(\mathbf{x}) + \\ &+ \left[\frac{1-\varphi^{\delta}(x)}{2}\right]\left[\frac{1-\varphi^{\varepsilon}(y)}{2}\right]\mathbf{F_3}(\mathbf{x}) + \left[\frac{1+\varphi^{\delta}(x)}{2}\right]\left[\frac{1-\varphi^{\varepsilon}(y)}{2}\right]\mathbf{F_4}(\mathbf{x}).\end{aligned} \tag{3.22}$$

Definition 3.2. *Let $\varphi : \mathbb{R} \to \mathbb{R}$ be a monotonous transition function. We say that (3.22) is a $\varphi^{\varepsilon,\delta}$-regularization of (3.1).*

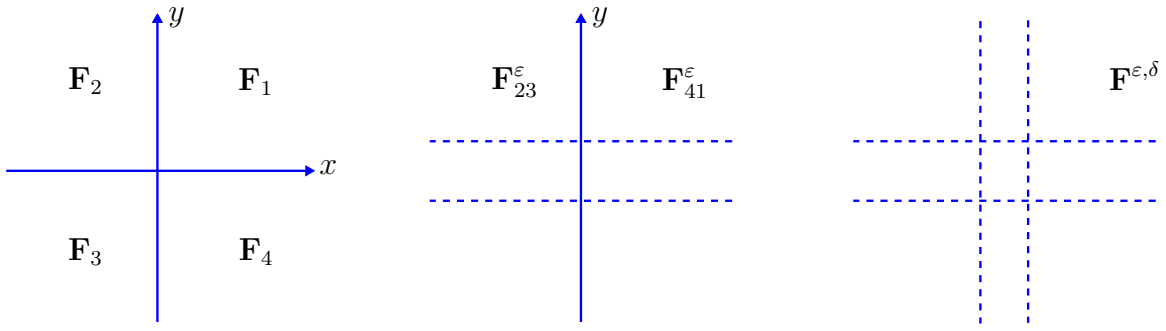

(a) Cross. (b) Horizontal. (c) Vertical.

Figure 19 – Regularization of the cross switching manifold.

For a particular set of vector fields $\mathcal{N} \subset \mathcal{D}^k_2$ and a fixed transition function φ, we define the respective set of regularizations

$$\mathcal{N}^{\varepsilon,\delta} = \left\{\mathbf{F}^{\varepsilon,\delta};\ \mathbf{F} \in \mathcal{N}\right\},$$

whose importance becomes clear over the next subsection.

3.2.2 Structural Stability

Let $\mathbf{F}^{\varepsilon,\delta}$ be the $\varphi^{\varepsilon,\delta}$-regularization of a particular $\mathbf{F} = (\mathbf{F}_1, \dots, \mathbf{F}_4) \in \mathcal{N}$ given by (3.1), where $\mathcal{N} \subset \mathcal{D}_2^k$ is a fixed subset. Suppose that $\mathbf{F}^{\varepsilon,\delta}$ is structurally stable in $\mathcal{N}^{\varepsilon,\delta}$, i.e., there exists an open neighborhood $\mathcal{U} \subset \mathcal{N}^{\varepsilon,\delta}$ of $\mathbf{F}^{\varepsilon,\delta}$ such that

$$\mathbf{H} \in \mathcal{U} \qquad \Rightarrow \qquad \mathbf{H} \sim \mathbf{F}^{\varepsilon,\delta}, \tag{3.23}$$

where $\sim$ represents topological equivalence.

Now, consider perturbations of $\mathbf{F}$ given by

$$\mathbf{F}_\mu = (\mathbf{F}_1 + \mu_1 \mathbf{P}_1, \dots, \mathbf{F}_4 + \mu_4 \mathbf{P}_4)$$

where $\mu = (\mu_1, \dots, \mu_4) \in \mathbb{R}^4$ and $\mathbf{P} = (\mathbf{P}_1, \dots, \mathbf{P}_4) \in \mathcal{N}$. Moreover, suppose also that $\mathcal{N}$ satisfies the following condition

$$\mathbf{F} \in \mathcal{N} \qquad \Rightarrow \qquad \mathbf{F}_\mu \in \mathcal{N} \tag{PH}$$

henceforth, called **perturbation hypothesis**, or PH for short.

Observe that, from (3.22) and (PH), it follows that the $\varphi^{\varepsilon,\delta}$-regularization of $\mathbf{F}_\mu$ is an element of $\mathcal{N}^{\varepsilon,\delta}$ given by

$$\mathbf{F}_\mu^{\varepsilon,\delta} = \mathbf{F}^{\varepsilon,\delta} + \mathcal{P}_\mu^{\varepsilon,\delta},$$

where $\mathcal{P}_\mu^{\varepsilon,\delta}$ depends on μ_i and $\mathbf{P}_i$ and satisfy $\mathcal{P}_\mu^{\varepsilon,\delta} \to \mathbf{0}$ when $\mu \to \mathbf{0}$. Hence, we have that

$$\mathbf{F}_\mu^{\varepsilon,\delta} = \mathbf{F}^{\varepsilon,\delta} + \mathcal{P}_\mu^{\varepsilon,\delta} \to \mathbf{F}^{\varepsilon,\delta} \tag{3.24}$$

when $\mu \to \mathbf{0}$.

In particular, from (3.23) and (3.24) follows the existence of an open neighborhood $V \subset \mathbb{R}^4$ of $\mu = \mathbf{0}$ such that

$$\mu \in V \qquad \Rightarrow \qquad \mathbf{F}_\mu^{\varepsilon,\delta} \in \mathcal{U} \qquad \Rightarrow \qquad \mathbf{F}_\mu^{\varepsilon,\delta} \sim \mathbf{F}^{\varepsilon,\delta}. \tag{3.25}$$

That is, if we define the set

$$\mathcal{W}_i = \left\{ \mathbf{F}_i + \mu_i \mathbf{P}_i;\ \pi_i^{-1}(\mu_i) \in V \right\}$$

for every $i \in \{1,2,3,4\}$, then from (PH) follows that $\mathcal{W} = \mathcal{W}_1 \times \cdots \times \mathcal{W}_4$ is an open neighborhood of $\mathbf{F}$ in $\mathcal{N}$ such that

$$\mathbf{G} \in \mathcal{W} \qquad \Rightarrow \qquad \mathbf{G}^{\varepsilon,\delta} \sim \mathbf{F}^{\varepsilon,\delta}. \tag{3.26}$$

Now, suppose that a similar result to Theorem 2.2, which is valid for regular systems in $\mathcal{R}^k$, can be proved for Filippov systems in $\mathcal{D}_2^k$. More precisely, suppose that after a proper blow-up of $\mathbf{F}^{\varepsilon,\delta}$ we obtain a singular perturbation problem that recovers the sliding field of $\mathbf{F}$. Let $B(\cdot)$ be the operator given by the mentioned blow-up. Since blow-ups are just changes of variables, then from (3.26) follows that

$$\mathbf{G} \in \mathcal{W} \qquad \Rightarrow \qquad \mathbf{G}^{\varepsilon,\delta} \sim \mathbf{F}^{\varepsilon,\delta} \qquad \Rightarrow \qquad B(\mathbf{G}^{\varepsilon,\delta}) \sim B(\mathbf{F}^{\varepsilon,\delta}) \qquad \Rightarrow \qquad \mathbf{G}^s \sim \mathbf{F}^s,$$

i.e., $\mathbf{F}^s$ is structurally stable upon small perturbations of $\mathbf{F}$ in $\mathcal{N}$.

In particular, since Theorem 2.2 is actually truth in the set of regular systems $\mathcal{R}^k$, then we do have proved[2] the theorem bellow which, in a sense, serve as a converse to the Main Result of [46], where the structural stability of the regularization is studied given conditions on the piecewise field.

Theorem 3.1. *Let $\varphi : \mathbb{R} \to \mathbb{R}$ be a monotonous transition function, $\mathcal{N} \subset \mathcal{R}^k$ a subset satisfying the (PH) hypothesis and $\mathbf{F} \in \mathcal{N}$ such that $\mathbf{F}^\varepsilon$ is structurally stable in $\mathcal{N}^\varepsilon$. Then, there exists an open neighborhood $\mathcal{W} \subset \mathcal{N}$ of $\mathbf{F}$ such that*

$$\mathbf{G} \in \mathcal{W} \qquad \Rightarrow \qquad \mathbf{G}^s \sim \mathbf{F}^s,$$

i.e., $\mathbf{F}^s$ is structurally stable upon small perturbations of $\mathbf{F}$ in $\mathcal{N}$.

Whereas for systems in $\mathcal{D}_2^k$, we actually do have a similar result to Theorem 2.2: the Theorem 4.1, which can be found in [37, p. 498] and is explored over the next chapter of this text and, therefore, its details are omitted here. However, it remains an open problem to determine if this theorem is enough to assure the conjecture below.

Conjecture 3.2. *Let $\varphi : \mathbb{R} \to \mathbb{R}$ be a monotonous transition function, $\mathcal{N} \subset \mathcal{D}_2^k$ a subset satisfying the (PH) hypothesis and $\mathbf{F} \in \mathcal{N}$ such that $\mathbf{F}^{\varepsilon,\delta}$ is structurally stable in $\mathcal{N}^{\varepsilon,\delta}$. Then, there exists an open neighborhood $\mathcal{W} \subset \mathcal{N}$ of $\mathbf{F}$ such that*

$$\mathbf{G} \in \mathcal{W} \qquad \Rightarrow \qquad \mathbf{G}^s \sim \mathbf{F}^s,$$

i.e., $\mathbf{F}^s$ is structurally stable upon small perturbations of $\mathbf{F}$ in $\mathcal{N}$.

[2] Some natural and trivial adaptations on the notes are necessary though.

Using the conjecture above, we are able to study the structural stability of the sliding saddles realized in the previous section. In fact, it is easy to verify that the sets $\mathcal{C}_2$, $\mathcal{L}_2$ and $\mathcal{A}_2$ considered in Section 3.1 satisfy the (PH) hypothesis and, therefore, Conjecture 3.2 is applicable. In order to do so, for every example below, let $\varphi : \mathbb{R} \to \mathbb{R}$ be a monotonous transition function such that $\varphi(0) = 0$ which, in the examples below, assures that $(0,0)$ is an isolated singularity of the regularization $\mathbf{F}^{\varepsilon,\delta}$, regardless of the values of ε and δ.

Example 3.4 (Constant)**.** *Let $\mathbf{F} \in \mathcal{C}_2$ be the field obtained at Example 3.1, i.e., $\mathbf{F}$ is formed of constant fields and realizes a sliding saddle. It can be verified using (3.22) that its $\varphi^{\varepsilon,\delta}$-regularization is given by*

$$\mathbf{F}^{\varepsilon,\delta}(x,y) = \left(\varphi\left(\frac{x}{\delta}\right), -\varphi\left(\frac{y}{\varepsilon}\right)\right)$$

and, since $\varphi(0) = 0$, then $(0,0)$ is the only singularity of $\mathbf{F}^{\varepsilon,\delta}$, regardless of the values of ε and δ

Beyond that, one can verify that the Jacobian matrix of $\mathbf{F}^{\varepsilon,\delta}$ at $(0,0)$ is

$$\mathbf{J}_C = \begin{bmatrix} \frac{\varphi'(0)}{\delta} & 0 \\ 0 & -\frac{\varphi'(0)}{\varepsilon} \end{bmatrix},$$

whose eigenvalues are the real numbers $\frac{\varphi'(0)}{\delta} > 0$ and $-\frac{\varphi'(0)}{\varepsilon} < 0$, since $\varphi'(0) > 0$. That is, $(0,0)$ is an isolated hyperbolic singularity and, therefore, from Hartman-Grobman Theorem follows the existence of an open neighborhood $U \subset \mathbb{R}^2$ of $(0,0)$ where $\mathbf{F}^{\varepsilon,\delta}\big|_U \sim \mathbf{J}_C$. But, since $\mathbf{J}_C$ is hyperbolic, then it is structurally stable as a linear operator. Hence, from the continuity of the Jacobian operator follows the structural stability of $\mathbf{F}^{\varepsilon,\delta}\big|_U$ in $\mathcal{C}_2^{\varepsilon,\delta}$.

Therefore, from Conjecture 3.2 it follows that $\mathbf{F}^s\big|_U$ is structurally stable upon small perturbations of $\mathbf{F}\big|_U$ in $\mathcal{C}_2$. In other words, the sliding saddle realized by $\mathbf{F}$ is structurally stable in $\mathcal{C}_2$ at a neighborhood of the origin.

Example 3.5 (Linear)**.** *Let $\mathbf{F} \in \mathcal{L}_2$ be the field obtained at Example 3.2, i.e., $\mathbf{F}$ is formed of linear fields and realize a sliding saddle. It can be verified using (3.22) that its $\varphi^{\varepsilon,\delta}$-regularization is given by*

$$\mathbf{F}^{\varepsilon,\delta}(x,y) = \left(x + y\varphi\left(\frac{x}{\delta}\right)\varphi\left(\frac{y}{\varepsilon}\right), -2y - x\varphi\left(\frac{y}{\varepsilon}\right)\varphi\left(\frac{x}{\delta}\right)\right)$$

and, since $\varphi(0) = 0$, then $(0,0)$ is an isolated singularity of $\mathbf{F}^{\varepsilon,\delta}$, regardless of the values of ε and δ

Beyond that, one can verify that the Jacobian matrix of $\mathbf{F}^{\varepsilon,\delta}$ at $(0,0)$ is

$$\mathbf{J}_L = \begin{bmatrix} 1 & \varphi^2(0) \\ -\varphi^2(0) & -2 \end{bmatrix},$$

whose eigenvalues are the real numbers $1 > 0$ *and* $-2 < 0$*, since* $\varphi(0) = 0$*, which implies that* $\mathbf{J}_L$ *is hyperbolic.*

Therefore, the same argument used in Example 3.4 assures that the sliding saddle realized by $\mathbf{F}$ *is structurally stable upon small perturbations in* $\mathcal{L}_2$ *at a neighborhood of the origin.*

Example 3.6 (Affine)**.** *Let* $\mathbf{F} \in \mathcal{A}_2$ *be the field obtained at Example 3.3, i.e.,* $\mathbf{F}$ *is formed of affine fields and realizes a sliding saddle. It can be verified using (3.22) that its* $\varphi^{\varepsilon,\delta}$*-regularization is given by*

$$\mathbf{F}^{\varepsilon,\delta}(x,y) = \left(x + \varphi\left(\frac{x}{\delta}\right)\left(2 + y\varphi\left(\frac{y}{\varepsilon}\right)\right), -2y - \varphi\left(\frac{y}{\varepsilon}\right)\left(3 + x\varphi\left(\frac{x}{\delta}\right)\right)\right)$$

and, since $\varphi(0) = 0$*, then* $(0,0)$ *is an isolated singularity of* $\mathbf{F}^{\varepsilon,\delta}$*, regardless of the values of* ε *and* δ

Beyond that, one can verify that the Jacobian matrix of $\mathbf{F}^{\varepsilon,\delta}$ *at* $(0,0)$ *is*

$$\mathbf{J}_A = \begin{bmatrix} 1 + \frac{2\varphi'(0)}{\delta} & \varphi^2(0) \\ -\varphi^2(0) & -2 - \frac{3\varphi'(0)}{\varepsilon} \end{bmatrix},$$

whose eigenvalues are the real numbers $1 + \frac{2\varphi'(0)}{\delta} > 0$ *and* $-2 - \frac{3\varphi'(0)}{\varepsilon} < 0$*, since* $\varphi(0) = 0$ *and* $\varphi'(0) > 0$*, which implies that* $\mathbf{J}_A$ *is hyperbolic.*

Therefore, as before, the same argument used in Example 3.4 assures that the sliding saddle realized by $\mathbf{F}$ *is structurally stable upon small perturbations in* $\mathcal{A}_2$ *at a neighborhood of the origin.*

4 Double Discontinuity

In this chapter, reproducing the contents of [44], we investigate the dynamics and structural stability of a tridimensional piecewise system with a singular switching manifold similar to that studied in the previous chapter: the double discontinuity. In the first section, we properly state the problem and propose a solution in the second section. The third and fourth sections are then devoted to the use of this proposed framework to describe the dynamics presented by double discontinuities generated by constant and affine vector fields, respectively. Finally, in the last section, we study the structural stability. Many, if not all, of the results obtained here, can be naturally adapted to the planar case studied in the previous chapter.

4.1 Statement of the Problem

One of the fundamental hypothesis in the theory described in Chapter 1 is the fact that $0 \in \mathbb{R}$ is a **regular value** of the function $h : \mathbb{R} \to \mathbb{R}$ and, therefore, the switching manifold $\Sigma = h^{-1}(\{0\})$ is a regular surface. In that case, as we have seen, there exists at least one well-defined and established dynamics associated: the Filippov dynamics. A natural question to ask then is: can a Filippov-like dynamics be defined for the case when $0 \in \mathbb{R}$ is a **singular value** of the function $h : \mathbb{R} \to \mathbb{R}$, i.e., when the switching manifold is not a regular surface?

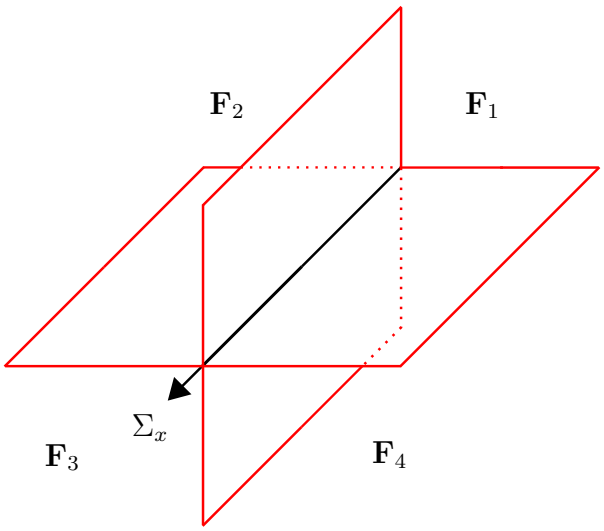

Figure 20 – Double discontinuity.

In the next sections, we would like to study the particular case known as the **double discontinuity**. This particular configuration of the switching manifold is the simplest one between the four singular configurations (known as Gutierrez-Sotomayor or simple manifolds) that, according to [26], breaks the regularity condition in a dynamically stable manner. The double discontinuity is described in detail below.

Let $\mathbf{F}_i : \mathbb{R}^3 \to \mathbb{R}^3$ be vector fields of class $C^k(\mathbb{R}^3)$ with $i \in \{1, 2, 3, 4\}$. The piecewise smooth vector field $\mathbf{F} : \mathbb{R}^3 \to \mathbb{R}^3$ given by

$$\mathbf{F}(x, y, z) = \begin{cases} \mathbf{F}_1(x, y, z), & \text{if } y \geqslant 0 \text{ and } z \geqslant 0, \\ \mathbf{F}_2(x, y, z), & \text{if } y \leqslant 0 \text{ and } z \geqslant 0, \\ \mathbf{F}_3(x, y, z), & \text{if } y \leqslant 0 \text{ and } z \leqslant 0, \\ \mathbf{F}_4(x, y, z), & \text{if } y \geqslant 0 \text{ and } z \leqslant 0, \end{cases} \tag{4.1}$$

and denoted by $\mathbf{F} = (\mathbf{F}_1, \mathbf{F}_2, \mathbf{F}_3, \mathbf{F}_4)$ is said to have a **double discontinuity** as switching manifold, see Figure 20. The set of all vector fields $\mathbf{F}$ defined as above will be denoted by

$$\mathcal{D}_3^k \equiv C^k(\mathbb{R}^3) \times C^k(\mathbb{R}^3) \times C^k(\mathbb{R}^3) \times C^k(\mathbb{R}^3)$$

and equipped with the Whitney product topology.

The double discontinuity, as defined above, consists of the planes xy and xz perpendicularly intersecting at the x-axis, $\Sigma_x = \{(x, 0, 0);\ x \in \mathbb{R}\}$. For points in $\Sigma \backslash \Sigma_x$, the ordinary Filippov dynamics described in Section 1.3 can be locally applied. However, for points $(x, 0, 0) \in \Sigma_x$ that theory cannot be directly applied. In fact, $\Sigma = h^{-1}(\{0\})$, where $h : \mathbb{R}^3 \to \mathbb{R}$ given by $h(x, y, z) = yz$ has $0 \in \mathbb{R}$ as a singular value, since $Dh(x, 0, 0)$ is not a surjective map for $(x, 0, 0) \in \Sigma_x$.

Therefore, we state the problem: given $\mathbf{F} \in \mathcal{D}_3^k$, can we define a Filippov-like dynamics over Σ_x? How does it generally behave there? In the next section, we present a framework, based on [8, 37, 40, 49], to approach this problem.

4.2 Framework

The first step consists of the application of a polar blow-up at the origin of the slice represented at Figure 21a or, in other words, a **cylindrical blow-up** at Σ_x. More specifically, assuming that the components of $\mathbf{F} \in \mathcal{D}_3^k$ can be written as

$$\mathbf{F}_i = (w_i, p_i, q_i),$$

we apply the blow-up $\phi_1 : \mathbb{R} \times S^1 \times \mathbb{R}^+ \to \mathbb{R}^3$ given by

$$\phi_1(x, \theta, r) = (x, r\cos\theta, r\sin\theta),$$

which induces a piecewise smooth vector field $\tilde{\mathbf{F}} = [(\phi_1)_*^{-1}\mathbf{F}] \circ \phi_1$ whose components are given by

$$\tilde{\mathbf{F}}_i = \left(w_i, \frac{q_i\cos\theta - p_i\sin\theta}{r}, p_i\cos\theta + q_i\sin\theta\right),$$

where w_i, p_i and q_i must be calculated at the point $\phi_1(x, \theta, r)$. We then define the set

$$\tilde{\mathcal{D}}_3^k = \left\{\tilde{\mathbf{F}} = [(\phi_1)_*^{-1}\mathbf{F}] \circ \phi_1;\ \mathbf{F} \in \mathcal{D}_3^k\right\}$$

of all blow-up induced vector fields.

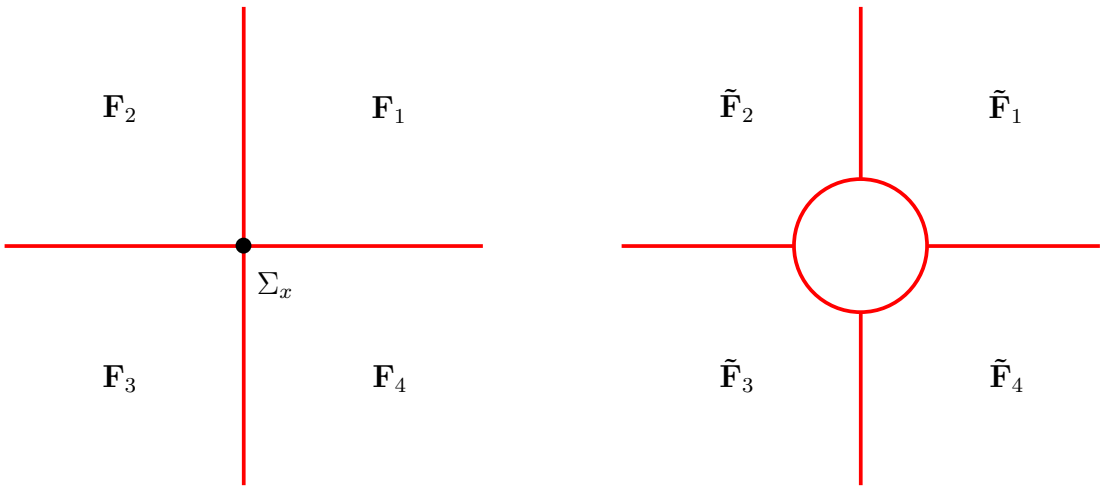

(a) Slice. (b) Blow-up.

Figure 21 – Framework process at slice-level.

An extremely important observation at this point consists in the theorem stated below with minor adaptations to our notation relative to the original one found in [37][1].

Theorem 4.1 (Retrieved from [37], page 498)**.** *The map* $\phi_1 : \mathbb{R} \times S^1 \times \mathbb{R}^+ \to \mathbb{R}^3$ *given by* $\phi_1(x, \theta, r) = (x, r\cos\theta, r\sin\theta)$ *induces a vector field* $\tilde{\mathbf{F}}$ *satisfying that any discontinuity* $q \in \tilde{\Sigma} = \phi_1^{-1}(\Sigma)$ *is regular.*

Hence, since the induced vector field $\tilde{\mathbf{F}}$ has only **regular discontinuities**, then classical Filippov theory, as presented at Section 1.3, is enough for its analysis. More precisely, we

[1] Up to our knowledge, this theorem where actually first stated in [8, p. 449]. However, [37] also provides analogous results for the triple, cone, and Whitney discontinuities. See Figure 1. Regarding the double discontinuity, similar versions of the theorem can also be found in [40], within the context of foliations, and in [49], which is actually a survey.

have now a piecewise smooth vector field $\tilde{\mathbf{F}}$ given by the four smooth vector fields $\tilde{\mathbf{F}}_i$, which induces the four **slow-fast systems**

$$\begin{cases} \dot{x} = w_i \\ r\dot{\theta} = q_i \cos\theta - p_i \sin\theta \\ \dot{r} = p_i \cos\theta + q_i \sin\theta \end{cases}, \tag{4.2}$$

where $\dot{\square} = {}^{d\square}/_{dt}$; w_i, p_i and q_i must be calculated at the point $\phi_1(x, \theta, r)$; and r is the time rescaling factor.

The study of the dynamics of (4.1) has therefore been reduced to the study of the slow-fast systems (4.2). In particular, the dynamics over Σ_x, previously undefined, can now be associated with (4.2) at $r = 0$, which is given by the combination of the dynamics of the **reduced system**

$$\begin{cases} \dot{x} = w_i \\ 0 = q_i \cos\theta - p_i \sin\theta \\ \dot{r} = p_i \cos\theta + q_i \sin\theta \end{cases} \tag{4.3}$$

and the dynamics of the **layer system**

$$\begin{cases} x' = 0 \\ \theta' = q_i \cos\theta - p_i \sin\theta \\ r' = 0 \end{cases}, \tag{4.4}$$

where $\square' = {}^{d\square}/_{d\tau}$ with $t = r\tau$; and the components w_i, p_i and q_i must be calculated at the point $\phi_1(x, \theta, 0) = (x, 0, 0)$.

More geometrically, the dynamics over Σ_x in (4.1) can now be associated to the dynamics over the cylinder $C = \mathbb{R} \times S^1$ divided in the four infinite stripes

$$S_2 = \mathbb{R} \times [{}^{\pi}/_{2}, \pi], \qquad S_1 = \mathbb{R} \times [0, {}^{\pi}/_{2}],$$
$$S_3 = \mathbb{R} \times [\pi, {}^{3\pi}/_{2}], \qquad S_4 = \mathbb{R} \times [{}^{3\pi}/_{2}, 2\pi],$$

as represented at Figure 22, where the slow-fast systems given by (4.3) and (4.4) acts, respectively. As we previously stated at Theorem 4.1, the four lines where these stripes intersect admits at most regular discontinuities. Finally, the analysis of the dynamics on each stripe S_i can then be carried out using GSP-Theory.

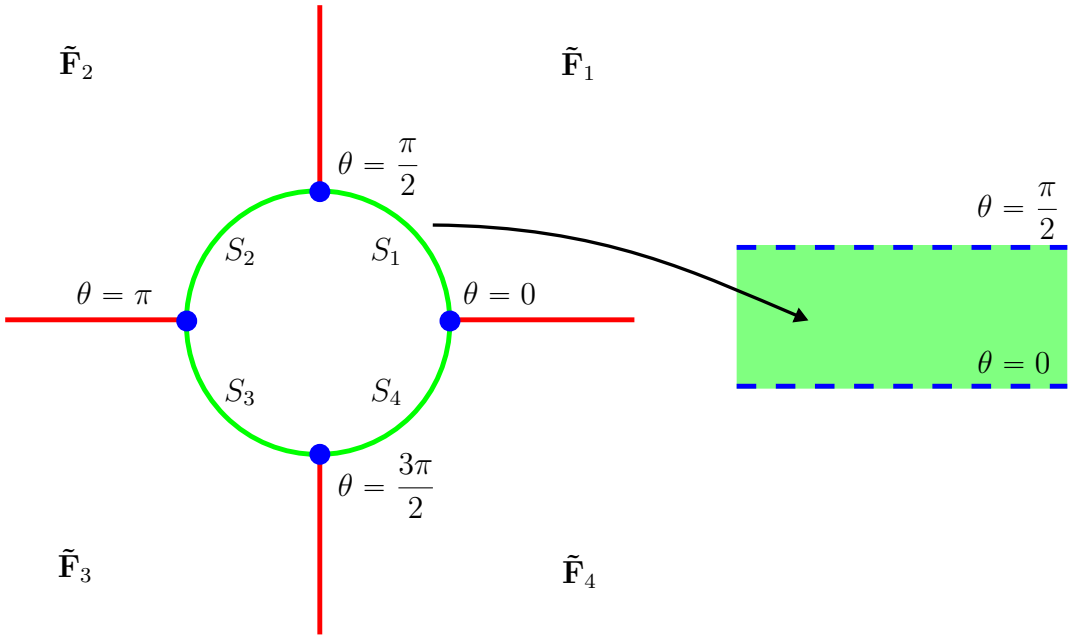

Figure 22 – Green cylinder C divided in the four stripes S_i. A scheme of the stripe S_1 is also put in evidence.

In particular, the first two equations of the system (4.3) are independent of r and, therefore, it can be decoupled as

$$\begin{cases} \dot{x} = w_i \\ 0 = q_i \cos\theta - p_i \sin\theta \end{cases}, \tag{4.5}$$

which gives the **reduced dynamics** over S_i; and

$$\dot{r} = p_i \cos\theta + q_i \sin\theta, \tag{4.6}$$

which gives the respective **slow radial dynamics** or, in other words, it indicates how the external dynamics communicates with the dynamics (4.5) over the cylinder: entering ($\dot{r} > 0$), leaving ($\dot{r} < 0$) or staying ($\dot{r} = 0$) at S_i.

Analogously, the first two equations of the system (4.4) are independent of r and, therefore, it can also be decoupled as

$$\begin{cases} x' = 0 \\ \theta' = q_i \cos\theta - p_i \sin\theta \end{cases}, \tag{4.7}$$

which gives the **layer dynamics** over S_i; and

$$r' = 0, \tag{4.8}$$

which gives the respective **fast radial dynamics** over the cylinder.

Summarizing, we conclude that the dynamics over Σ_x behaves as described in the **fundamental lemma** below, whose proof consists in the analysis done above.

Lemma 4.1 (Fundamental Dynamics)**.** *Given $\mathbf{F} \in \mathcal{D}_3^k$ with components $\mathbf{F}_i = (w_i, p_i, q_i)$, let $\tilde{\mathbf{F}} \in \tilde{\mathcal{D}}_3^k$ be the vector field induced by the blow-up*

$$\phi_1(x, \theta, r) = (x, r\cos\theta, r\sin\theta).$$

Then, this blow-up associates the dynamics over Σ_x with the following dynamics over the cylinder $C = \mathbb{R} \times S^1 = S_1 \cup \ldots \cup S_4$: over each stripe S_i acts a slow-fast dynamics whose reduced dynamics is given by

$$\begin{cases} \dot{x} = w_i \\ 0 = q_i\cos\theta - p_i\sin\theta \end{cases}, \tag{4.9}$$

with slow radial dynamics $\dot{r} = p_i\cos\theta + q_i\sin\theta$; and layer dynamics given by

$$\begin{cases} x' = 0 \\ \theta' = q_i\cos\theta - p_i\sin\theta \end{cases}, \tag{4.10}$$

with fast radial dynamics $r' = 0$. Finally, at every equation above the functions w_i, p_i and q_i must be calculated at the point $\phi_1(x, \theta, 0) = (x, 0, 0)$.

In order to perform a deeper analysis of the dynamics given by Lemma 4.1 with GSP-Theory as described at Section 2.2, let S_i be one of the cylinder's stripe and let

$$\mathcal{M}_i = \big\{(x, \theta) \in \mathbb{R} \times S^1;\ f_i(x, \theta, 0) = 0\big\}$$

be its slow manifold, where $f_i(x, \theta, 0) = q_i\cos\theta - p_i\sin\theta$.

Given $(x_0, \theta_0, 0) \in \mathcal{M}_i \times \{0\}$, the Jacobian matrix of the complete layer system (4.4) over this point is

$$\mathbf{J}_{\text{fast}} = \begin{bmatrix} 0 & 0 & 0 \\ (f_i)_x & (f_i)_\theta & 0 \\ 0 & 0 & 0 \end{bmatrix},$$

where $(f_i)_x$ and $(f_i)_\theta$ represents the partial derivatives calculated at $(x_0, \theta_0, 0)$. The eigenvalues of this matrix are the elements of the set $\{0, 0, (f_i)_\theta\}$ and, therefore, (x_0, θ_0) is normally hyperbolic if, and only if, $(f_i)_\theta \neq 0$. However, we observe that, since we are over the slow manifold, then $(f_i)_\theta = 0$ leads to the homogeneous linear system

$$\begin{cases} f_i = 0 \\ (f_i)_\theta = 0 \end{cases} \sim \begin{cases} q_i \cos\theta - p_i \sin\theta = 0 \\ q_i \sin\theta + p_i \cos\theta = 0 \end{cases} \sim \begin{bmatrix} \cos\theta & -\sin\theta \\ \sin\theta & \cos\theta \end{bmatrix} \begin{bmatrix} q_i \\ p_i \end{bmatrix} = \begin{bmatrix} 0 \\ 0 \end{bmatrix}$$

whose unique solution is the trivial, $p_i = q_i = 0$, since the trigonometrical matrix above is invertible ($\det \equiv 1$) for every $\theta \in S^1$ and, therefore, we conclude that $(f_i)_\theta \neq 0$ whenever

$$p_i \neq 0 \quad \text{or} \quad q_i \neq 0, \tag{WFH}$$

henceforth, called **weak fundamental hypothesis**, or WFH for short. We also observe that

$$(f_i)_x = (q_i)_x \cos\theta - (p_i)_x \sin\theta$$

which, as above, supposing $(f_i)_x = 0$ leads to the homogeneous linear system

$$\begin{cases} q_i \cos\theta - p_i \sin\theta = 0 \\ (q_i)_x \cos\theta - (p_i)_x \sin\theta = 0 \end{cases} \sim \begin{bmatrix} q_i & p_i \\ (q_i)_x & (p_i)_x \end{bmatrix} \begin{bmatrix} \cos\theta \\ \sin\theta \end{bmatrix} = \begin{bmatrix} 0 \\ 0 \end{bmatrix}$$

which only admits the absurd solution $\cos\theta = \sin\theta = 0$ if the matrix above is invertible. Hence, we can ensure $(f_i)_x \neq 0$ by imposing this absurd, i.e.,

$$0 \neq \det \begin{bmatrix} q_i & p_i \\ (q_i)_x & (p_i)_x \end{bmatrix} = q_i (p_i)_x - p_i (q_i)_x \tag{SFH}$$

which always implies the weak fundamental hypothesis and, therefore, will be called **strong fundamental hypothesis**, or SFH for short.

Theorem 4.2. *The radial dynamics can only be transversal ($\dot{r} \neq 0$) to the cylinder C over the slow manifold $\mathcal{M}_i$. More over, under (WFH), it is in fact transversal.*

Proof. The first part of the statement is assured by Lemma 4.1. For the second part, just observe that $\dot{r} = -(f_i)_\theta \neq 0$ under (WFH). □

Theorem 4.3. *The slow manifold $\mathcal{M}_i$ is locally a graph $(x, \theta(x))$ under (WFH). However, if $\|(f_i)_\theta\|$ admits a global positive minimum, then $\mathcal{M}_i$ is globally a graph $(x, \theta(x))$. Either way, $\theta(x)$ is of class C^k.*

Proof. The first part is assured by the usual Implicit Function Theorem applied to $f_i(x_0, \theta_0, 0) = 0$ over $\mathcal{M}_i$, since under (WFH) we have $\|(f_i)_\theta\| > 0$. Analogously, the second part is assured by the Global Implicit Function Theorem found in [57, p. 253], which requires a stronger hypothesis. □

Theorem 4.4. *The slow manifold $\mathcal{M}_i$ is normally hyperbolic at every point that satisfies (WFH).*

Proof. Just observe that the only non-trivial eigenvalue, $(f_i)_\theta$, is non-zero under (WFH). □

Theorem 4.5. *The hyperbolic singularities of the reduced system (4.9) acts as hyperbolic saddle or node singularities of S_i under (WFH).*

Proof. Let $\mathbf{P} = (x_0, \theta_0) \in \mathcal{M}_i$ be a hyperbolic singularity of the reduced system, i.e., $w_i(x_0, 0, 0) = 0$ with eigenvalue $\lambda_1 = (w_i)_x(x_0, 0, 0) \neq 0$. We have two possibilities:

- $\lambda_1 > 0 \Rightarrow (j^s, j^u) = (0, 1)$; or
- $\lambda_1 < 0 \Rightarrow (j^s, j^u) = (1, 0)$,

where j^s and j^u are the dimensions of the stable and unstable manifolds of $\mathbf{P}$ with respect to the reduced system, respectively.

On the other hand, under (WFH) we also have the non-trivial eigenvalue $\lambda_2 = (f_i)_\theta(x_0, \theta_0, 0) \neq 0$ for the layer system and, therefore, the two possibilities:

- $\lambda_2 > 0 \Rightarrow (k^s, k^u) = (0, 1)$; or
- $\lambda_2 < 0 \Rightarrow (k^s, k^u) = (1, 0)$,

where k^s and k^u are the dimensions of the stable and unstable manifolds of $\mathbf{P}$ with respect to the layer system, respectively.

Hence, observing that $j = \dim \mathbf{P} = 0$ and remembering Theorem 2.1, any combination of the signs of λ_1 and λ_2 leads to the total sum of dimensions

$$(j^s + k^s) + (j^u + k^u) = 2 = \dim S_i,$$

and, therefore, $\mathbf{P}$ acts as a hyperbolic singularity of S_i. Finally, the saddle-node duality comes from the fact that both non-trivial eigenvalues above have no imaginary parts. □

In other words, under (WFH), the slow manifold $\mathcal{M}_i$ is, at the very least, locally a graph. More than that, it is the entry-point for the external dynamics to the cylinder. Besides that, it is normally hyperbolic at its full extension, assuring then not only persistence and well-behaved stability for its invariant compact parts, but also that $\mathcal{M}_i$ is always attracting or repelling the surrounding (layer) dynamics. All these nice

properties come at the low cost of (WFH). Therefore, it is not a surprise that, for every system studied below, we require at least (WFH), but also always test for (SFH), whose importance will become clear when studying affine systems.

4.3 Constant Dynamics

Let $\mathcal{C}_3 \subset \mathcal{D}_3^k$ be the set of all piecewise smooth vector fields $\mathbf{F}$ with a double discontinuity given by the constant vector fields

$$\mathbf{F}_i(x, y, z) = (d_{i1}, d_{i2}, d_{i3}), \tag{4.11}$$

where $d_{ij} \in \mathbb{R}$ for all i and j. According to Lemma 4.1, the dynamics over Σ_x of such a field is blow-up associated to the following dynamics over the cylinder $C = \mathbb{R} \times S^1 = S_1 \cup \ldots \cup S_4$: over each stripe S_i acts a slow-fast dynamics whose reduced dynamics is given by

$$\begin{cases} \dot{x} = d_{i1} \\ 0 = d_{i3} \cos\theta - d_{i2} \sin\theta \end{cases}, \tag{4.12}$$

with radial slow dynamics $\dot{r} = d_{i2} \cos\theta + d_{i3} \sin\theta$; and layer dynamics given by

$$\begin{cases} x' = 0 \\ \theta' = d_{i3} \cos\theta - d_{i2} \sin\theta \end{cases}, \tag{4.13}$$

with radial fast dynamics $r' = 0$.

Besides that, for (4.11), we have $p_i = d_{i2}$ and $q_i = d_{i3}$ so that (WFH) is satisfied as long as

$$d_{i2} \neq 0 \quad \text{or} \quad d_{i3} \neq 0, \tag{4.14}$$

whereas (SFH) is **never** satisfied, since $(p_i)_x = (q_i)_x = 0$.

Therefore, our goal at this section is to fully describe the dynamics of (4.11) over the cylinder C under the hypothesis (4.14). In order to do so, we are going to systematically analyze the slow-fast systems (4.12)–(4.13) for the two cases suggested by (4.14). This analysis takes place in Sections 4.3.1 and 4.3.2, resulting in Theorem 4.6 stated and exemplified at Section 4.3.3.

4.3.1 Case $d_{i2} \neq 0$

In order to explicitly define the slow manifold $\mathcal{M}_i$, observe that whenever $\cos\theta \neq 0$ the second equation of (4.12) gives us

$$0 = d_{i3}\cos\theta - d_{i2}\sin\theta \Leftrightarrow \tan\theta = \frac{d_{i3}}{d_{i2}} \Leftrightarrow \theta = \arctan\left(\frac{d_{i3}}{d_{i2}}\right) + n\pi = \theta_i + n\pi,$$

where $n \in \mathbb{Z}$. Therefore, without loss of generality, the slow manifold can be written as $\mathcal{M}_i = L_i \cup L_i^\pi$, where

$$L_i = \{(x,\theta) \in \mathbb{R} \times [0, 2\pi]\,;\ \theta = \theta_i\} \text{ and}$$
$$L_i^\pi = \{(x,\theta) \in \mathbb{R} \times [0, 2\pi]\,;\ \theta = \theta_i + \pi\},$$

which consists of two straight lines inside the cylinder $C = \mathbb{R} \times [0, 2\pi]$, as the red part of Figure 23.

Observe that, since $\theta_i \in \left(-\frac{\pi}{2}, \frac{\pi}{2}\right)$ and $\theta_i + \pi \in \left(\frac{\pi}{2}, \frac{3\pi}{2}\right)$, then either $L_i \subset S_1$ and $L_i^\pi \subset S_3$ or $L_i \subset S_4$ and $L_i^\pi \subset S_2$. In other words, this straight lines are always at intercalated stripes. Therefore, a given stripe S_i might or might not contain one of this straight lines, depending exclusively on the value of θ_i.[2] This completes the qualitative analysis of the shape of the slow manifold.

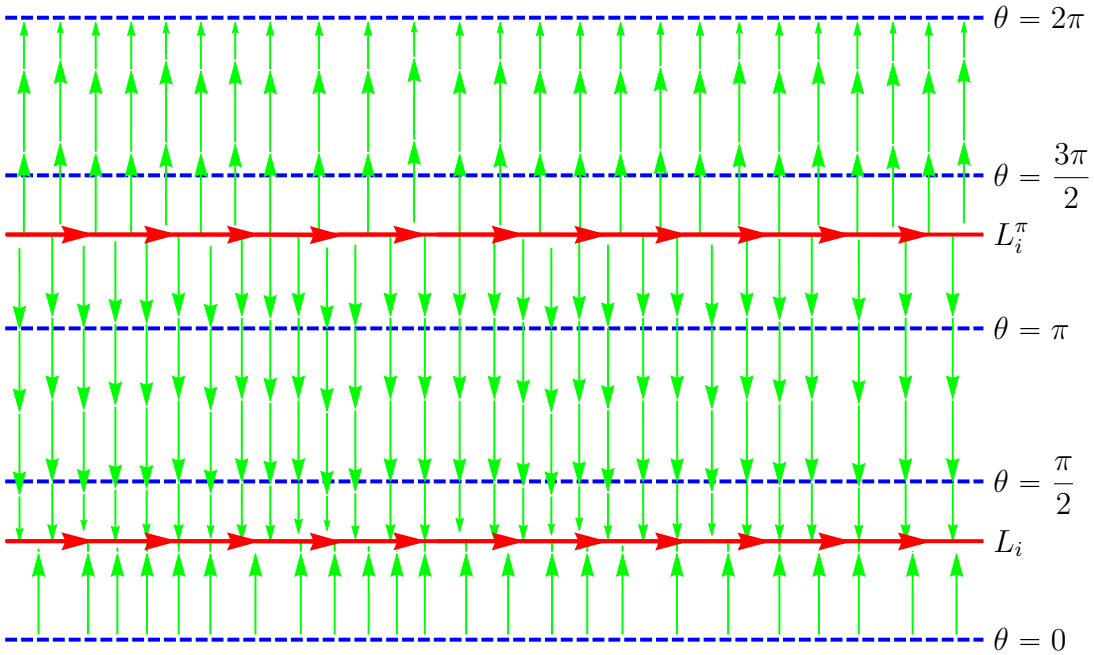

Figure 23 – Constant double discontinuity dynamics for $d_{i1} = 1 > 0$, $d_{i2} = 0.7 > 0$ and $d_{i3} = 1 > 0$. At this example we have $\theta_i = \arctan\frac{1}{0.7} \approx 0.96$. Therefore, for example, S_1 has $\theta = \theta_i$ as an attracting visible part of the slow manifold; whereas S_2 has none.

[2] In particular, when $d_{i3} = 0$ we have $\theta_i = 0$ and, therefore, the straight lines L_i and L_i^π are given by $\theta = 0$ and $\theta = \pi$, respectively, which are part of the stripes' boundary.

Over both the straight lines $\mathcal{M}_i = L_i \cup L_i^\pi$, we have the one-dimensional dynamics given by the first equation of (4.12), i.e., $\dot{x} = d_{i1}$. Analyzing this equation we observe that, considering the usual growth direction of the x-axis, the dynamics over $\mathcal{M}_i$ is increasing if $d_{i1} > 0$ and decreasing if $d_{i1} < 0$. This completes the qualitative analysis of the reduced dynamics.

Regarding the layer dynamics, we have the layer system (4.13) which says that for each fixed value of $x \in \mathbb{R}$, we have a one-dimensional dynamics given by the second equation of (4.13). In particular, assuming that $\cos\theta > 0$ and $d_{i2} > 0$, then

$$\theta' > 0 \Leftrightarrow d_{i3}\cos\theta - d_{i2}\sin\theta > 0 \Leftrightarrow \tan\theta < \frac{d_{i3}}{d_{i2}} \Leftrightarrow \theta < \arctan\left(\frac{d_{i3}}{d_{i2}}\right) = \theta_i,$$

since the arctangent function is strictly increasing. Likewise and under the same conditions, we have that

$$\theta' < 0 \Leftrightarrow \theta > \arctan\left(\frac{d_{i3}}{d_{i2}}\right) = \theta_i$$

and, therefore, we conclude that for $d_{i2} > 0$, the straight line L_i is attractor of surrounding layer dynamics and, therefore, L_i^π is a repellor, as the green part of Figure 23. An analogous study for $d_{i2} < 0$ allows us to reach the results summarized in Table 1.

	$d_{i2} < 0$	$d_{i2} > 0$
L_i	repellor	attractor
L_i^π	attractor	repellor

Table 1 – Layer dynamics around the straight lines L_i and L_i^π that compose the slow manifold $\mathcal{M}_i = L_i \cup L_i^\pi$.

Finally, at $\cos\theta = 0$ with $d_{i2} \neq 0$ the reduced system (4.12) tells us that $\mathcal{M}_i = \varnothing$ and, therefore, there is only the fast dynamics (4.13) which reduces to

$$\begin{cases} x' &= 0 \\ \theta' &= -d_{i2} \end{cases} \quad \text{and} \quad \begin{cases} x' &= 0 \\ \theta' &= d_{i2} \end{cases}$$

for $\theta = \dfrac{\pi}{2}$ and $\theta = \dfrac{3\pi}{2}$, respectively, whose dynamics is consistent with Table 1. This completes the qualitative analysis of the layer dynamics and, therefore, the qualitative analysis of this case. See Example 4.1.

4.3.2 Case $d_{i2} = 0$

Now, the reduced system (4.12) can be written as

$$\begin{cases} \dot{x} &= d_{i1} \\ 0 &= d_{i3}\cos\theta \end{cases}, \tag{4.15}$$

whose slow manifold $\mathcal{M}_i$ is implicitly given by the equation $0 = d_{i3}\cos\theta$ which actually means $0 = \cos\theta$, since we are under (WFH) and, therefore, $d_{i3} \neq 0$. In other words, $\mathcal{M}_i = L_i \cup L_i^\pi$ with L_i and L_i^π being the straight lines given by $\theta = \dfrac{\pi}{2}$ and $\theta = \dfrac{3\pi}{2}$, respectively.[3] The dynamics over and around $\mathcal{M}_i$ behaves exactly as in the case $d_{i2} \neq 0$, but exchanging d_{i2} with d_{i3} at Table 1.

4.3.3 Theorem and Examples

Summarizing, we conclude that the dynamics over Σ_x for constant fields behaves as described in the theorem below, whose proof consists in the analysis done above in Sections 4.3.1 and 4.3.2.

Theorem 4.6 (Constant Dynamics)**.** *Given $\mathbf{F} \in \mathcal{C}_3$ with constant components $\mathbf{F}_i = (d_{i1}, d_{i2}, d_{i3})$ such that $d_{i2} \neq 0$ or $d_{i3} \neq 0$, let $\tilde{\mathbf{F}} \in \tilde{\mathcal{C}}_3$ be the vector field induced by the blow-up $\phi_1(x, \theta, r) = (x, r\cos\theta, r\sin\theta)$. Then, this blow-up associates the dynamics over Σ_x with the following dynamics over the cylinder $C = \mathbb{R} \times S^1 = S_1 \cup \ldots \cup S_4$: over each stripe S_i acts a slow-fast dynamics whose slow manifold is given by $\mathcal{M}_i = L_i \cup L_i^\pi$, where L_i^π is a π-translation of L_i in θ and*

1. *case $d_{i2} \neq 0$, then*

$$L_i = \left\{(x, \theta) \in \mathbb{R} \times [0, 2\pi]\,;\ \theta = \arctan\left(\frac{d_{i3}}{d_{i2}}\right)\right\};$$

2. *case $d_{i2} = 0$ and $d_{i3} \neq 0$, then*

$$L_i = \left\{(x, \theta) \in \mathbb{R} \times [0, 2\pi]\,;\ \theta = \frac{\pi}{2}\right\};$$

which, in both cases, consists of two straight lines inside the cylinder C, possibly invisible relative to S_i. Over this straight lines acts the reduced dynamics $\dot{x} = d_{i1}$ and, around then, acts the layer dynamics described in Table 1, but exchanging d_{i2} with d_{i3} if $d_{i2} = 0$.

[3] Here, again, the straight lines L_i and L_i^π are part of the boundary of the stripes.

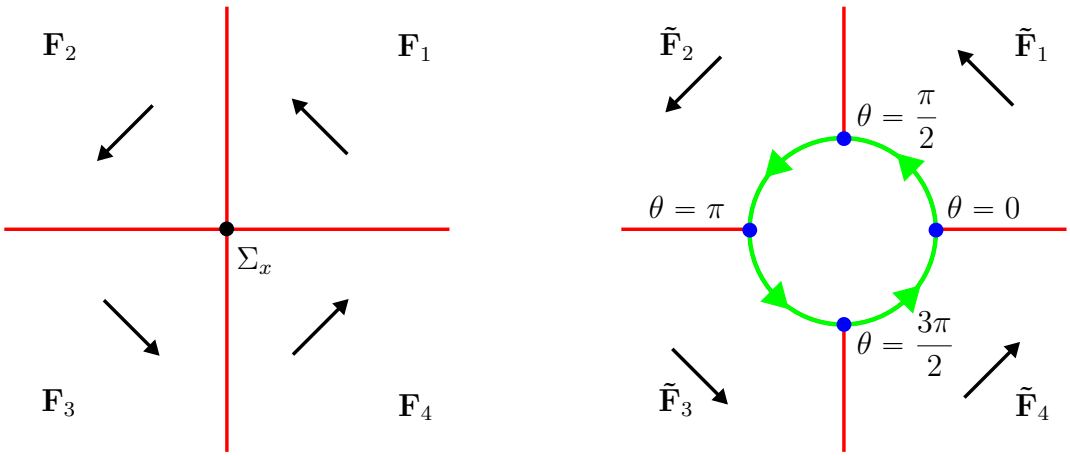

(a) Before the blow-up. (b) After the blow-up.

Figure 24 – Slices of the system studied at Example 4.1.

Example 4.1. *Let* $\mathbf{F} \in \mathcal{C}_3$ *be given by the constant vector fields*

$$\mathbf{F}_2(x,y,z) = (1,-1,-1), \qquad \mathbf{F}_1(x,y,z) = (1,-1,1),$$
$$\mathbf{F}_3(x,y,z) = (1,1,-1), \qquad \mathbf{F}_4(x,y,z) = (1,1,1),$$

that behaves as represented at Figure 24a. Using Theorem 4.6 we can verify that, over the cylinder C *given by the blow-up of* Σ_x*, this system behaves as expected, i.e., as represented at Figure 24b.*

For instance, over the stripe $S_1 = \mathbb{R} \times [0, \pi/2]$ *we have*

$$(d_{11}, d_{12}, d_{13}) = \mathbf{F}_1(x,y,z) = (1,-1,1)$$

such that, according to Theorem 4.6, induces over S_1 *a slow-fast system with* $L_1 \subset \mathcal{M}_1$ *given by*

$$\theta = \theta_1 = \arctan\left(\frac{d_{13}}{d_{12}}\right) = \arctan\left(\frac{1}{-1}\right) = -\frac{\pi}{4},$$

and, therefore, the slow manifold $\mathcal{M}_1$ *consists of the straight lines* $L_1 \subset S_4$ *and* $L_1^\pi \subset S_2$ *given by* $\theta = \theta_1 = -\dfrac{\pi}{4}$ *and* $\theta = \theta_1 + \pi = \dfrac{3\pi}{4}$*, respectively. In particular, none of these lines are visible at* S_1*. Over these lines acts the reduced dynamics* $\dot{x} = d_{11} = 1$*. Finally, since* $d_{12} = -1 < 0$*, then* L_1 *is repellor and* L_1^π *is attractor of surrounding layer dynamics, according to Table 1.*

Therefore, we conclude that the dynamics generated by $\mathbf{F}_1$ *over the whole cylinder* C *behaves as represented in Figure 25. In particular, the dynamics over the stripe*

S_1 behaves as represented in Figure 24b. The dynamics over the other stripes can be similarly verified to be as represented. □

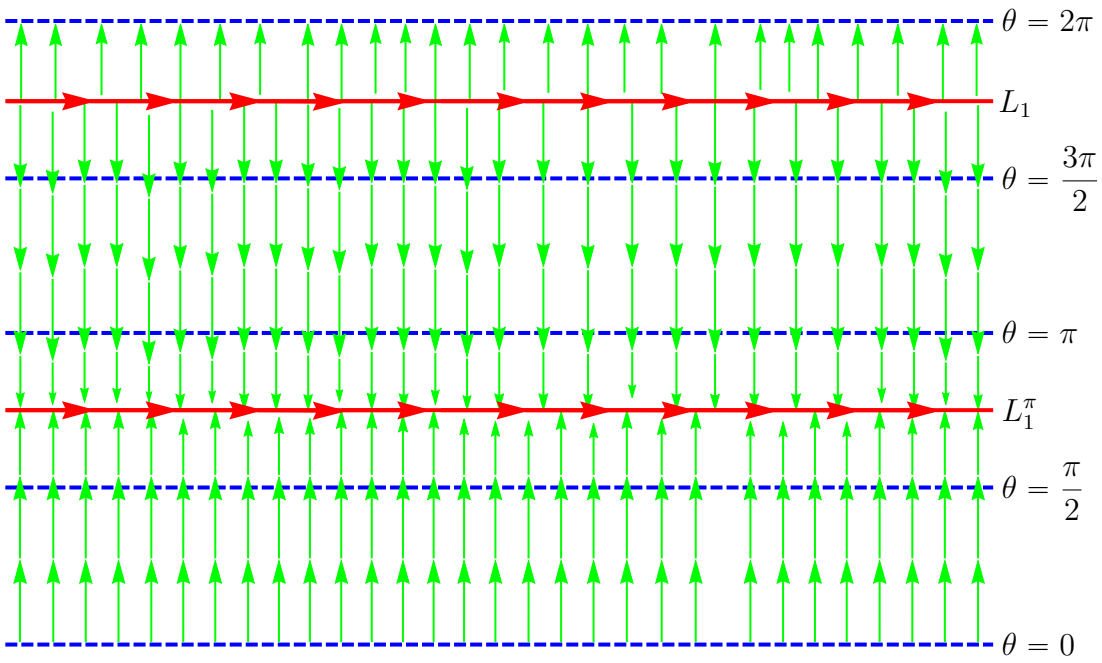

Figure 25 – Dynamics over C generated by the field $\mathbf{F}_1$ studied at Example 4.1. The dynamics over S_1 behaves as represented in Figure 24b.

4.4 Affine Dynamics

Let $\mathcal{A}_3 \subset \mathcal{D}_3^k$ be the set of all piecewise smooth vector fields $\mathbf{F}$ with a double discontinuity given by the affine vector fields

$$\begin{aligned}\mathbf{F}_i(x,y,z) = (&a_{i1}x + b_{i1}y + c_{i1}z + d_{i1},\\ &a_{i2}x + b_{i2}y + c_{i2}z + d_{i2},\\ &a_{i3}x + b_{i3}y + c_{i3}z + d_{i3}),\end{aligned} \tag{4.16}$$

where $a_{ij}, b_{ij}, c_{ij}, d_{ij} \in \mathbb{R}$ for all i and j. According to Lemma 4.1, the dynamics over Σ_x of such a field is blow-up associated to the following dynamics over the cylinder $C = \mathbb{R} \times S^1 = S_1 \cup \ldots \cup S_4$: over each stripe S_i acts a slow-fast dynamics whose reduced dynamics is given by

$$\begin{cases} \dot{x} = a_{i1}x + d_{i1} \\ 0 = (a_{i3}x + d_{i3})\cos\theta - (a_{i2}x + d_{i2})\sin\theta \end{cases}, \tag{4.17}$$

with radial slow dynamics $\dot{r} = (a_{i2}x + d_{i2})\cos\theta + (a_{i3}x + d_{i3})\sin\theta$; and layer dynamics given by

$$\begin{cases} x' = 0 \\ \theta' = (a_{i3}x + d_{i3})\cos\theta - (a_{i2}x + d_{i2})\sin\theta \end{cases}, \tag{4.18}$$

with radial fast dynamics $r' = 0$.

Besides that, for (4.16), we have $p_i = a_{i2}x + d_{i2}$ and $q_i = a_{i3}x + d_{i3}$ so that (WFH) is satisfied as long as

$$a_{i2}x + d_{i2} \neq 0 \quad \text{or} \quad a_{i3}x + d_{i3} \neq 0, \tag{4.19}$$

whereas, since $(p_i)_x = a_{i2}$ and $(q_i)_x = a_{i3}$, then (SFH) is satisfied as long as

$$\begin{aligned} 0 \neq p_i(q_i)_x - q_i(p_i)_x = \\ = (a_{i2}x + d_{i2})a_{i3} - (a_{i3}x + d_{i3})a_{i2} = \\ = a_{i3}d_{i2} - a_{i2}d_{i3} =: \gamma_i, \end{aligned} \tag{4.20}$$

which not only assures the fundamental hypothesis but also avoids the already studied constant case, as we will see below.

As in the constant case, our goal at this section is to fully describe the dynamics of (4.16) over the cylinder C under the hypothesis (4.20). In order to do so, we are going to systematically analyze the slow-fast systems (4.17)–(4.18) for the cases suggested by (4.19) and outlined at Table 2.

	$a_{i2}x + d_{i2} \neq 0$	$a_{i2}x + d_{i2} = 0$
$a_{i2} \neq 0$	A	B
$a_{i2} = 0$	C	D

Table 2 – Division (4.16) dynamics in study cases.

Observe that case (B) actually complements case (A). Moreover, observe that at case (D) we have $a_{i2} = 0$ and $d_{i2} = 0$ which implies the absurd $\gamma_i = 0$. Therefore, cases (A) and (B) complement each other and it will be studied at Section 4.4.1; case (C) will be studied at Section 4.4.2. The resulting Theorem 4.7 is stated and exemplified at Section 4.4.3.

4.4.1 Case $a_{i2} \neq 0$

Lets start with case (A), i.e., assume that $a_{i2} \neq 0$ and $a_{i2}x + d_{i2} \neq 0$. In order to explicitly define $\mathcal{M}_i$, observe that whenever $\cos\theta \neq 0$ the second equation of (4.17) gives us

$$
\begin{aligned}
0 &= (a_{i3}x + d_{i3})\cos\theta - (a_{i2}x + d_{i2})\sin\theta \Leftrightarrow \\
&\Leftrightarrow \tan\theta = \frac{a_{i3}x + d_{i3}}{a_{i2}x + d_{i2}} =: h(x) \Leftrightarrow \\
&\Leftrightarrow \theta = \arctan\left(\frac{a_{i3}x + d_{i3}}{a_{i2}x + d_{i2}}\right) + n\pi = \theta_i(x) + n\pi,
\end{aligned}
$$

where $n \in \mathbb{Z}$. Therefore, without loss of generality, the slow manifold can be written as $\mathcal{M}_i = H_i \cup H_i^\pi$, where

$$
\begin{aligned}
H_i &= \{(x,\theta) \in \mathbb{R} \times [0, 2\pi];\ \theta = \theta_i(x)\} \text{ and} \\
H_i^\pi &= \{(x,\theta) \in \mathbb{R} \times [0, 2\pi];\ \theta = \theta_i(x) + \pi\},
\end{aligned}
$$

which consists of two arctangent-normalized hyperboles inside the cylinder $C = \mathbb{R} \times S^1$. In fact, since $a_{i2} \neq 0$, then $h(x)$ is a hyperbole such that

$$
\frac{d}{dx}h(x) = \frac{d}{dx}\left[\frac{a_{i3}x + d_{i3}}{a_{i2}x + d_{i2}}\right] = \frac{a_{i3}d_{i2} - d_{i3}a_{i2}}{(a_{i2}x + d_{i2})^2} = \frac{\gamma_i}{(a_{i2}x + d_{i2})^2}
$$

or, in other words, it is an increasing hyperbole if $\gamma_i > 0$ and decreasing if $\gamma_i < 0$[4]. Besides that, observe that $h(x)$ has a vertical asymptote at

$$
a_{i2}x + d_{i2} = 0 \Leftrightarrow x = -\frac{d_{i2}}{a_{i2}} =: \alpha_i
$$

which satisfies

$$
\lim_{x \to \alpha_i^\pm} h(x) = \mp\infty \quad \text{and} \quad \lim_{x \to \alpha_i^\pm} h(x) = \pm\infty
$$

if $\gamma_i > 0$ and $\gamma_i < 0$, respectively; and $h(x)$ has a horizontal asymptote at

$$
\lim_{x \to \pm\infty} h(x) = \lim_{x \to \pm\infty}\left(\frac{a_{i3}x + d_{i3}}{a_{i2}x + d_{i2}}\right) = \frac{a_{i3}}{a_{i2}}.
$$

Translating the information above about the hyperbole $h(x)$ to the arctangent-normalized hyperbole H_i, we get that it

- is an increasing curve if $\gamma_i > 0$ and decreasing if $\gamma_i < 0$;

[4] If $\gamma_i = 0$, then $h(x)$ is a constant function and, therefore, H_i and H_i^π are straight lines. In other words, the constant case is recovered.

- has a vertical asymptote at $x = \alpha_i$ which satisfies

$$\lim_{x\to\alpha_i^{\pm}} \theta_i(x) = \mp\frac{\pi}{2} \quad \text{and} \quad \lim_{x\to\alpha_i^{\pm}} \theta_i(x) = \pm\frac{\pi}{2}$$

  if $\gamma_i > 0$ and $\gamma_i < 0$, respectively;

- has a horizontal asymptote at $\theta = \arctan\left(\dfrac{a_{i3}}{a_{i2}}\right) =: \beta_i$.

More precisely, the hyperbole H_i behave as the red part of Figure 26a. However, putting together the hyperboles H_i and H_i^{π} we get that they actually behave as two arctangent-like curves as represented at Figure 26b.

These arctangent-like curves will be denoted by A_i and A_i^{π}. Based on the analysis done before, we conclude that they are given by

$$\begin{aligned} A_i &= \{(x,\theta) \in [-\infty, \alpha_i] \times [0, 2\pi]\,;\ \theta = \theta_i(x) + \pi\} \cup \\ &\quad \cup \{(x,\theta) \in [\alpha_i, +\infty] \times [0, 2\pi]\,;\ \theta = \theta_i(x)\}\,, \\ A_i^{\pi} &= \{(x,\theta) \in [-\infty, \alpha_i] \times [0, 2\pi]\,;\ \theta = \theta_i(x)\} \cup \\ &\quad \cup \{(x,\theta) \in [\alpha_i, +\infty] \times [0, 2\pi]\,;\ \theta = \theta_i(x) + \pi\}\,, \end{aligned}$$

and, therefore, on one hand, A_i is an arctangent-like curve with $\theta = \beta_i + \pi$ and $\theta = \beta_i$ as negative and positive[5] horizontal asymptotes, respectively; on the other hand, A_i^{π} is an arctangent-like curve with $\theta = \beta_i$ and $\theta = \beta_i + \pi$ as negative and positive horizontal asymptotes, respectively.[6] Moreover, because of the very definition of β_i, the positioning of the asymptotes inside the cylinder behaves similarly as the straight lines L_i and L_i^{π} in Section 4.3. This completes the qualitative analysis of the shape of the slow manifold and, from now on we will write $\mathcal{M}_i = A_i \cup A_i^{\pi}$.

Over both the arctangents $\mathcal{M}_i = A_i \cup A_i^{\pi}$, we have the one-dimensional dynamics given by the first equation of (4.17), i.e., $\dot{x} = a_{i1}x + d_{i1}$. Analyzing this equation we observe that, if $a_{i1} \neq 0$, then there are hyperbolic critical points at

$$x = -\frac{d_{i1}}{a_{i1}} =: \delta_i,$$

being these points attractors if $a_{i1} < 0$ and repellers if $a_{i1} > 0$, as represented at Figure 26b. Since we are under (SFH), then Theorem 4.5 tells us that, in this case, these hyperbolic singularities are actually hyperbolic singularities of the whole stripe S_i. If $a_{i1} = 0$, then

[5] Where negative means $x \to -\infty$ and positive means $x \to +\infty$.

[6] In particular, when $a_{i3} = 0$ we have $\beta_i = 0$ and, therefore, the horizontal asymptotes are given by $\theta = 0$ and $\theta = \pi$, which are part of the stripes' boundary.

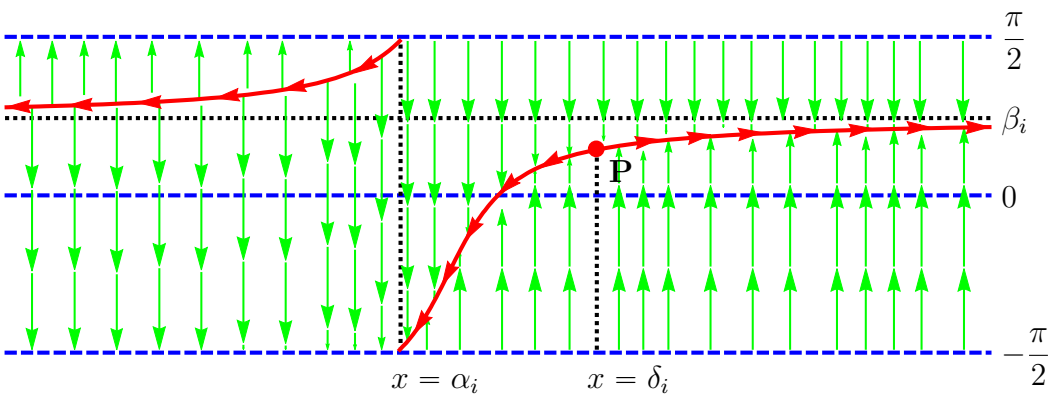

(a) Hyperbole H_i.

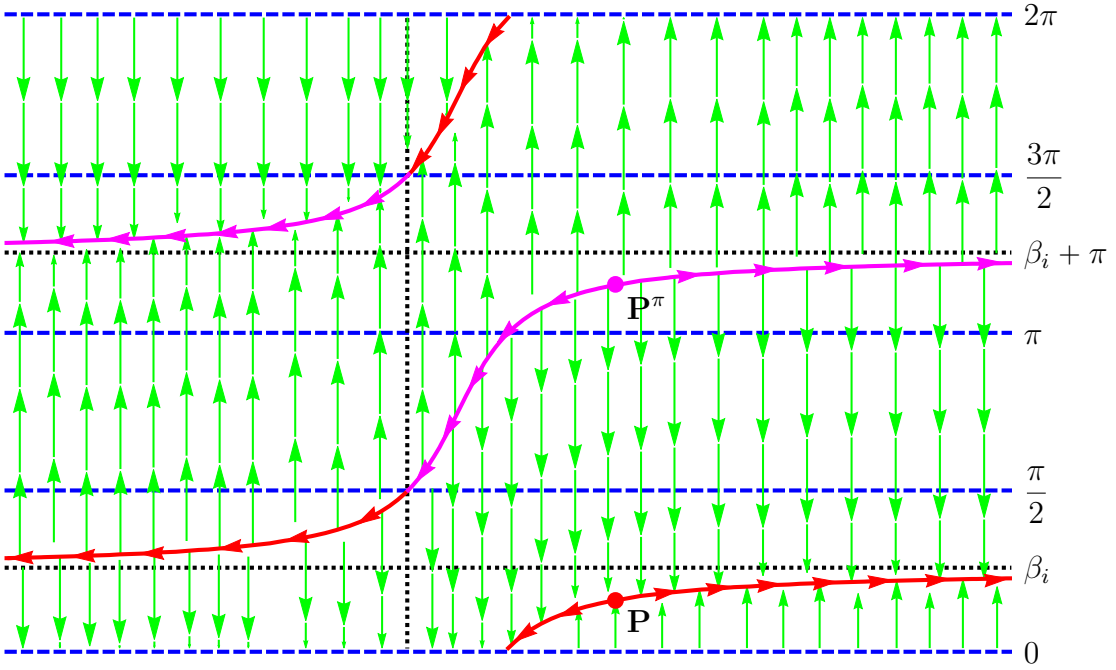

(b) Hyperboles H_i and H_i^π together at the cylinder C forming the arctangents A_i and A_i^π.

Figure 26 – Affine double discontinuity dynamics for $a_{i1} = 1$, $d_{i1} = -1$, $a_{i2} = 1$, $d_{i2} = 1$, $a_{i3} = 1$ and $d_{i3} = 0$. At this example we have $\alpha_i = -1$, $\beta_i = \frac{\pi}{4}$ and $\delta_i = 1$. Therefore, for example, S_1 has part of the hyperbole H_i as a visible part of the slow manifold; whereas S_2 has only part of A_i^π visible.

there is no critical point and the dynamics over $\mathcal{M}_i$ is exactly as in the constant case described in Section 4.3. This completes the qualitative analysis of the reduced dynamics.

Regarding the layer dynamics, we have the layer system (4.18) which says that for each fixed value of $x \in \mathbb{R}$, we have a one-dimensional dynamics given by the second equation of (4.18). In particular, assuming that $\cos\theta > 0$ and $a_{i2}x + d_{i2} > 0$, then

$$\theta' > 0 \Leftrightarrow \theta < \theta_i(x),$$

since the arctangent function is strictly increasing. Likewise, and under the same conditions, we have that

$$\theta' < 0 \Leftrightarrow \theta > \theta_i(x),$$

and, therefore, we conclude that for $a_{i2}x + d_{i2} > 0$, the piece of curve $\theta = \theta_i(x)$ is attractor of the surrounding dynamics and, therefore, $\theta = \theta_i(x) + \pi$ is repellor. Moreover, if $a_{i2} > 0$, then $a_{i2}x + d_{i2} > 0$ happens for $x > \alpha_i$; if $a_{i2} < 0$, then $a_{i2}x + d_{i2} > 0$ happens for $x < \alpha_i$. Completing this analysis and comparing with the definition of A_i and A_i^π we reach the results summarized at Table 3 and represented as the green part of Figure 26. Moreover, at $\cos\theta = 0$ with $a_{i2} \neq 0$ and $a_{i2}x + d_{i2} \neq 0$, (4.18) give us the layer systems

$$\begin{cases} x' &= 0 \\ \theta' &= -(a_{i2}x + d_{i2}) \end{cases} \quad \text{and} \quad \begin{cases} x' &= 0 \\ \theta' &= a_{i2}x + d_{i2} \end{cases}$$

for $\theta = \dfrac{\pi}{2}$ and $\theta = \dfrac{3\pi}{2}$, respectively, whose dynamics is consistent with Table 3. This completes the qualitative analysis of the layer dynamics for case (A).

Now, lets consider the case (B), which complements the case (A) studied above defining the missing dynamics over $a_{i2}x + d_{i2} = 0$ ($\Leftrightarrow x = \alpha_i$) with $a_{i2} \neq 0$. At this case, the reduced system (4.17) becomes

$$\begin{cases} \dot{x} &= a_{i1}x + d_{i1} \\ 0 &= (a_{i3}x + d_{i3})\cos\theta \end{cases},$$

whose slow manifold $\mathcal{M}_i$ is implicitly given by the equation $0 = (a_{i3}x + d_{i3})\cos\theta$ which actually means $0 = \cos\theta$, since we are under SFH and, therefore $a_{i3}x + d_{i3} \neq 0$. In other words, $\mathcal{M}_i = \left\{ \left(\alpha_i, \dfrac{\pi}{2}\right), \left(\alpha_i, \dfrac{3\pi}{2}\right) \right\}$. Over these points acts the dynamics $\dot{x} = a_{i1}x + d_{i1}$, which is consistent with case (A). Regarding the fast dynamics, we have the layer system

$$\begin{cases} x' &= 0 \\ \theta' &= (a_{i3}x + d_{i3})\cos\theta \end{cases} \sim \begin{cases} x' &= 0 \\ \theta' &= -\dfrac{\gamma_i}{a_{i2}}\cos\theta \end{cases},$$

since $x = \alpha_i$, which can be easily verified to be consistent with the layer dynamics given by Table 3 and, therefore, it is consistent with case (A). Therefore, we conclude that case whole (B) is consistent with case (A). In other words, the dynamics over the asymptote $a_{i2}x + d_{i2} = 0$ agrees with the surrounding dynamics.

	$a_{i2} < 0$	$a_{i2} > 0$
A_i	repellor	attractor
A_i^π	attractor	repellor

Table 3 – Layer dynamics around the arctangents A_i and A_i^π that compose the slow manifold $\mathcal{M}_i = A_i \cup A_i^\pi$.

4.4.2 Case $a_{i2} = 0$

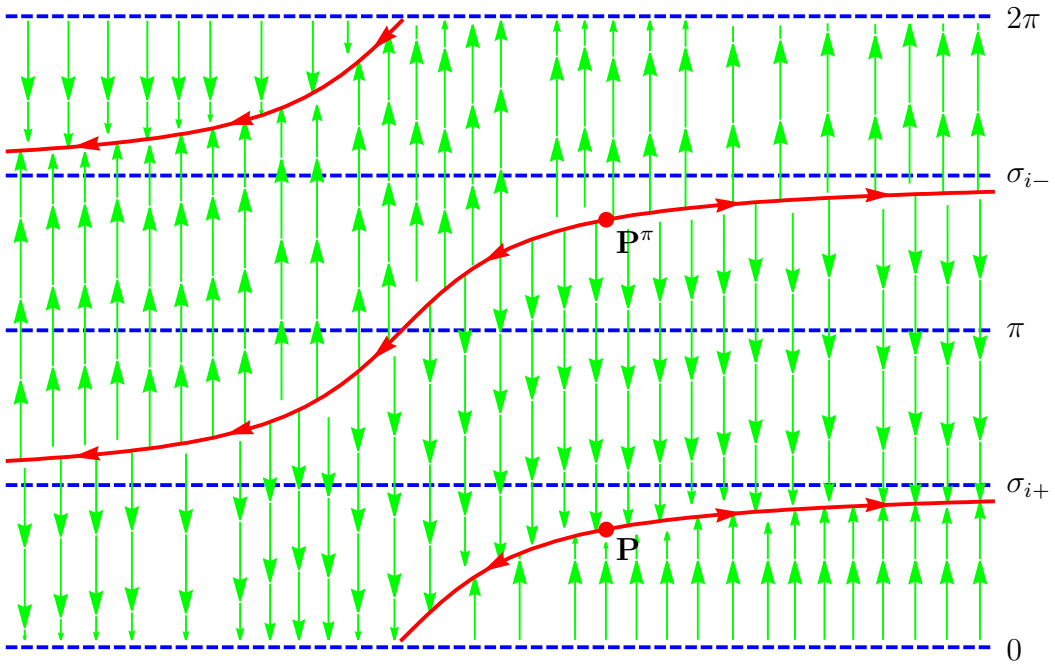

Figure 27 – Affine double discontinuity dynamics for $a_{i1} = 1$, $d_{i1} = -1$, $a_{i2} = 0$, $d_{i2} = 1$, $a_{i3} = 1$ and $d_{i3} = 1$. At this example we have $\delta_i = 1$ and $\sigma_{i\pm} = \pm\dfrac{\pi}{2}$.

For case (C), remember that we have $a_{i2} = 0$ and $a_{i2}x + d_{i2} \neq 0$ implying $d_{i2} \neq 0$. Therefore, everything at the beginning of Section 4.4.1 is true. However, whenever $\cos\theta \neq 0$, the explicit expression for the slow manifold $\mathcal{M}_i$ is now

$$\theta = \arctan\left(\frac{a_{i3}x + d_{i3}}{d_{i2}}\right) + n\pi = \theta_i(x) + n\pi,$$

where $n \in \mathbb{Z}$. Therefore, without loss of generality, the slow manifold can be written as $\mathcal{M}_i = A_i \cup A_i^{\pi}$, where

$$\begin{aligned} A_i &= \{(x,\theta) \in \mathbb{R} \times [0, 2\pi]\,;\ \theta = \theta_i(x)\} \text{ and} \\ A_i^{\pi} &= \{(x,\theta) \in \mathbb{R} \times [0, 2\pi]\,;\ \theta = \theta_i(x) + \pi\}\,, \end{aligned}$$

which consists of two arctangent-like curves inside the cylinder $C = \mathbb{R} \times S^1$ as the red part of Figure 27. In fact, since $a_{i2} = 0$, then $h(x)$ is a straight line and, therefore,

$$\theta = \theta_i(x) = \arctan\left(h(x)\right)$$

is an arctangent curve. Besides that, we have

$$\frac{d}{dx}h(x) = \frac{\gamma_i}{(a_{i2}x + d_{i2})^2} = \frac{\gamma_i}{d_{i2}^2}$$

and, therefore, A_i and A_i^π are increasing curves if $\gamma_i > 0$ and decreasing if $\gamma_i < 0$[7]. Moreover, since

$$\begin{aligned}\lim_{x\to\pm\infty}\theta_i(x) &= \lim_{x\to\pm\infty}\left[\arctan\left(\frac{a_{i3}x+d_{i3}}{d_{i2}}\right)\right] = \\ &= \arctan\left[\lim_{x\to\pm\infty}\left(\frac{a_{i3}x+d_{i3}}{d_{i2}}\right)\right] = \\ &= \arctan\left[\pm\operatorname{sgn}\left(\frac{a_{i3}}{d_{i2}}\right)\infty\right] = \\ &= \pm\operatorname{sgn}\left(\frac{a_{i3}}{d_{i2}}\right)\frac{\pi}{2} = \pm\operatorname{sgn}\left(\frac{\gamma_i}{d_{i2}^2}\right)\frac{\pi}{2} = \\ &= \pm\operatorname{sgn}(\gamma_i)\frac{\pi}{2} =: \sigma_{i\pm},\end{aligned}$$

then A_i has σ_{i-} and σ_{i+} as negative and positive horizontal asymptote, respectively; while A_i^π has σ_{i+} and σ_{i-} as negative and positive horizontal asymptote, respectively. This completes the qualitative analysis of the shape of the slow manifold.

Over both the arctangents $\mathcal{M}_i = A_i \cup A_i^\pi$, we have the one-dimensional dynamics given by the first equation of (4.17), i.e., $\dot{x} = a_{i1}x + d_{i1}$ which behaves as described in Section 4.4.1. This completes the qualitative analysis of the reduced dynamics.

Regarding the layer dynamics, a completely analogous analysis such as that made for the previous cases allows us to conclude that it behaves as described in Table 3, including the case $\cos\theta = 0$, but exchanging a_{i2} with d_{i2}.

4.4.3 Theorem and Examples

Summarizing, we conclude that the dynamics over Σ_x for affine fields behaves as described in the theorem below, whose proof consists in the analysis done above.

Theorem 4.7 (Affine Dynamics)**.** *Given $\mathbf{F} \in \mathcal{A}_3$ with affine components $\mathbf{F}_i$ given by (4.16) and such that $\gamma_i \neq 0$, let $\tilde{\mathbf{F}} \in \tilde{\mathcal{A}}_3$ be the vector field induced by the blow-up $\phi_1(x,\theta,r) = (x, r\cos\theta, r\sin\theta)$. Then, this blow-up associates the dynamics over Σ_x with the following dynamics over the cylinder $C = \mathbb{R}\times S^1 = S_1 \cup \ldots \cup S_4$: over each stripe S_i acts a slow-fast dynamics whose slow manifold is given by $\mathcal{M}_i = A_i \cup A_i^\pi$, where A_i^π is a π-translation of A_i in θ and*

1. *case $a_{i2} \neq 0$, then*

[7] Again, if $\gamma_i = 0$ ($\Leftrightarrow a_{i3} = 0$), then $h(x)$ is a constant function and, therefore, A_i and A_i^π are straight lines. In other words, the constant case is recovered.

$$A_i = \{(x,\theta) \in [-\infty, \alpha_i] \times [0, 2\pi]\,;\ \theta = \theta_i(x) + \pi\} \cup$$
$$\cup\, \{(x,\theta) \in [\alpha_i, +\infty] \times [0, 2\pi]\,;\ \theta = \theta_i(x)\}$$

with $\theta_i(x) = \arctan\left(\dfrac{a_{i3}x + d_{i3}}{a_{i2}x + d_{i2}}\right)$, *which consists in an arctangent-like curve inside the cylinder* C *with* $\theta = \beta_i + \pi$ *and* $\theta = \beta_i$ *as negative and positive horizontal asymptotes, respectively;*

2. *case* $a_{i2} = 0$, *then*

$$A_i = \{(x,\theta) \in \mathbb{R} \times [0, 2\pi]\,;\ \theta = \theta_i(x)\}$$

with $\theta_i(x) = \arctan\left(\dfrac{a_{i3}x + d_{i3}}{d_{i2}}\right)$, *which consists in an arctangent-like curve inside the cylinder* C *with* $\theta = \sigma_{i-}$ *and* $\theta = \sigma_{i+}$ *as negative and positive horizontal asymptotes, respectively.*

Both arctangents are increasing if $\gamma_i > 0$ *and decreasing if* $\gamma_i < 0$. *Over them act the reduced dynamics* $\dot{x} = a_{i1}x + d_{i1}$ *and, around them, acts the layer dynamics described in Table 3, but exchanging* a_{i2} *with* d_{i2} *if* $a_{i2} = 0$. *Finally, the new parameters above are given by* $\alpha_i = -\dfrac{d_{i2}}{a_{i2}}$, $\beta_i = \arctan\left(\dfrac{a_{i3}}{a_{i2}}\right)$, $\gamma_i = a_{i3}d_{i2} - d_{i3}a_{i2}$, $\delta_i = -\dfrac{d_{i1}}{a_{i1}}$ *and* $\sigma_{i\pm} = \pm\,\mathrm{sgn}\,(\gamma_i)\dfrac{\pi}{2}$.

Example 4.2. *Let* $\mathbf{F} \in \mathcal{A}_3$ *be given by affine vector fields such that*

$$\mathbf{F}_2 : \begin{bmatrix} a_{21} & d_{21} \\ a_{22} & d_{22} \\ a_{23} & d_{23} \end{bmatrix} = \begin{bmatrix} 1 & -2 \\ -1 & 1 \\ -1 & 0 \end{bmatrix}, \qquad \mathbf{F}_1 : \begin{bmatrix} a_{11} & d_{11} \\ a_{12} & d_{12} \\ a_{13} & d_{13} \end{bmatrix} = \begin{bmatrix} -1 & 2 \\ -1 & 1 \\ 1 & 0 \end{bmatrix},$$

$$\mathbf{F}_3 : \begin{bmatrix} a_{31} & d_{31} \\ a_{32} & d_{32} \\ a_{33} & d_{33} \end{bmatrix} = \begin{bmatrix} 1 & -2 \\ 1 & 1 \\ -1 & 0 \end{bmatrix}, \qquad \mathbf{F}_4 : \begin{bmatrix} a_{41} & d_{41} \\ a_{42} & d_{42} \\ a_{43} & d_{43} \end{bmatrix} = \begin{bmatrix} -1 & 2 \\ 1 & 1 \\ 1 & 0 \end{bmatrix},$$

with parameters c_{ij}*'s and* d_{ij}*'s arbitrary since, according to Theorem 4.7, they only affect the dynamics outside the cylinder. Using this theorem we can also verify that, over the cylinder* C *given by the blow-up of* Σ_x, *the system has a single* ***slow cycle*** *as represented at Figure 28.*

For instance, according to Theorem 4.7, the field $\mathbf{F}_1$ *induces a slow-fast system whose slow manifold* $\mathcal{M}_1 = A_1 \cup A_1^{\pi}$ *consists of arctangents with horizontal asymptotes*

$$\theta = \beta_1 = \arctan\left(\frac{a_{13}}{a_{12}}\right) = \arctan(-1) = -\frac{\pi}{4}$$

at S_4 *and* $\theta = \beta_1 + \pi = \dfrac{3\pi}{4}$ *at* S_2*. Besides that, since*

$$\gamma_1 = a_{13}d_{12} - a_{12}d_{13} = 1$$

then these arctangents are increasing. Therefore, we conclude that $\mathcal{M}_1 \cap S_1 \subset A_1^{\pi}$*, and it transversally crosses* S_1 *as represented at the lowest stripe of Figure 28 from* $\mathbf{R}_1$ *to* $\mathbf{Q}_1$*, where the point* $\mathbf{Q}_1$ *is given by*

$$\frac{\pi}{2} = \theta_1(x) = \arctan\left(\frac{a_{i3}x + d_{i3}}{a_{i2}x + d_{i2}}\right) = \arctan\left(\frac{x}{-x+1}\right),$$

which happens when $x \to 1^-$*; and the point* $\mathbf{R}_1$ *is given by*

$$0 = \theta_1(x) = \arctan\left(\frac{a_{i3}x + d_{i3}}{a_{i2}x + d_{i2}}\right) = \arctan\left(\frac{x}{-x+1}\right),$$

which happens when $x \to 0^+$*. Dynamically it also goes* $\mathbf{R}_1 \to \mathbf{Q}_1$*, since over* $\mathcal{M}_1 \cap S_1$ *acts the reduced dynamics* $\dot{x} = -x + 2$*, which has* $x = 2$ *as a stable singularity. Finally, since* $a_{12} = -1 < 0$ *and* $\mathcal{M}_1 \cap S_1 \subset A_1^{\pi}$*, then* $\mathcal{M}_1 \cap S_1$ *attracts the surrounding layer dynamics, according to Table 3.*

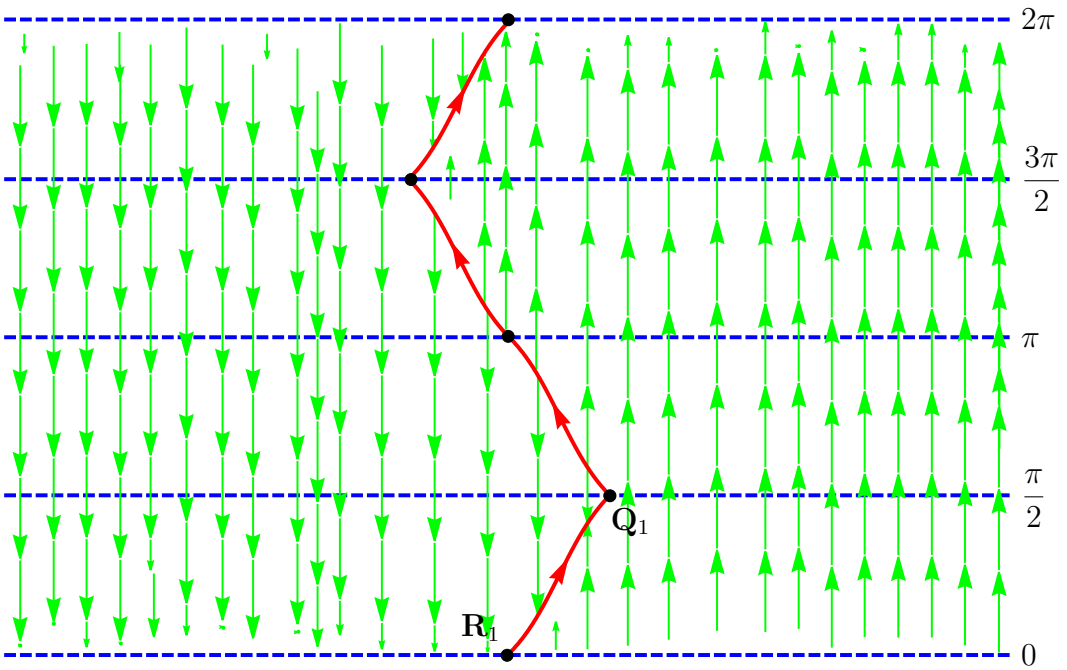

Figure 28 – Dynamics over C generated by the field $\mathbf{F}$ studied at Example 4.2.

Therefore, we conclude that the dynamics generated by $\mathbf{F}_1$ *over the stripe* S_1*, in fact, behave as represented at Figure 28. The dynamics over the other stripes can be similarly verified to be as represented.* □

Corollary 4.1. *Every* $\mathbf{F} \in \mathcal{A}_3$ *with* $\gamma_i \neq 0$ *can induce at most one slow cycle over the cylinder.*

Proof. Given a stripe S_i, according to Theorem 4.7 the arctangents that forms the slow manifold $\mathcal{M}_i$ can either have a horizontal asymptote inside S_i or not.

If a horizontal asymptote is inside S_i, then a slow cycle construction is impossible, even if the asymptote is at one of the borders of S_i, since $\mathcal{M}_i$ does not cross transversally both borders of S_i.

However, if no horizontal asymptote is inside S_i, then a construction similar to that realized at Example 4.2 can occur. Finally, no more than one slow cycle can occur, since the arctangents are strictly monotonous and, therefore, transversally crosses S_i at most once. □

4.5 Structural Stability

Let $\mathbf{F} \in \mathcal{D}_3^k$ be a piecewise smooth vector field with a double discontinuity given by affine vector fields (4.16). The theorems obtained in the previous sections fully describe the affine double discontinuity dynamics over the cylinder C of the induced vector field $\tilde{\mathbf{F}} \in \tilde{\mathcal{D}}_3^k$. As an application, we would like to use this knowledge to study its structural stability. The first step in this process consists of defining a concept of structural stability which fits the systems we are studying. In order to do so, we are going to mimic the classical definition for the regular case, $\mathcal{R}^k(U)$, obtained from Definition 1.16, which can be easily extended to $\mathcal{D}_3^k$. In fact, on one hand, systems in $\mathcal{R}^k(U)$ have a single subset that should be kept invariant, $\Sigma = h^{-1}(0)$; on the other hand, systems in $\mathcal{D}_3^k$ have a set of subsets

$$\mathcal{I} = \{\Sigma_{12}, \Sigma_{23}, \Sigma_{34}, \Sigma_{14}, \Sigma_x\}$$

which should be kept invariants by topological equivalence. Therefore, a direct substitution gives us the following definition:

Definition 4.1. *Let* $\mathbf{F}, \mathbf{G} \in \mathcal{D}_3^k$*. We say that* $\mathbf{F}$ *and* $\mathbf{G}$ *are* ***topologically equivalent*** *and denote* $\mathbf{F} \sim \mathbf{G}$ *if, and only if, there exists a homeomorphism* $\varphi : \mathbb{R}^3 \to \mathbb{R}^3$ *that keeps every* $I \in \mathcal{I}$ *invariant and takes orbits of* $\mathbf{F}$ *into orbits of* $\mathbf{G}$ *preserving the orientation of time. From this definition the concept of structural stability in* $\mathcal{D}_3^k$ *is naturally obtained.*

For the blow-up induced vector fields, $\tilde{\mathcal{D}}_3^k$, the set of invariant subsets are given by

$$\tilde{\mathcal{I}} = \left\{\tilde{\Sigma}_{12}, \tilde{\Sigma}_{23}, \tilde{\Sigma}_{34}, \tilde{\Sigma}_{14}, C\right\}$$

and, therefore, we define:

Definition 4.2. *Let $\tilde{\mathbf{F}}, \tilde{\mathbf{G}} \in \tilde{\mathcal{D}}_3^k$. We say that $\tilde{\mathbf{F}}$ and $\tilde{\mathbf{G}}$ are **topologically equivalent** and denote $\tilde{\mathbf{F}} \sim \tilde{\mathbf{G}}$ if, and only if, there exists a homeomorphism $\tilde{\varphi} : \mathbb{R}\times S^1 \times \mathbb{R}^+ \to \mathbb{R}\times S^1 \times \mathbb{R}^+$ that keeps every $I \in \tilde{\mathcal{I}}$ invariant and takes orbits of $\tilde{\mathbf{F}}$ into orbits of $\tilde{\mathbf{G}}$ preserving the orientation of time. From this definition the concept of structural stability in $\tilde{\mathcal{D}}_3^k$ is naturally obtained.*

Now, let $\tilde{\mathbf{F}}, \tilde{\mathbf{G}} \in \tilde{\mathcal{D}}_3^k$ be topologically equivalent by a homeomorphism $\tilde{\varphi}$. In this case, we have that $\tilde{\varphi}\big|_I$ with $I \in \tilde{\mathcal{I}}$ are also homeomorphisms taking orbits into orbits and preserving the orientation of time. In other words, the existence of these homeomorphisms is a necessary condition for the topological equivalence. More precisely:

Proposition 4.1. *If $\tilde{\mathbf{F}} \sim \tilde{\mathbf{G}}$, then $\tilde{\mathbf{F}}\big|_I \sim \tilde{\mathbf{G}}\big|_I$ for every $I \in \tilde{\mathcal{I}}$.*

We are interested on the dynamics over the cylinder C. Therefore, given $\mathbf{F} \in \mathcal{D}_3^k$, we look for necessary and/or sufficient conditions for the structural stability of $\tilde{\mathbf{F}}\big|_C$. Beyond the intrinsic interest, given in Proposition 4.1 above, such conditions shall also reveal relevant information on the structural stability of $\tilde{\mathbf{F}}$ and, therefore, on the structural stability of $\mathbf{F}$. In fact, from Proposition 4.1 it follows the result below.

Corollary 4.2. *If $\tilde{\mathbf{F}}$ is structurally stable, then $\tilde{\mathbf{F}}\big|_I$ is structurally stable for every $I \in \tilde{\mathcal{I}}$.*

Proof. Given $I \in \tilde{\mathcal{I}}$, let $\tilde{\mathcal{W}} \subset \mathcal{D}_3^k$ be an open neighborhood of $\tilde{\mathbf{F}}$. Observe that

$$\tilde{\mathcal{W}}\big|_I = \left\{\tilde{\mathbf{H}}\big|_I;\ \tilde{\mathbf{H}} \in \tilde{\mathcal{W}}\right\}$$

is an open neighborhood of $\tilde{\mathbf{F}}\big|_I$.

Therefore, if $\tilde{\mathbf{F}}\big|_I$ was not structurally stable, would exist $\tilde{\mathbf{G}}\big|_I \in \tilde{\mathcal{W}}\big|_I$ such that $\tilde{\mathbf{F}}\big|_I \nsim \tilde{\mathbf{G}}\big|_I$ and, therefore, from Proposition 4.1 would follow that $\tilde{\mathbf{G}} \nsim \tilde{\mathbf{F}}$, then implying that $\tilde{\mathbf{F}}$ would not be structurally stable. □

Thus, from now on, we will exclusively study conditions for the structural stability of $\tilde{\mathbf{F}}\big|_C$. In order to do so, remember that over C acts a regular Filippov dynamics whose switching manifold is formed by the elements of

$$\tilde{\mathcal{I}}_C = \left\{\Sigma_0, \Sigma_{\frac{\pi}{2}}, \Sigma_\pi, \Sigma_{\frac{3\pi}{2}}\right\},$$

where $\Sigma_\theta = \{(x,\theta);\ x \in \mathbb{R}\}$. Therefore, without loss of generality for the previous results, it is natural to adopt the following definitions of equivalence and stability for C:

Definition 4.3. *Let $\tilde{\mathbf{F}}, \tilde{\mathbf{G}} \in \tilde{\mathcal{D}}_3^k$. We say that $\tilde{\mathbf{F}}$ and $\tilde{\mathbf{G}}$ are C-**topologically equivalent** and denote $\tilde{\mathbf{F}} \sim_c \tilde{\mathbf{G}}$ if, and only if, there exists a homeomorphism $\tilde{\varphi} : C \to C$ that keeps every $I \in \tilde{\mathcal{I}}_C$ invariant and takes orbits of $\tilde{\mathbf{F}}\big|_C$ into orbits of $\tilde{\mathbf{G}}\big|_C$ preserving the orientation of time. From this definition the concept of C-structural stability is naturally obtained.*

Although global and naturally derived from the regular case, C-structural stability, as presented above, is still a fairly complex property to prove and, in fact, to the best of the author's knowledge, it is an open problem to characterize it through simple conditions and, therefore, shall be treated in future works.

However, many of the difficulties found at characterizing C-structural stability comes from its global aspect. In fact, conditions for a semi-local approach can be found in [7] and, in order to apply these results, a *regular* and *compact* Filippov section of the cylinder C must be taken.

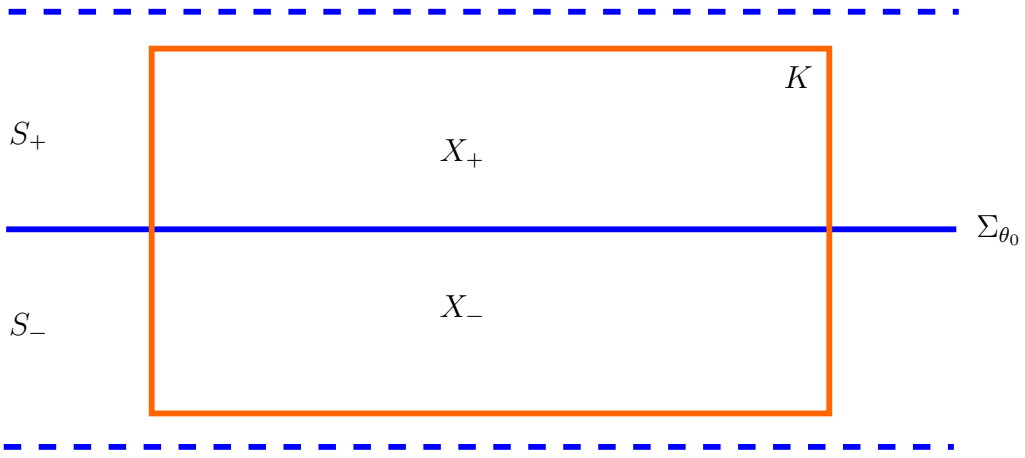

Figure 29 – Regular Filippov system $\mathbf{X} = (\mathbf{X}_-, \mathbf{X}_+)$ defined at a convex compact set $K \subset C_+ \cup C_-$ with switching manifold Σ_{θ_0}.

More precisely, given $\mathbf{F} \in \mathcal{D}_3^k$ and two consecutive stripes C_+ and C_- meeting at a straight line $\Sigma_{\theta_0} \in \tilde{\mathcal{I}}_C$, let $\mathbf{X}_+$ and $\mathbf{X}_-$ be the smooth vector fields induced over $C_+ \cap K$ and $C_- \cap K$, respectively, as described at the previous sections and where $K \subset C_+ \cup C_-$ is a convex compact set, see Figure 29. Observe that $\mathbf{X} = (\mathbf{X}_-, \mathbf{X}_+)$ is a *regular* and *compact* Filippov system with a connected (due to the convexity of K) switching manifold Σ_{θ_0}.

Then, a direct application of Theorem B from [7, p. 5] and the Proposition 1.1 from [39, p. 122] give us the following result:

Proposition 4.2. *Given $\mathbf{F} \in \mathcal{D}_3^k$, two consecutive stripes C_+ and C_- and a convex compact set $K \subset C_+ \cup C_-$, then the induced Filippov system $\mathbf{X} = (\mathbf{X}_-, \mathbf{X}_+)$ is structurally stable inside K if, and only if, the following sets of conditions are satisfied:*

(I) $\mathbf{X}_+$ *and* $\mathbf{X}_-$ *are robustly*[8] *Morse-Smale, i.e., they have:*

- *(C.1) finitely many critical elements*[9]*, all hyperbolic;*
- *(C.2) no saddle-connections;*
- *(C.3) only critical elements as non-wandering points;*

(II) $\mathbf{X}_+$ *and* $\mathbf{X}_-$ *robustly satisfies that:*

- *(C.4) none of them vanishes at a point of Σ_{θ_0};*
- *(C.5) they are tangent to Σ_{θ_0} at only finitely many points with both never tangent at the same point;*
- *(C.6) they are colinear at only finitely many points;*

(III) $\mathbf{X}$ *have:*

- *(C.7) only hyperbolic periodic orbits;*
- *(C.8) no separatrix-connections or relations*[10]*;*
- *(C.9) only trivial recurrent orbits.*

Observe that (I) refers only to the usual dynamics of $\mathbf{X}_+$ and $\mathbf{X}_-$ over the smooth parts. On the other hand, (II) considers only the values of $\mathbf{X}_+$ and $\mathbf{X}_-$ over the switching manifold Σ_{θ_0}. Finally, only (III) refers to the actual Filippov dynamics of $\mathbf{X}$. With that in mind, over the next, and final sections, we will apply Theorem 4.6 and Theorem 4.7 to analyze this conditions for the particular cases of constant and affine double discontinuities, respectively, and therefore derive semi-local structural stability theorems or, more precisely:

Definition 4.4. *We say that $\mathbf{F} \in \mathcal{D}_3^k$ is (I, K)-**semi-local structurally stable** if, and only if, the induced Filippov system $\mathbf{X} = (\mathbf{X}_-, \mathbf{X}_+)$ is structurally stable inside a convex compact set $K \subset C_+ \cup C_-$, where C_+ and C_- are two consecutive stripes meeting at $I \in \tilde{\mathcal{I}}_C$.*

In fact, given the bifurcation described below, it is natural to study the constant and affine cases separately, since the first is always structurally unstable inside the last one. More precisely:

[8] In other words, the property is stable under small perturbations.
[9] Singularities and periodic orbits.
[10] Unstable separatrices arriving at the same point are said to be **related**.

Proposition 4.3. *Every* $\mathbf{F} \in \mathcal{C}_3$ *is structurally unstable as an element of* $\mathcal{A}_3$.

Proof. Let $\mathbf{F} \in \mathcal{C}_3 \subset \mathcal{D}_3^k$ be a piecewise smooth vector field with a double discontinuity given by constant vector fields

$$\mathbf{F}_i(x, y, z) = (d_{i1}, d_{i2}, d_{i3}),$$

where $d_{ij} \in \mathbb{R}$ for all i and j.

Assume, without loss of generality, that $d_{i1} > 0$. Then, according to Theorem 4.6, over the slow manifold we have the dynamics $\dot{x} = d_{i1}$. As $d_{i1} > 0$, then it is strictly increasing and, in particular, has no singularities.

However, considering $\mathbf{F}$ as an element of $\mathcal{A}_3 \subset \mathcal{D}_3^k$ and, in particular, perturbing $\mathbf{F}_i$ inside $\mathcal{A}_3$ with $a_{i1} \neq 0$, then we would now have the dynamics $\dot{x} = a_{i1}x + d_{i1}$ over the slow manifold. As $d_{i1} > 0$ and $a_{i1} \neq 0$, then it does now have a single singularity at $x = \delta_i$ and, besides that, half of its stability was inverted when compared with the unperturbed dynamics.

In other words, $\mathbf{F}$ as an element of $\mathcal{A}_3$ violates the robustness of condition (C.1) of Proposition 4.2 and, therefore, is structurally unstable. □

4.5.1 Constant Dynamics

Let $\mathbf{F} \in \mathcal{C}_3$ be a piecewise smooth vector field with a double discontinuity given by constant vector fields

$$\mathbf{F}_i(x, y, z) = (d_{i1}, d_{i2}, d_{i3}), \tag{4.21}$$

with $d_{i2} \neq 0$ or $d_{i3} \neq 0$. Remember that, in this case, Theorem 4.6 provides a full description of the dynamics of (4.21) and, therefore, we would like to combine it with Proposition 4.2 to derive a semi-local structural stability theorem.

In order to apply this results, given $\Sigma_{\theta_0} \in \tilde{\mathcal{I}}_C$, let $\mathbf{X} = (\mathbf{X}_-, \mathbf{X}_+)$ be the Filippov system induced by (4.21) in a convex compact set $K \subset C_+ \cup C_-$, where C_+ and C_- are two consecutive stripes meeting at Σ_{θ_0} as represented at Figure 29. According to Theorem 4.6, the following are the possible categories of dynamics for a stripe $S_i \in \{C_+, C_-\}$, which we now analyze against conditions (C.1) — (C.5) of Proposition 4.2 case by case in order to discover those that can possibly generate structural stable systems, henceforth called **candidates**:

1. $d_{i2} \neq 0$:

   a) $d_{i3} \neq 0$:
   One, and only one, of the straight lines L_i or L_i^π is visible inside the stripe. Hence, if $d_{i1} = 0$, then we have a continuum of singularities, i.e., a violation of condition (C.1). However, if $d_{i1} \neq 0$, then no critical elements are present and, therefore (C.1) and (C.2) validates. About (C.3), since the slow manifold acts as α or ω-limit of the surrounding dynamics, then it also validates if $d_{i1} \neq 0$. Even more, since over the borders of S_i there is only transversal layer dynamics, then (C.4) and (C.5) also validates. Finally, observe that, invoking theorems such as *continuity theorems* and *Thom Transversality Theorem*, we easily conclude the robustness of the properties validated above when perturbing inside $\mathcal{C}_3$. Therefore, this case is a *candidate* if, and only if, $d_{i1} \neq 0$.

   b) $d_{i3} = 0$:
   The only difference between this case and the previous is the fact that, now, one of straight lines L_i or L_i^π is over one of the borders of the stripe S_i and, therefore, (C.5) is possibly violated, whatever d_{i1}. More specifically, if L_i or L_i^π coincides with Σ_{θ_0}, then we have instability; otherwise, we have a *candidate*.

2. $d_{i2} = 0$ and $d_{i3} \neq 0$:
   This case is similar to the previous one ($d_{i2\neq 0}$ and $d_{i3} = 0$): whatever d_{i1}, if L_i or L_i^π coincides with Σ_{θ_0}, then we have instability; otherwise, we have a *candidate*.

The analysis of the remaining conditions (C.6) — (C.9) requires the combined dynamics of the stripes C_+ and C_-. Therefore, in order to decide stability, we shall now analyze all the combinations of candidates obtained above, and summarized at Table 4, against these conditions.

	$d_{i2} \neq 0$	$d_{i2} = 0$
$d_{i3} \neq 0$	$d_{i1} \neq 0$	$\theta_i \neq \theta_0$
$d_{i3} = 0$	$\theta_i \neq \theta_0$	unstable

Table 4 – Conditions under which the stripe S_i is a semi-local structural stability candidate.

Actually, most of the remaining conditions can be easily dropped. In fact, according to Theorem 4.6, none of the candidates have periodic orbits and, besides that, because of the α and ω-limit nature of $\mathcal{M}_i$, an orbit that enters S_i never touches the same border again and, therefore, (C.7) always validates, because there is no periodic orbits. Likewise, there is no singularities, usual or not and, therefore, there is no separatrix-connections or relations, i.e., (C.8) always validates. Finally, as long as $d_{i1} \neq 0$, Poincaré-Bendixson Theorem assures that no non-trivial recurrent orbits can happen inside S_i and, besides that, again because of the α and ω-limit nature of $\mathcal{M}_i$, neither can they happen

thought the switching manifold and, therefore, (C.9) also always validates. At this point, the following theorem has been proved:

Theorem 4.8 (Constant Dynamics Stability)**.** *Let $\mathbf{F} \in \mathcal{C}_3$ be given by (4.21) with $d_{i2} \neq 0$ or $d_{i3} \neq 0$. Given $\Sigma_{\theta_0} \in \tilde{\mathcal{I}}_C$, let $\mathbf{X} = (\mathbf{X}_-, \mathbf{X}_+)$ be the Filippov system induced around Σ_{θ_0} and inside a convex compact set $K \subset C_+ \cup C_-$, where C_+ and C_- are two consecutive stripes meeting at Σ_{θ_0}. Then, $\mathbf{F}$ is (Σ_{θ_0}, K)-semi-local structurally stable in $\mathcal{C}_3$ if, and only if, $\mathbf{X}_+$ and $\mathbf{X}_-$ satisfies at least one of the conditions*

1. *$d_{i1}d_{i2}d_{i3} \neq 0$; or*
2. *$d_{i1} \neq 0$, $d_{i2}^2 + d_{i3}^2 \neq 0$ and $\theta_i \neq \theta_0$;*

and, additionally, $\mathbf{X}_+$ and $\mathbf{X}_-$ are non-colinear over Σ_{θ_0}, except at finitely many points.

Example 4.3. *Lets see an example of instability around the discontinuity manifold $\Sigma_{\frac{\pi}{2}} \in \tilde{\mathcal{I}}_C$ of the cylinder generated by constant vector fields. More precisely, take $\mathbf{F} \in \mathcal{C}_3$ with*

$$\mathbf{F}_1(x, y, z) = (1, -1, 1) \quad \text{and} \quad \mathbf{F}_2(x, y, z) = (-1, 1, 1),$$

whose dynamics over the stripes $S_1 \cup S_2$, represented at Figure 30 below, can be determined as in Example 4.1 using Theorem 4.6.

Since $d_{11}d_{12}d_{13} = -1 \neq 0$ and $d_{21}d_{22}d_{23} = -1 \neq 0$, then the first part of Theorem 4.8 is satisfied. However, the induced dynamics $\mathbf{X}_1$ and $\mathbf{X}_2$ over the stripes S_1 and S_2, respectively, are colinear over their whole intersection, the discontinuity manifold $\Sigma_{\frac{\pi}{2}}$.

In fact, as represented at Figure 30a, for $\mathbf{F}_1$ the slow manifold consists of the straight lines given by $\theta = \theta_1 = -\dfrac{\pi}{4}$ and $\theta = \theta_1 + \pi = \dfrac{3\pi}{4}$; over then acts the increasing dynamics $\dot{x} = 1$. Besides that, the first line is repellor and, the second, attractor of the allround dynamics. On the other hand, as represented at Figure 30b, for $\mathbf{F}_2$ the slow manifold consists of the straight lines given by $\theta = \theta_2 = \dfrac{\pi}{4}$ and $\theta = \theta_1 + \pi = \dfrac{5\pi}{4}$; over then acts the decreasing dynamics $\dot{x} = -1$. Besides that, the first line is attractor and, the second, repellor of the surrounding layer dynamics. In other words, the only differences between their dynamics is a π-translation in θ and inverse stability.

This symmetry assures the colinearity of $\mathbf{X}_1$ and $\mathbf{X}_2$ over $\Sigma_{\frac{\pi}{2}}$, as represented at Figure 30c. Hence, the final part of Theorem 4.8 is violated and, therefore, this configuration is structurally unstable around $\Sigma_{\frac{\pi}{2}}$, whatever the convex compact set K considered. Geometrically, the instability here comes from the fact that each point of colinearity is associated with a pseudo-singularity of the sliding vector field of the Filippov system

$\mathbf{X} = (\mathbf{X}_1, \mathbf{X}_2)$ *and, at our configuration we have a continuum of them. This whole continuum of pseudo-singularities can be easily destroyed by perturbing any of associated vector fields.* □

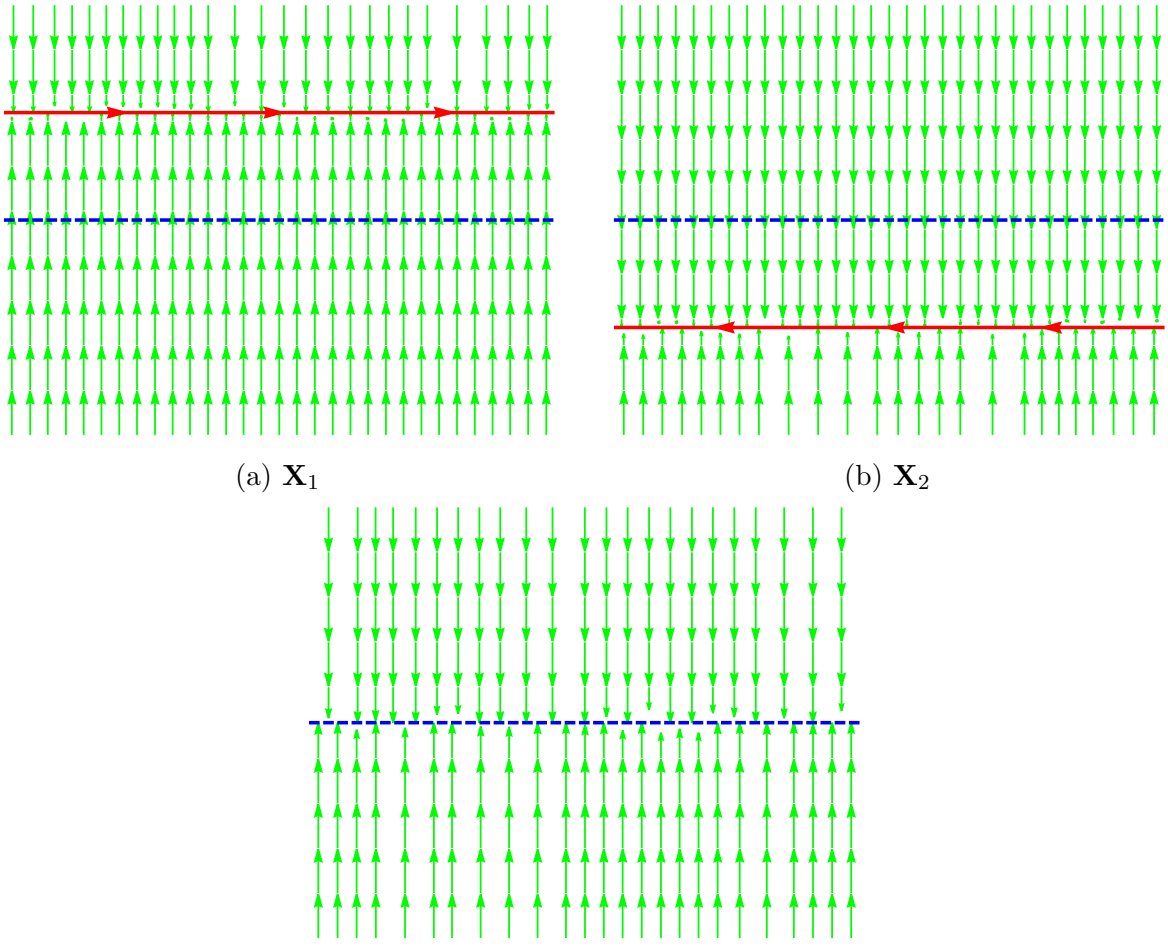

(a) $\mathbf{X}_1$ (b) $\mathbf{X}_2$

(c) $\mathbf{X} = (\mathbf{X}_1, \mathbf{X}_2)$

Figure 30 – Dynamics over the stripes $S_1 \cup S_2$ generated by the fields studied at Example 4.3.

4.5.2 Affine Dynamics

Let $\mathbf{F} \in \mathcal{A}_3$ be a piecewise smooth vector field with a double discontinuity given by affine vector fields

$$\begin{aligned} \mathbf{F}_i(x, y, z) = (&a_{i1}x + b_{i1}y + c_{i1}z + d_{i1}, \\ &a_{i2}x + b_{i2}y + c_{i2}z + d_{i2}, \\ &a_{i3}x + b_{i3}y + c_{i3}z + d_{i3}), \end{aligned} \tag{4.22}$$

with $\gamma_i \neq 0$. Remember that, in this case, Theorem 4.7 provides a full description of the dynamics of (4.22) and, therefore, as in the previous section, we would like to combine it with Proposition 4.2 to derive a semi-local structural stability theorem.

In order to apply this results, given $\Sigma_{\theta_0} \in \tilde{\mathcal{I}}_C$, let $\mathbf{X} = (\mathbf{X}_-, \mathbf{X}_+)$ be the Filippov system induced by (4.22) in a convex compact set $K \subset C_+ \cup C_-$, where C_+ and C_- are two consecutive stripes meeting at Σ_{θ_0} as represented at Figure 29. According to Theorem 4.7, the following are the possible categories of dynamics for a stripe $S_i \in \{C_+, C_-\}$, which we now analyze against conditions (C.1) — (C.5) of Proposition 4.2 case by case in order to discover those that can possibly generate structural stable systems, i.e., the *candidates*:

1. $a_{i2} \neq 0$:

   a) $a_{i3} \neq 0$:
   The characterizing property of this case is the fact that $\beta_i \neq 0$ and, therefore, the horizontal asymptotes resides inside the stripes, possibly even S_i. As a consequence, there is always a visible part of the slow manifold inside S_i. Hence, if $a_{i1} = 0$ and $d_{i1} = 0$, then we have a continuum of singularities; if $a_{i1} = 0$ and $d_{i1} \neq 0$, then we have a similar bifurcation to that described at Proposition 4.3 when perturbing. Either way, (C.1) is violated. However, if $a_{i1} \neq 0$, then Theorem 4.5 assures the existence of at most one robust singularity $\mathbf{P}$, always hyperbolic and, therefore, (C.1) and (C.2) validates, since obviously the is no periodic orbits inside S_i. As in the constant case, the α or ω-limit nature of the slow manifold also assures (C.3). For (C.4) and (C.5), observe that the fast dynamics is always transversal and, therefore, we only need the additional condition $\mathbf{P} \notin \Sigma_{\theta_0}$. Finally, as in the constant case, invoking theorems such as *continuity theorems* and *Thom Transversality Theorem*, we easily conclude the robustness of the properties validated above when perturbing inside $\mathcal{A}_3$. Therefore, this case is a *candidate* if, and only if, $a_{i1} \neq 0$ and $\mathbf{P} \notin \Sigma_{\theta_0}$.

   b) $a_{i3} = 0$:
   The only difference between this case and the previous is the fact that $\beta_i = 0$ and, therefore, the horizontal asymptotes are exactly at the borders $\theta = 0$ and $\theta = \pi$ of the stripes. However, since we are working inside a convex compact set K, then the same arguments of the previous case apply here.

2. $a_{i2} = 0$:
   Finally, the only difference between this case and the previous ($a_{i2} \neq 0$ and $a_{i3} = 0$) is the fact that now the horizontal asymptotes are exactly at the borders $\theta = \pi/2$ and $\theta = 3\pi/2$ of the stripes. Therefore, the same arguments applies.

The analysis of the remaining conditions (C.6) — (C.9) requires the combined dynamics of the stripes C_+ and C_-. Therefore, in order to decide stability, we need to analyze all the combinations of candidates obtained above against these conditions. Generally, it is fairly easy to perform this analysis given a specific combination. However,

a translation of these final conditions to parametric ones, although possible, would lead to a relatively large number[11] of conditions that, worse than that, would carry little to no geometrical meaning. Hence, leaving these final conditions "untranslated" is a better approach and, therefore, the following theorem has been proved:

Theorem 4.9 (Affine Dynamics Stability)**.** *Let $\mathbf{F} \in \mathcal{A}_3$ be given by (4.22) with $\gamma_i \neq 0$. Given $\Sigma_{\theta_0} \in \tilde{\mathcal{I}}_C$, let $\mathbf{X} = (\mathbf{X}_-, \mathbf{X}_+)$ be the Filippov system induced around Σ_{θ_0} and inside a convex compact set $K \subset C_+ \cup C_-$, where C_+ and C_- are two consecutive stripes meeting at Σ_{θ_0}. Then, $\mathbf{F}$ is (Σ_{θ_0}, K)-semi-local structurally stable in $\mathcal{A}_3$ if, and only if, $\mathbf{X}_+$ and $\mathbf{X}_-$ satisfies*

1. *$a_{i1} \neq 0$ and $\mathbf{P} \notin \Sigma_{\theta_0}$, where $\mathbf{P}$ is the only singularity of $\mathbf{X}_\pm$;*
2. *conditions (C.6) — (C.9) of Proposition 4.2.*

Example 4.4. *Lets see an example of instability around the discontinuity manifold $\Sigma_0 \in \tilde{\mathcal{I}}_C$ of the cylinder generated by affine vector fields. More precisely, take $\mathbf{F} \in \mathcal{A}_3$ with $\mathbf{F}_4$ and $\mathbf{F}_1$ affine vector fields given by (4.22) such that*

$$\mathbf{F}_4 : \begin{bmatrix} a_{41} & d_{41} \\ a_{42} & d_{42} \\ a_{43} & d_{43} \end{bmatrix} = \begin{bmatrix} -1 & 1 \\ 0 & -1 \\ 1 & 0 \end{bmatrix} \quad \textit{and} \quad \mathbf{F}_1 : \begin{bmatrix} a_{11} & d_{11} \\ a_{12} & d_{12} \\ a_{13} & d_{13} \end{bmatrix} = \begin{bmatrix} 1 & -1 \\ 0 & 1 \\ 1 & 0 \end{bmatrix},$$

whose dynamics over the stripes $S_4 \cup S_1$, represented at Figure 31 below, can be determined as in Example 4.2 using Theorem 4.7.

Regarding $\mathbf{F}_4$, since $a_{42} = 0$ and $\gamma_4 = -1 < 0$, then Theorem 4.7 tells us that the slow manifold is a decreasing arctangent with horizontal asymptotes $\theta = -\pi/2$ and $\theta = \pi/2$, as represented at Figure 31a. This manifold crosses the line $\theta = \theta_0 = 0$ at $x \in \mathbb{R}$ such that

$$0 = \theta_0 = \theta_4(x) = \arctan\left(\frac{a_{43}x + d_{43}}{d_{42}}\right) = \arctan(-x) \Leftrightarrow x = 0,$$

i.e., at the point $\mathbf{Q}_4 = (0, 0)$. Besides that, over the slow manifold acts the dynamics $\dot{x} = -x + 1$ whose only singularity at the point

$$\mathbf{P}_4 = (\delta_4, \theta_4(\delta_4)) = (1, \arctan(-1)) = \left(1, -\frac{\pi}{4}\right),$$

[11] More specifically, Theorem 4.7 give us a normal form with 8 possible dynamics for each stripe. Combining them 2 by 2 (with repetition) leave us with 36 combinations. Even if half of the combinations lead to a repeating condition, we would still be left with 18 conditions!

is stable, since $a_{41} < 0$. *Even more, since* $a_{42} = 0$ *and* $d_{42} < 0$ *then, according to Table 3, the slow manifold repels the layer dynamics around. Therefore, remembering of Theorem 4.5 we conclude that* $\mathbf{P}_4$, *as a singularity of* $\mathbf{X}_4$, *is a hyperbolic* saddle.

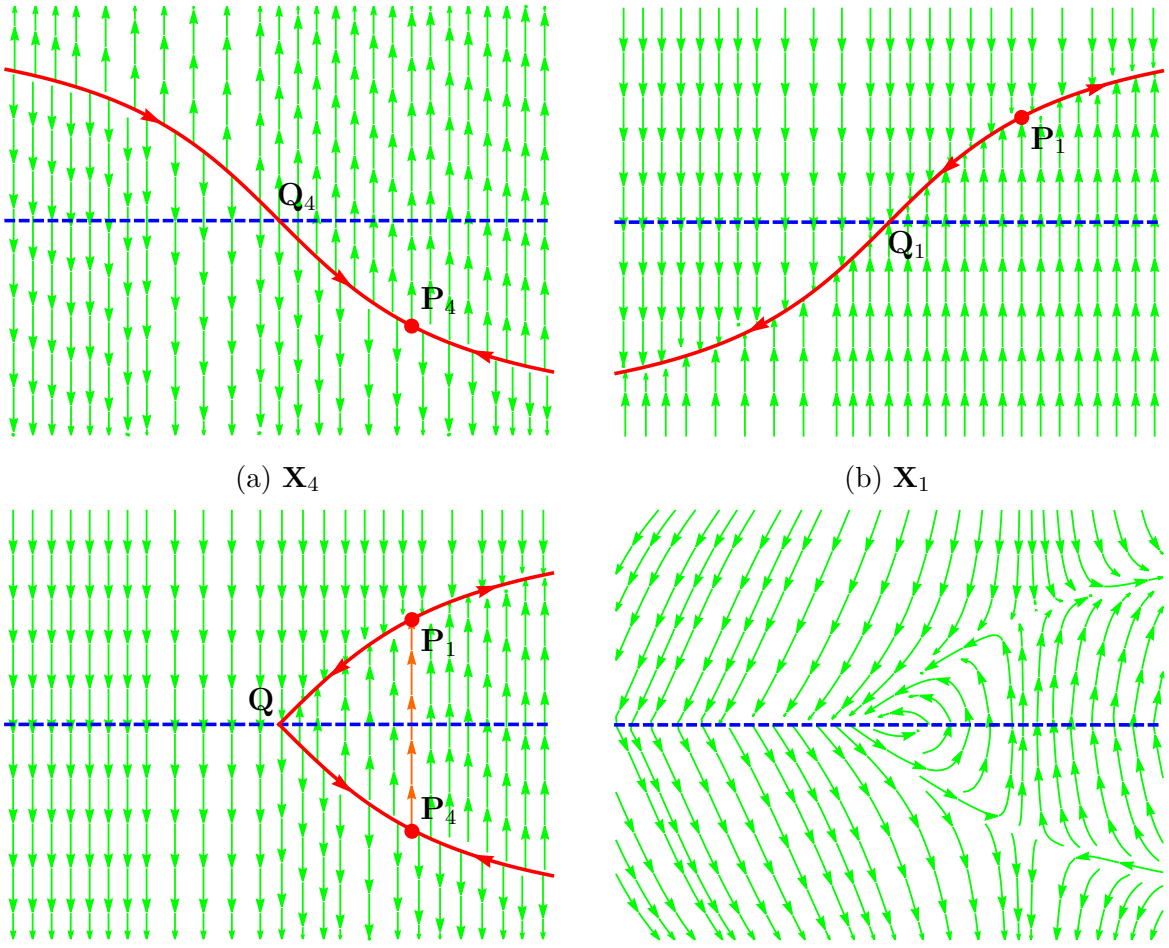

(a) $\mathbf{X}_4$ (b) $\mathbf{X}_1$

(c) $\mathbf{X} = (\mathbf{X}_4, \mathbf{X}_1)$ (d) $\mathbf{X} = (\mathbf{X}_4, \mathbf{X}_1)$ with $r > 0$

Figure 31 – Dynamics over the stripes $S_4 \cup S_1$ generated by the fields studied at Example 4.4.

On the other hand, regarding $\mathbf{F}_1$, *since* $a_{12} = 0$ *and* $\gamma_1 = 1 > 0$, *then Theorem 4.7 tells us that the slow manifold is a decreasing arctangent with horizontal asymptotes* $\theta = -\pi/2$ *and* $\theta = \pi/2$, *as represented at Figure 31b. This manifold crosses the line* $\theta = \theta_0 = 0$ *at* $x \in \mathbb{R}$ *such that*

$$0 = \theta_0 = \theta_1(x) = \arctan\left(\frac{a_{13}x + d_{13}}{d_{12}}\right) = \arctan(x) \Leftrightarrow x = 0,$$

i.e., also at the point $\mathbf{Q}_1 = (0, 0)$. *Besides that, over the slow manifold acts the dynamics* $\dot{x} = x - 1$ *whose only singularity at the point*

$$\mathbf{P}_1 = (\delta_1, \theta_1(\delta_1)) = (1, \arctan(1)) = \left(1, \frac{\pi}{4}\right),$$

is unstable, since $a_{11} > 0$. *Even more, since* $a_{12} = 0$ *and* $d_{12} > 0$ *then, according to Table 3, the slow manifold attracts the layer dynamics around. Therefore, remembering Theorem 4.5 we conclude that* $\mathbf{P}_1$, *as a singularity of* $\mathbf{X}_1$, *is also a hyperbolic* saddle.

Hence, as represented at Figure 31c, since $\mathbf{Q}_4 = \mathbf{Q}_1$ *with* $\mathbf{P}_4$ *and* $\mathbf{P}_1$ *hyperbolic saddles, then the Filippov system* $\mathbf{X} = (\mathbf{X}_4, \mathbf{X}_1)$ *has a separatrix-connection and, therefore, it violates condition (C.8) of Proposition 4.2, whatever the convex compact set* K *considered. In other words, according to Theorem 4.9, this configuration is structurally unstable around the discontinuity manifold* Σ_0.

Finally, we observe that, as represented at Figure 31c, there is actually two separatrix-connections between the saddles $\mathbf{P}_4$ *and* $\mathbf{P}_1$. *These connections enclose a* rotating region, *represented at Figure 31d.* □

5 Further Directions

Regarding Chapter 3, as for the realization of sliding saddles, a natural further direction of investigation consists in the proof of Conjecture 3.1. Another one consists in the use of the already obtained results to derive normal forms for the more general, non-linear, case. As for the structural stability, besides the proof of Conjecture 3.2, another further direction of investigation consist in a deeper analysis of the regularizations (in the examples presented there) through Peixoto Theorem, for instance, in order to search for global stability both in the linear and non-linear case.

Regarding Chapter 4, as for the structural stability, since the semi-local approach, as in Definition 4.4, is a necessary condition for the global one, as in Definition 4.3, then it is reasonable to conjecture that a set of conditions for the global case would be given by Proposition 4.2, taken from [7], plus an additional set of conditions similar to (III), but involving the whole cylinder, rather just one of its discontinuities. Another further direction consists in the adaptation of the results studied in this chapter to the planar case studied in Chapter 3.

In both chapters, Sliding Saddles and Double Discontinuities, the investigation on the existence of minimal sets (limit cycles, homoclinic and heteroclinic orbits, etc.) is a must which, especially for double discontinuities, can now be investigated even when dealing with the singular part, given the detailed dynamical descriptions here provided. In this context, the works [9, 36, 43] are interesting sources of inspiration.

Finally, in this text, we only dealt with one of the Gutierrez-Sotomayor algebraic manifolds, the double discontinuity. Therefore, a natural further direction of investigation consists in a similar analysis of the dynamics of non-smooth systems presenting one of the other singular configurations as switching manifold, namely, the triple, cone, and Whitney discontinuities. For this, [37] is an important reference, since it provides the necessary blow-ups and results.

Bibliography

1 AMADOR, J. A.; OLIVAR, G.; ANGULO, F. Smooth and Filippov models of sustainable development: bifurcations and numerical computations. *Differential Equations and Dynamical Systems*, Springer India, v. 21, n. 1-2, p. 173–184, Jan 2013. Available in: <https://doi.org/10.1007/s12591-012-0138-2>. Cited on page 15.

2 ARROWSMITH, D. K.; PLACE, C. M. *An Introduction to Dynamical Systems*. Cambridge University Press, 1990. ISBN 9780521316507. Available in: <https://books.google.com.br/books?id=HOU6q6wHCncC>. Cited on page 14.

3 BARRY, A. M.; WIDIASIH, E.; MCGEHEE, R. Nonsmooth frameworks for an extended Budyko model. *Discrete and Continuous Dynamical Systems - B*, v. 22, n. 6, p. 2447–2463, Aug 2017. Available in: <http://dx.doi.org/10.3934/dcdsb.2017125>. Cited on page 15.

4 BERNARDO, M. di; GAREFALO, F.; GLIELMO, L.; VASCA, F. Switchings, bifurcations, and chaos in DC/DC converters. *IEEE Transactions on Circuits and Systems I*, v. 45, n. 2, p. 133–141, Feb 1998. Available in: <https://doi.org/10.1109/81.661675>. Cited on page 15.

5 BERNARDO, M. D.; JOHANSSON, K. H.; VASCA, F. Self-Oscillations and Sliding in Relay Feedback Systems: Symmetry and Bifurcations. *International Journal of Bifurcation and Chaos*, v. 11, n. 4, p. 1121–1140, Apr 2001. Available in: <https://doi.org/10.1142/S0218127401002584>. Cited on page 15.

6 BROGLIATO, B. *Nonsmooth Mechanics: Models, Dynamics and Control*. 2. ed. Springer-Verlag London, 1999. ISBN 978-1-4471-0557-2. Available in: <https://doi.org/10.1007/978-1-4471-0557-2>. Cited on page 15.

7 BROUCKE, M. E.; PUGH, C.; SIMIC, S. N. Structural Stability of Piecewise Smooth Systems. *Computational and Applied Mathematics*, v. 20, n. 1-2, p. 51–89, 2001. Available in: <https://www.researchgate.net/publication/237673372_Structural_stability_of_piecewise_smooth_systems>. Cited 4 times on pages 16, 22, 83, and 93.

8 BUZZI, C. A.; SILVA, P. R. da; TEIXEIRA, M. A. Slow–fast systems on algebraic varieties bordering piecewise-smooth dynamical systems. *Bulletin des Sciences Mathématiques*, v. 136, n. 4, p. 444–462, Jun 2012. Available in: <https://doi.org/10.1016/j.bulsci.2011.06.001>. Cited 3 times on pages 18, 59, and 60.

9 CARVALHO, T.; EUZÉBIO, R. D.; TEIXEIRA, M. A.; TONON, D. J. Birth of limit cycles from a 3D triangular center of a piecewise smooth vector field. *IMA Journal of Applied Mathematics*, Oxford University Press, v. 82, n. 3, p. 561–578, Feb 2017. Available in: <https://doi.org/10.1093/imamat/hxx003>. Cited on page 93.

10 CARVALHO, T. de; NOVAES, D. D.; GONçALVES, L. F. Sliding Shilnikov connection in Filippov-type predator–prey model. *Nonlinear Dynamics*, v. 100, n. 3, p. 2973—-2987, May 2020. Available in: <https://doi.org/10.1007/s11071-020-05672-w>. Cited on page 15.

11 COLOMBO, A.; JEFFREY, M. R. Nondeterministic chaos, and the two-fold singularity in piecewise smooth flows. *SIAM Journal on Applied Dynamical Systems*, SIAM, Philadelphia, PA, v. 10, n. 2, p. 423–451, 2011. Available in: <https://doi.org/10.1137/100801846>. Cited on page 34.

12 CRISTIANO, R.; PAGANO, D. J.; FREIRE, E.; PONCE, E. Revisiting the Teixeira singularity bifurcation analysis: application to the control of power converters. *Int. J. Bifurcation Chaos*, World Scientific, Singapore, v. 28, n. 9, p. 31, Aug 2018. ISSN 0218-1274; 1793-6551/e. Available in: <https://doi.org/10.1142/S0218127418501067>. Cited on page 15.

13 DIECI, L.; LOPEZ, L. Sliding motion in Filippov differential systems: theoretical results and a computational approach. *SIAM Journal on Numerical Analysis*, SIAM, v. 47, n. 3, p. 2023–2051, Jun 2009. Available in: <https://doi.org/10.1137/080724599>. Cited 2 times on pages 18 and 20.

14 DIECI, L.; LOPEZ, L. Sliding motion on discontinuity surfaces of high co-dimension. A construction for selecting a Filippov vector field. *Numerische Mathematik*, Springer, v. 117, n. 4, p. 779–811, 2011. Available in: <https://doi.org/10.1007/s00211-011-0365-4>. Cited 2 times on pages 18 and 20.

15 DIECI, L.; ELIA, C.; LOPEZ, L. A Filippov sliding vector field on an attracting co-dimension 2 discontinuity surface, and a limited loss-of-attractivity analysis. *Journal of Differential Equations*, v. 254, n. 4, p. 1800–1832, 2013. Available in: <https://doi.org/10.1016/j.jde.2012.11.007>. Cited 2 times on pages 18 and 20.

16 DIECI, L.; DIFONZO, F. A comparison of Filippov sliding vector fields in codimension 2. *Journal of Computational and Applied Mathematics*, v. 262, p. 161–179, May 2014. Available in: <https://doi.org/10.1016/j.cam.2013.10.055>. Cited 2 times on pages 18 and 20.

17 DIECI, L.; ELIA, C.; LOPEZ, L. Sharp sufficient attractivity conditions for sliding on a co-dimension 2 discontinuity surface. *Mathematics and Computers in Simulation*, v. 110, p. 3–14, 2015. Available in: <https://doi.org/10.1016/j.matcom.2013.12.005>. Cited 2 times on pages 18 and 20.

18 DIECI, L. Sliding motion on the intersection of two manifolds: Spirally attractive case. *Communications in Nonlinear Science and Numerical Simulation*, v. 26, n. 1, p. 65–74, 2015. Available in: <https://doi.org/10.1016/j.cnsns.2015.02.002>. Cited 2 times on pages 18 and 20.

19 DIECI, L.; ELIA, C.; LOPEZ, L. Uniqueness of Filippov sliding vector field on the intersection of two surfaces in $\mathbb{R}^3$ and implications for stability of periodic orbits. *Journal of Nonlinear Science*, v. 25, n. 6, p. 1453–1471, 2015. Available in: <https://doi.org/10.1007/s00332-015-9265-6>. Cited 2 times on pages 18 and 20.

20 DIECI, L.; ELIA, C. Piecewise smooth systems near a co-dimension 2 discontinuity manifold: Can one say what should happen? *Discrete and Continuous Dynamical Systems - S*, v. 9, n. 4, p. 1039–1068, 2016. Available in: <http://doi.org/10.3934/dcdss.2016041>. Cited 2 times on pages 18 and 20.

21 FENICHEL, N. Geometric singular perturbation theory for ordinary differential equations. *Journal of Differential Equations*, v. 31, n. 1, p. 53–98, Jan 1979. Available in: <https://doi.org/10.1016/0022-0396(79)90152-9>. Cited 3 times on pages 18, 37, and 40.

22 FILIPPOV, A. F. *Differential Equations with Discontinuous Righthand Sides*. Springer Netherlands, 1988. (18). ISBN 9401577935. Available in: <https://doi.org/10.1007/978-94-015-7793-9>. Cited 3 times on pages 15, 25, and 29.

23 GLENDINNING, P.; JEFFREY, M. R. *An Introduction to Piecewise Smooth Dynamics*. Birkhäuser Basel, 2019. (Advanced Courses in Mathematics - CRM Barcelona). ISBN 978-3-030-23689-2. Available in: <https://doi.org/10.1007/978-3-030-23689-2>. Cited on page 15.

24 GOMIDE, O. M. L.; TEIXEIRA, M. A. On structural stability of 3D Filippov systems. *Mathematische Zeitschrift*, Springer, v. 294, n. 1-2, p. 419–449, 2020. Available in: <https://doi.org/10.1007/s00209-019-02252-6>. Cited on page 16.

25 GUARDIA, M.; SEARA, T. M.; TEIXEIRA, M. A. Generic bifurcations of low codimension of planar Filippov systems. *Journal of Differential equations*, Elsevier, v. 250, n. 4, p. 1967–2023, 2011. Available in: <http://dx.doi.org/10.1016/j.jde.2010.11.016>. Cited on page 16.

26 GUTIERREZ, C.; SOTOMAYOR, J. Stable Vector Fields on Manifolds with Simple Singularities. *Proceedings of the London Mathematical Society*, v. 45, n. 1, p. 97–112, Jul 1982. Available in: <https://doi.org/10.1112/plms/s3-45.1.97>. Cited 2 times on pages 16 and 59.

27 HINRICHS, N.; OESTREICH, M.; POPP, K. On the Modelling of Friction Oscillators. *Journal of Sound Vibration*, v. 216, n. 3, p. 435–459, Sep 1998. Available in: <https://doi.org/10.1006/jsvi.1998.1736>. Cited on page 15.

28 JEFFREY, M. R. Dynamics at a switching intersection: Hierarchy, isonomy, and multiple sliding. *SIAM Journal on Applied Dynamical Systems*, SIAM, v. 13, n. 3, p. 1082–1105, 2014. Available in: <https://doi.org/10.1137/13093368X>. Cited 2 times on pages 17 and 18.

29 JEFFREY, M. R. *Hidden Dynamics: The mathematics of switches, decisions, and other discontinuous behaviour*. Springer, 2018. Available in: <https://doi.org/10.1007/978-3-030-02107-8>. Cited on page 18.

30 JEFFREY, M. R. *Modeling with Nonsmooth Dynamics*. Springer, 2020. Available in: <https://doi.org/10.1007/978-3-030-35987-4>. Cited on page 16.

31 KAKLAMANOS, P.; KRISTIANSEN, K. U. Regularization and geometry of piecewise smooth systems with intersecting discontinuity sets. *SIAM Journal on Applied Dynamical Systems*, SIAM, v. 18, n. 3, p. 1225–1264, Jul 2019. Available in: <https://doi.org/10.1137/18M1214470>. Cited on page 18.

32 KATOK, A.; HASSELBLATT, B. *Introduction to the Modern Theory of Dynamical Systems*. Cambridge University Press, 1997. (Encyclopedia of Mathematics and its Applications). ISBN 9780521575577. Available in: <https://books.google.com.br/books?id=9nL7ZX8Djp4C>. Cited on page 14.

33 KOWALCZYK, P.; PIIROINEN, P. T. Two-parameter sliding bifurcations of periodic solutions in a dry-friction oscillator. *Physica D*, Elsevier (North-Holland), Amsterdam, v. 237, n. 8, p. 1053–1073, Jun 2008. ISSN 0167-2789. Available in: <https://doi.org/10.1016/j.physd.2007.12.007>. Cited on page 15.

34 LEIFELD, J. Non-smooth homoclinic bifurcation in a conceptual climate model. *European Journal of Applied Mathematics*, Cambridge University Press, Cambridge, v. 29, n. 5, p. 891–904, Apr 2018. Available in: <https://doi.org/10.1017/S0956792518000153>. Cited on page 15.

35 LLIBRE, J.; SILVA, P. R. da; TEIXEIRA, M. A. Regularization of Discontinuous Vector Fields on $\mathbb{R}^3$ via Singular Perturbation. *Journal of Dynamics and Differential Equations*, v. 19, n. 2, p. 309–331, Jun 2007. Available in: <https://doi.org/10.1007/s10884-006-9057-7>. Cited on page 18.

36 LLIBRE, J.; PONCE, E.; TERUEL, A. E. Horseshoes near homoclinic orbits for piecewise linear differential systems in R3. *International Journal of Bifurcation and Chaos*, World Scientific, v. 17, n. 04, p. 1171–1184, 2007. Available in: <http://dx.doi.org/10.1142/S0218127407017756>. Cited on page 93.

37 LLIBRE, J.; SILVA, P. R. da; TEIXEIRA, M. A. Sliding vector fields for non-smooth dynamical systems having intersecting switching manifolds. *Nonlinearity*, v. 28, n. 2, p. 493–507, Jan 2015. Available in: <https://doi.org/10.1088/0951-7715/28/2/493>. Cited 6 times on pages 18, 20, 55, 59, 60, and 93.

38 NOVAES, D. D. *Regularization and minimal sets for non-smooth dynamical systems*. Thesis (PhD) — Universidade Estadual de Campinas, Jun 2015. Available in: <http://repositorio.unicamp.br/jspui/handle/REPOSIP/305995>. Cited on page 37.

39 PALIS, J.; MELO, W. de. *Geometric Theory of Dynamical Systems*. Springer-Verlag New York, 1982. ISBN 978-1-4612-5703-5. Available in: <https://doi.org/10.1007/978-1-4612-5703-5>. Cited on page 83.

40 PANAZZOLO, D.; SILVA, P. R. da. Regularization of discontinuous foliations: Blowing up and sliding conditions via Fenichel theory. *Journal of Differential Equations*, v. 263, n. 12, p. 8362–8390, Dec 2017. Available in: <http://dx.doi.org/10.1016/j.jde.2017.08.042>. Cited 4 times on pages 16, 18, 59, and 60.

41 PILTZ, S. H.; PORTER, M. A.; MAINI, P. K. Prey switching with a linear preference trade-off. *SIAM Journal on Applied Dynamical Systems*, Society for Industrial and Applied Mathematics (SIAM), Philadelphia, PA, v. 13, n. 2, p. 658–682, Apr 2014. Available in: <https://doi.org/10.1137/130910920>. Cited on page 15.

42 PROKOPIOU, S. A.; BYRNE, H. M.; JEFFREY, M. R.; ROBINSON, R. S.; MANN, G. E.; OWEN, M. R. Mathematical analysis of a model for the growth of the bovine corpus luteum. *Journal of Mathematical Biology*, Springer, Berlin/Heidelberg, v. 69, n. 6-7, p. 1515–1546, 2014. Available in: <https://doi.org/10.1007/s00285-013-0722-2>. Cited on page 15.

43 SILVA, G. T. da. *Ciclos em Sistemas Lineares por Partes Contínuos Tridimensionais*. Dissertation (MSc) — Universidade Estadual de Campinas, Mar 2017. Available in: <http://repositorio.unicamp.br/jspui/handle/REPOSIP/322368>. Cited on page 93.

44 SILVA, G. T. da; MARTINS, R. M. Dynamics and structural stability of piecewise smooth dynamical systems presenting a double discontinuity. *arXiv:2009.08971*, Sep 2020. Available in: <https://arxiv.org/abs/2009.08971>. Cited on page 58.

45 SMIRNOV, G. V. *Introduction to the Theory of Differential Inclusions*. American Mathematical Society, 2002. ISBN 9780821829776. Available in: <https://books.google.com.br/books?id=6EUPCgAAQBAJ>. Cited 3 times on pages 25, 27, and 28.

46 SOTOMAYOR, J.; TEIXEIRA, M. A. Regularization of discontinuous vector fields. *International Conference on Differential Equations*, Jan 1996. Available in: <https://www.researchgate.net/publication/268245331_Regularization_of_discontinuous_vector_fields>. Cited 4 times on pages 16, 20, 37, and 55.

47 SPRAKER, J. S. A Comparison of the Carathéodory and Filippov Solution Sets. *Journal of Mathematical Analysis and Applications*, v. 198, n. 2, p. 571–580, 1996. Available in: <https://doi.org/10.1006/jmaa.1996.0099>. Cited 2 times on pages 15 and 29.

48 TEIXEIRA, M. A. Stability conditions for discontinuous vector fields. *Journal of Differential Equations*, v. 88, n. 1, p. 15–29, Nov 1990. Available in: <https://doi.org/10.1016/0022-0396(90)90106-Y>. Cited 3 times on pages 16, 34, and 35.

49 TEIXEIRA, M. A.; SILVA, P. R. da. Regularization and singular perturbation techniques for non-smooth systems. *Physica D: Nonlinear Phenomena*, v. 241, n. 22, p. 1948–1955, Nov 2012. Available in: <http://dx.doi.org/10.1016/j.physd.2011.06.022>. Cited 6 times on pages 16, 18, 40, 41, 59, and 60.

50 UTKIN, V. I. *Sliding Modes in Control and Optimization*. Springer-Verlag, 1992. ISBN 978-3-642-84379-2. Available in: <https://doi.org/10.1007/978-3-642-84379-2>. Cited 2 times on pages 15 and 29.

51 VALENCIA-CALVO, J.; OLIVAR-TOST, G.; MORCILLO-BASTIDAS, J. D.; FRANCO-CARDONA, C. J.; DYNER, I. Non-Smooth Dynamics in Energy Market Models: A Complex Approximation From System Dynamics and Dynamical Systems Approach. *IEEE Access*, v. 8, p. 128877–128896, 2020. Available in: <https://doi.org/10.1109/ACCESS.2020.3008709>. Cited on page 15.

52 WANG, B.; XU, J.; WAI, R.; CAO, B. Adaptive Sliding-Mode With Hysteresis Control Strategy for Simple Multimode Hybrid Energy Storage System in Electric Vehicles. *IEEE Transactions on Industrial Electronics*, v. 64, n. 2, p. 1404–1414, Oct 2017. Available in: <https://doi.org/10.1109/TIE.2016.2618778>. Cited on page 15.

53 WANG, A.; XIAO, Y.; ZHU, H. Dynamics of a Filippov epidemic model with limited hospital beds. *Mathematical Biosciences and Engineering*, v. 15, n. 3, p. 739–764, Jun 2018. Available in: <http://dx.doi.org/10.3934/mbe.2018033>. Cited on page 15.

54 WEBBER, S.; JEFFREY, M. R. Two-fold singularities in nonsmooth dynamics—Higher dimensional analogs. *Chaos*, v. 30, n. 9, p. 093142, Sep 2020. Available in: <https://doi.org/10.1063/5.0002144>. Cited on page 18.

55 WEINAN, E. A Proposal on Machine Learning via Dynamical Systems. *Communications in Mathematics and Statistics*, Springer Science and Business Media LLC, v. 5, n. 1, p. 1–11, Mar 2017. Available in: <https://doi.org/10.1007/s40304-017-0103-z>. Cited on page 14.

56 WOJEWODA, J.; STEFAŃSKI, A.; WIERCIGROCH, M.; KAPITANIAK, T. Hysteretic effects of dry friction: Modelling and experimental studies. *Philos. Trans. R. Soc. A*, Royal Society Publishing, London, v. 366, n. 1866, p. 747–765, Oct 2008. Available in: <https://doi.org/10.1098/rsta.2007.2125>. Cited on page 15.

57 ZHANG, W.; GE, S. S. A global implicit function theorem without initial point and its applications to control of non-affine systems of high dimensions. *Journal of Mathematical Analysis and Applications*, Elsevier, v. 313, n. 1, p. 251–261, Sep 2006. Available in: <https://doi.org/10.1016/j.jmaa.2005.08.072>. Cited on page 64.